Title
Deep-sea bioturbation and the role of the sea urchin Echinocrepis rostrata

Permalink
https://escholarship.org/uc/item/4m54n420

Author
Vardaro, Michael F.

Publication Date
2008

Peer reviewed|Thesis/dissertation

UNIVERSITY OF CALIFORNIA, SAN DIEGO

Deep-sea Bioturbation and the Role of the Sea Urchin *Echinocrepis rostrata*

A dissertation submitted in partial satisfaction of the
requirements for the degree of Doctor of Philosophy

in

Marine Biology

by

Michael F. Vardaro

Committee in charge:

       Kenneth L. Smith, Jr., Chair
       Nicholas D. Holland, Co-Chair
       Miriam Kastner
       David P. Phillips
       Victor D. Vacquier

2008

The dissertation of Michael F. Vardaro is approved, and it is acceptable in quality and form for publication on microfilm:

_____

_____

_____

_____
Co-Chair

_____
Chair

University of California, San Diego

2008

To my grandfather, Stanley, who nurtured

my love of science from the very beginning

TABLE OF CONTENTS

LIST OF FIGURES

II

III

IV

V

VI

LIST OF TABLES

II

III

V

VI

ACKNOWLEDGEMENTS

Chapter II, in full, is a reprint of the material as it appeared in Deep-Sea Research, Part I (Vardaro MF, Parmley D, Smith KL, Jr. (2007) A study of possible "reef effects" caused by a long-term time-lapse camera in the deep North Pacific. Deep-Sea Research I 54: 1231-1240). I was the primary author of the above paper.

2008, **Ph.D. in Marine Biology**, University of California, San Diego

2004, **M.S. in Oceanography**, Texas A&M University, College Station, TX

1998, **B.S. in Biology**, Georgetown University, Washington, D.C.

JOURNAL PUBLICATIONS

Vardaro, M.F., Parmley, D., Smith, K. L. (2007) A study of possible "reef effects" caused by a long-term time-lapse camera in the deep North Pacific. Deep-Sea Research I. 54(8): 1231-1240.

Vardaro, M.F., MacDonald, I.R., Bender, L.C., Guinasso, N.L., Jr. (2005) Dynamic processes observed at a gas hydrate outcropping on the continental slope of the Gulf of Mexico. Geo-Marine Letters. 26(1): 1432-1157

MacDonald, I.R., Bender, L.C., **Vardaro, M.**, Bernard, B., Brooks, J.M. (2005) Thermal and visual time series at a seafloor gas hydrate deposit on the Gulf of Mexico slope. EPSL. 233: 45-59.

MacDonald, I.R., **Vardaro, M.**, Bender, L. (2003) A temperature and photographic time-series from a seafloor gas hydrate deposit on the Gulf of Mexico slope. Geophysical Research Abstracts. 5: p. 12714.

Eastlack M, Walter G, Lenrow D, Dudley G, Swift A, Yim S, Gregory C, **Vardaro M**, Vandenborne K. (1999) A Comparison of In Vitro Enzymatic Assays with In Vivo 31P MRS of Muscle Metabolism. Medicine and Science in Sports and Exercise, Vol. 31:5, p. S242.

Russ, D.W., Binder-Macleod, S.A., Elliot, M.A., Swift, A., Vandenborne, K., **Vardaro, M.**, Walter, G. (1999) Metabolic cost of different stimulation trains during fatigue of skeletal muscle. FASEB Journal. 13(5): A690, Part 2, Suppl.

OTHER PUBLICATIONS

Vardaro, M.F., Smith, K.L., Jr. (2008) Climate variation and bioturbation on the sea floor in the abyssal North Pacific. ASLO Ocean Sciences Meeting. Orlando, FL. p. 49.

Vardaro, M.F., Parmley, D., Smith, K. L. (2007) A study of possible "reef effects" caused by a long-term time-lapse camera in the deep North Pacific. ASLO Aquatic Sciences Meeting. Santa Fe, NM. p. 43.

Vardaro, M.F., Smith, K.L., Jr. (2006) Deep-sea bioturbation and the role of the sea urchin *Echinocrepis rostrata*. 11th International Deep Sea Biology Symposium. Southampton, UK. p. 83.

Vardaro, M.F., Bender, L.C., MacDonald, I.R. (2003) Long-term Measurement of Sediment Resuspension and Gas Hydrate Stability at a Gulf of Mexico Seep Site. Eos Trans. AGU. 84(46) Fall Meet. Suppl., Abstract OS51B-0859.

MacDonald, I.R., Bender, L.C., **Vardaro, M.F.** (2003) Temperature Time-Series from a Seafloor Gas Hydrate Deposit on the Gulf of Mexico Slope. Eos Trans. AGU. 84(46) Fall Meet. Suppl., Abstract OS51B-0858.

Vardaro, M.F., MacDonald, I.R. (2003) Long-term Observation of Hydrate Mound Topography and Ecology. The Oceanography Society – Oceanology International Americas 2003 Ocean Conference. New Orleans, LA. p. 64.

Vardaro, M.F., Bender, L.C., MacDonald, I.R. (2002) Long-term Observation of Temporal Changes in Hydrate Mound Topography and Ecology. Gulf of Mexico Hydrates Research Consortium Ann. Mtg., Oxford, MS. p. 1.

Noyszewski, E.A., Wehrli, S., Kudchodkar, S., **Vardaro, M.**, Reddy, R. (2000) High Resolution ^{13}C MRS Studies of Cartilage Metabolism in Intact Bovine Explants. Eighth Scientific Meeting of ISMRM, p. 226.

ABSTRACT OF THE DISSERTATION

Deep-sea Bioturbation and the Role of the Sea Urchin *Echinocrepis rostrata*

by

Michael F. Vardaro

Doctor of Philosophy in Marine Biology

University of California, San Diego, 2008

Kenneth L. Smith Jr., Chair
Nicholas D. Holland, Co-Chair

The following dissertation research studied bioturbation activity in the benthic community at a site in the eastern North Pacific (Station M; 34º50'N, 123º00'W; 4100 m depth). Time-lapse photography, animal collections and sediment core samples were used to examine whether bioturbation rates of *Echinocrepis rostrata* echinoids at Station M changed significantly over an 18-year period between 1989 and 2007, if these possible changes are correlated to food supply and surface conditions/climate, and how *E. rostrata* bioturbation affects deep-sea sediment chemistry.

First, animal aggregation behavior was addressed as a potential bias in the time-lapse camera data used to conduct the long-term observations at Station M. Genetic tests were conducted to determine the phylogenetic relationships among the three commonly

observed color morphs of *E. rostrata* (designated tan, purple and white). The reproductive behavior of *E rostrata*, which has never been described, was also examined. Abundance, size and speed data from the photographic record were used to track long-term changes in bioturbation by *E. rostrata*, and how those changes were correlated to variations in climate and particulate organic carbon (POC) flux rates. Radioactive isotope activity, carbon content and chlorophyll concentrations were measured in the top four cm of thirty-two paired push core samples collected at Station M from sediment trails recently created by *E. rostrata* and local undisturbed sediment.

The results showed that the rate of bioturbation of *E. rostrata* echinoids at Station M was correlated to food supply and climate indices. Aggregation behavior and possible multiple species of *Echinocrepis* were ruled out as confounding factors which might have affected the data used to conduct the bioturbation study, while examination of the reproductive anatomy of *E. rostrata* showed that this species is unlikely to broadcast spawn or reproduce seasonally. Finally, there was no conclusive evidence of the effect of *E. rostrata* bioturbation on sediment chemistry; however, further research is required.

I

General Introduction

Far from being the featureless, monotonous, mostly lifeless mud plain that it was initially thought to be, the abyssal plain is now known to support high levels of biodiversity and undergo constant change due to a degree of biological and geological activity that rivals that found anywhere else on the globe (Hessler and Sanders 1967; Gage 1996; Gage et al. 2002). The abyssal plain is also the eventual destination for the particulate organic carbon (POC) produced in the surface ocean (Martin et al. 1987; Lampitt 1992; Lee et al. 1998; Kiørboe 2001; Kiørboe and Thygesen 2001; Stemmann et al. 2004; Buesseler et al. 2007). The POC that reaches the seafloor, in the form of phytodetrital aggregates, does not simply accumulate on the seafloor and remain in a refractory state; instead, it is consumed and reworked by deep-sea benthic organisms, sequestered in sediments, remineralized, and eventually a large percentage of the carbon (Thunell et al. 1994; Thunell et al. 2000) is transported back to the surface over hundreds to thousands of years (Bauer et al. 1992; Reimers et al. 1992; Smallwood et al. 1999; Miller et al. 2000). The biologically mediated cycling of carbon from CO_2 in the atmosphere to incorporation by phytoplankton, from planktonic organisms to the export of POC into the deep ocean, and from phytodetritus ingested by benthic organisms back into the water column as dissolved CO_2 is collectively known as the "biological pump" which is a major control on carbon in the ocean and atmosphere (Sarmiento and Siegenthaler 1992; Bopp et al. 2005; Marinov et al. 2006). However, many of these processes occur at depth and are difficult to measure directly.

Both the quantity and quality of POC that is deposited on the seafloor, and the abundance of benthic organisms (Ruhl 2007), fluctuate in relation to climate (Smith et al. 1994; Smith et al. 2001; Ruhl and Smith 2004); however, the connections between the

amount of POC that reaches the seafloor, benthic population size, and bioturbation levels have yet to be extensively studied. The biological mixing of sediment, or bioturbation, is an important factor in changing geochemical gradients, redistributing nutrients and restructuring bacterial and microfaunal communities (Meysman et al. 2006). If bioturbation levels also fluctuate with climate, the amount of carbon that is sequestered in the sediments could be affected by changes in surface conditions as well. The pelagic-benthic coupling between surface production, benthic fauna abundance, and seabed carbon sequestration is a crucial process that has profound impacts on the seafloor biology, chemistry and geology (Gray 1974; Aller 1982; Smith et al. 1997; Biles et al. 2002; Solan et al. 2004). In spite of the importance of the deep-sea in the carbon cycle, there is a paucity of data on deep-sea processes.

One of the major reasons for the lack of biogeochemical data from the deep ocean is the difficulty inherent in sampling and observing communities at extreme depths. Traditional techniques, such as sediment coring and bottom trawling, do not always provide an accurate picture of the ecosystem. Marine biologists and geologists have used deep-sea photography to identify objects of interest in the deep ocean since the late 1960s (Ewing and Davis 1967; Menzies et al. 1973; Grassle et al. 1975; Lemche et al. 1976); however, all deployments before 1974 recovered only instantaneous snapshots of the seafloor. In 1974, Gerard and Thorndike created the Bottom Ocean Monitor (BOM), which was deployed for 202 days and took still photographs of the ocean bottom every 4 hours (Paul et al. 1978). Adding a time dimension to the photographic record significantly increased our understanding of the mechanisms and rates of deep-sea processes, and illustrated how little was known about the dynamic benthic environment.

The cost of operating research vessels and submersibles over the ensuing years has led to greater reliance on *in situ* monitoring devices such as time-lapse cameras and video systems. Video cameras require more data storage capacity and have lower resolution than still photography (Carter et al. 1979), so time-lapse still photography remains the method of choice for long-term deep-sea studies. A small sample of the scientific applications of time-lapse photography include observation and measurement of deep ocean floor processes (Thorndike et al. 1982; Gardner et al. 1984; Bett and Rice 1993; Smith et al. 1993; Bett et al. 2001; Solan and Kennedy 2002), feeding rates of abyssal scavengers (Hargrave 1985; Ramsay et al. 1997; Kemp et al. 2006), and the behavior and mortality of hydrothermal vent tubeworms (Tunnicliffe et al. 1990) and gastropods (Martell et al. 2002).

The following dissertation research used time-lapse photography and manned and robotic submersibles (ROVs) to study bioturbation activity in the benthic community at a site in the eastern North Pacific (Station M; 34º50'N, 123º00'W; 4100 m depth). This location, approximately 220 km west of Pt. Conception, CA**,** has been the subject of multiple long-term benthic and pelagic studies that provided 18 years of background data, including sediment trap collections as well as an 18-year set of time-lapse photographs of the seafloor. The long-term time-series study was established at this site because the activity of the California Current above it leads to seasonal and interannual variations in surface productivity. Seasonal pulses of phytodetritus and other forms of organic matter often begin in June or July and can last until December (Smith et al. 1994), though this cycle can vary extensively in intensity and duration from year to year (Baldwin et al. 1998). The variable food supply at Station M has seasonal impacts on sediment

community oxygen consumption (SCOC, Smith and Kaufmann 1999; Smith et al. 2001), abundance of sediment infauna (Drazen et al. 1998), megafaunal behavior (Kaufmann and Smith 1997) and megafaunal abundance (Ruhl and Smith 2004; Ruhl 2007).

A strong El Niño Southern Oscillation (ENSO) event in 1997 and 1998 caused numerous and persistent ecological changes in the northeast Pacific Ocean (Kahru and Mitchell 2002a; Kahru and Mitchell 2002b; Bograd and Lynn 2003; Brinton and Townsend 2003; Lavaniegos and Ohman 2003). A deficit in the abyssal food supply in 1998 was found by comparing the food supply (POC flux rates) and demand (SCOC levels) from 1989-1998 (Smith et al. 2001); the supply:demand ratio shifted back to surplus levels in 1999 (Smith et al. 2006). Ruhl (2004; 2007; 2008) found that the abundance and distribution of various species of mobile epibenthic megafauna at Station M were correlated with the climate-related, interannual variation in POC flux.

One of the most active and abundant epibenthic organisms observed at Station M is *Echinocrepis rostrata*, an irregular sea urchin that ranges in width between 50 to 150 mm and exhibits three color morphs: white, tan, and purple (Smith et al. 1993; Kaufmann and Smith 1997; Ruhl 2007; Vardaro et al. 2007). *Echinocrepis* echinoids mediate bioturbation through their locomotion and feeding behaviors, which create visible and distinctive trails several centimeters deep in the sediment that can persist for months (Kaufmann and Smith 1997). In addition to its abundance at Station M and bioturbation activity, *E. rostrata* was an ideal proxy species to use in this study because of its distinctive color and shape, which simplified identification from the time-lapse photographic record, and its movement speed, which was slow enough to remain in the field of view of the time-lapse camera for days to weeks at a time, but fast enough to be

measurable in hourly time-lapse photographs. The genus *Echinocrepis* was first described by Alexander Agassiz in a report on the echinoids dredged up by the Challenger Expedition (Agassiz 1879; 1881), with two species identified: *E. cuneata* in the Antarctic and *E. rostrata* in the eastern Pacific, described from samples recovered by Mironov (1973). *Echinocrepis* belongs to the family Pourtalesiidae in the order Holasteroida (Mortensen 1950). Holasteroida is an abyssal order that includes heart urchins (David 1988; Smith 2004). There are seven globally distributed genera of pourtalesiids, all of which exhibit unique spines and pedicellariae, irregularly-shaped tests, and oral structures that are significantly different from the conventional five-fold radial architecture of regular echinoids (Agassiz 1881; Mironov 1975; Gage 1987; Mooi and David 1996; David et al. 2003; Saucede et al. 2004; Smith 2004; Mironov 2008).

Chapters II-VI of this dissertation present research that used time-lapse photography, animal collections and sediment core samples to examine the behavior and biology of *E. rostrata*, whether bioturbation rates of *E. rostrata* echinoids at Station M changed significantly over time, if these possible changes are correlated to food supply and surface conditions/climate, and how bioturbation by *E. rostrata* affects deep-sea sediment chemistry. Chapters II and III examine possible confounding factors which might have affected the data used to conduct the bioturbation study, while Chapter IV deals with aspects of the reproductive biology of *E. rostrata* that have important implications for the recruitment and dispersal of the species.

Chapter II addresses animal aggregation behavior as a potential bias in the time-lapse camera data used to conduct the long-term observations at Station M. Aggregation responses of fish and invertebrate populations following the introduction of

structures to seafloor habitats have been documented in shallow water artificial reefs and at deeper structures such as shipwrecks and oil extraction platforms. The objective of this chapter was to document any persistent increases in the abundance of fish (*Coryphaenoides* spp.) or invertebrates (*Echinocrepis rostrata*) over the four-month deployment period of the time-lapse camera system.

In **Chapter III** I present the results of gene sequence tests to determine phylogenetic relationships among the three color morphs of *E. rostrata* (designated tan, purple and white). Bioturbation and population studies would be much more complex if the morphotypes were actually different species. The mitochondrial (mt) 16S rDNA sequence, a portion of the mitochondrial genome commonly used in barcoding, was amplified from tissue samples from all three morphotypes, and their similarity was compared using Bayesian analysis. This chapter addressed whether the three *E. rostrata* morphotypes constituted different species, possible explanations for the color variations of the morphotypes, and whether the size differences among the morphotypes were significant.

Chapter IV examines the gonadal anatomy of *E. rostrata* to determine the reproductive strategy that would explain the low fecundity and large ova sizes found in the collected specimens. Optical and electron microscopy as well as *in situ* photographs were used to search for evidence of seasonal spawning or constant gamete production, whether *E. rostrata* females brood their larvae or broadcast spawn, and any anatomical or photographic evidence of the reproductive behavior of *E. rostrata*.

Chapter V uses the 18-year time-series photographic record from Station M and data from concurrent abundance studies to track long-term changes in bioturbation by *E.*

rostrata. Abundance, size and speed data from the photographic record were used to create an equation for bioturbation potential. The bioturbation equation was used to determine whether there was an increase in bioturbation over the 18-years of the time series. The levels of bioturbation by *E. rostrata* were then correlated with POC flux rates and climate indices to examine whether climate variation could lead to altered rates of carbon sequestration in deep sea sediments.

Chapter VI uses push cores collected by ROV in areas of recently disturbed sediment to look for evidence of sediment mixing caused by *E. rostrata* bioturbation. The upper few cm of the sediment cores were sectioned and the isotopic composition, CHN concentration, and chlorophyll content of the sediment core sections were analyzed to isolate any evidence of vertical sediment mixing and homogenization by *E. rostrata* in recently bioturbated cores.

Finally, **Chapter VII** presents the conclusions, broader ecological implications and potential future directions of this dissertation research.

References

Agassiz A (1879) Preliminary report on the echini of the exploring expedition of H.M.S. "Challenger," Sir C. Wyville Thomson Chief of Civilian Staff. Proceedings of the American Academy of Arts and Sciences 14: 190-212

Agassiz A (1881) Report on the scientific results of the voyage of H.M.S. Challenger during the years 1873-76: Zoology; v. III, pt. 9, Report on the Echinoidea. Longmans & Co., London

Aller RC (1982) The effects of macrobenthos on chemical properties of marine sediment and overlying water. In: McCall PL, Tevesz MJS (eds) Animal-sediment relations---the biogenic alteration of sediments. Topics in geobiology, Vol 2. Plenum Press, New York, pp 53-102

Baldwin RJ, Glatts RC, Smith KL, Jr. (1998) Particulate matter fluxes into the benthic boundary layer at a long time-series station in the abyssal NE Pacific: composition and fluxes. Deep-Sea Research II 45: 643-665

Bauer JE, Williams PM, Druffel ERM (1992) Super ^{14}C activity of dissolved organic carbon fractions in the north-central Pacific and Sargasso Sea. Nature 357: 667-670

Bett BJ, Malzone MG, Narayanaswamy BE, Wigham BD (2001) Temporal variability in phytodetritus and megabenthic activity at the seabed in the deep Northeast Atlantic. Progress in Oceanography 50: 349-368

Bett BJ, Rice AL (1993) The feeding-behavior of an abyssal Echiuran revealed by in-situ time-lapse photography. Deep-Sea Research I 40: 1767-1779

Biles CL, Paterson DM, Ford RB, Solan M, Raffaelli DG (2002) Bioturbation, ecosystem functioning and community structure. Hydrology and Earth System Sciences 6: 999-1005

Bograd SJ, Lynn RJ (2003) Long-term variability in the Southern California Current System. Deep-Sea Research II 50: 2355-2370

Bopp L, Aumont O, Cadule P, Alvain S, Gehlen M (2005) Response of diatoms distribution to global warming and potential implications: A global model study. Geophysical Research Letters 32: L19606 doi:19610.11029/12005GL023653

Brinton E, Townsend A (2003) Decadal variability in abundances of the dominant euphausiid species in southern sectors of the California Current. Deep-Sea Research II 50: 2449-2472

Buesseler KO, Lamborg CH, Boyd PW, Lam PJ, Trull TW, Bidigare RR, Bishop JKB, Casciotti KL, Dehairs F, Elskens M, Honda M, Karl DM, Siegel DA, Silver MW, Steinberg DK, Valdes J, Van Mooy B, Wilson S (2007) Revisiting carbon flux through the ocean's twilight zone. Science 316: 567-570

David B (1988) Origins of the deep-sea holasteroid fauna. In: Paul CRC, Smith AB (eds) Echinoderm phylogeny and evolutionary biology. Clarendon Press, Oxford, pp 331-346

David B, Magniez F, Villier L, de Wever P (2003) Conveying behavior of the deep sea pourtalesiid *Cystocrepis setigera* off Peru. In: Féral J-P, David B (eds) Echinoderm Research 2001. CRC Press, London, pp 253-257

Drazen JC, Baldwin RJ, Smith KL, Jr. (1998) Sediment community response to a temporally varying food supply at an abyssal station in the NE Pacific. Deep-Sea Research II 45: 893-913

Ewing M, Davis RA (1967) Deep-Sea Photography. Johns Hopkins Press, Baltimore

Gage JD (1987) Growth of the deep-sea irregular sea urchins *Echinosigra phiale* and *Hemiaster expergitus* in the Rockall Trough (N.E. Atlantic Ocean). Marine Biology 96: 19-30

Gage JD (1996) Why are there so many species in deep-sea sediments? Journal of Experimental Marine Biology and Ecology 200: 257-286

Gage JD, Hughes DJ, Gonzalez Vecino JL (2002) Sieve size influence in estimating biomass, abundance and diversity in samples of deep-sea macrobenthos. Marine Ecology Progress Series 225: 97-107

Gardner WD, Sullivan LG, Thorndike EM (1984) Long-term photographic, current, and nephelometer observations of manganese nodule environments in the Pacific. Earth and Planetary Science Letters 70: 95-109

Grassle JF, Sanders HJ, Hessler RR, Rowe GT, McLellan T (1975) Pattern and zonation - study of bathyal megafauna using research submersible Alvin. Deep-Sea Research 22: 457

Gray JS (1974) Animal-sediment relationships. Oceanogr. Mar. Biol. Ann. Rev. 12: 223–261

Hargrave BT (1985) Feeding rates of abyssal scavenging amphipods (*Eurythenes gryllus*) determined *in situ* by time-lapse photography. Deep-Sea Research 32: 443-450

Hessler RR, Sanders HL (1967) Faunal diversity in the deep-sea. Deep-Sea Research 14: 65-78

Kahru M, Mitchell BG (2002a) Influence of the El Niño-La Niña cycle on satellite-derived primary production in the California Current. Geophysical Research Letters 29: 1846 doi:1810.1029/2002GL014963

Kahru M, Mitchell BG (2002b) Seasonal and nonseasonal variability of satellite-derived chlorophyll and colored dissolved organic matter concentration in the California Current. Journal of Geophysical Research 106: 2517-2529

Kaufmann RS, Smith KL, Jr. (1997) Activity patterns of mobile epibenthic megafauna at an abyssal site in the eastern North Pacific: results from a 17-month time-lapse photographic study. Deep-Sea Research I 44: 559-579

Kemp KM, Jamieson AJ, Bagley PM, McGrath H, Bailey DM, Collins MA, Priede IG (2006) Consumption of large bathyal food fall, a six month study in the NE Atlantic. Marine Ecology Progress Series 310: 65-76

Kiørboe T (2001) Formation and fate of marine snow: small-scale processes with large-scale implications. Scientia Marina 65: 57-71

Kiørboe T, Thygesen UH (2001) Fluid motion and solute distribution around sinking aggregates. II. Implications for remote detection by colonizing zooplankters. Marine Ecology Progress Series 211: 15-25

Lampitt RS (1992) The contribution of deep-sea macroplankton to organic remineralization: results from sediment trap and zooplankton studies over the Madeira Abyssal Plain. Deep-Sea Research 39: 221-233

Lavaniegos BE, Ohman MD (2003) Long-term changes in pelagic tunicates of the California Current`. Deep-Sea Research II 50: 2473-2498

Lee C, Murray DW, Barber RT, Buesseler KO, Dymond J, Hedges JI, Honjo S, Manganini SJ, Marra J, Moser C, Peterson ML, Prell WL, Wakeham SG (1998) Particulate organic carbon fluxes: compilation of results from the 1995 US JGOFS Arabian Sea Process Study. Deep-Sea Research II 45: 2489-2501

Lemche H, Hansen B, Madsen FJ, Tendal OS, Wolff T (1976) Hadal life as analysed from photographs. Vidensk. Meddr dansknaturh. Foren. 139: 263-336

Marinov I, Gnanadesikan A, Toggweiler JR, Sarmiento JL (2006) The Southern Ocean biogeochemical divide. Nature 441: 964-967

Martell KA, Tunnicliffe V, MacDonald IR (2002) Biological features of a buccinid whelk (Gastropoda, Neogastropoda) at the Endeavour ventfields of Juan de Fuca Ridge, Northeast Pacific. J. Moll. Stud. 68: 45-53

Martin JH, Knauer GA, Karl DM, Broenkow WW (1987) VERTEX: carbon cycling in the northeast Pacific. Deep-Sea Research 34: 267-285

Menzies RJ, George RY, Rowe GT (1973) Abyssal Environment and Ecology of the World Oceans. Wiley-Interscience, New York

Meysman FJR, Middelburg JJ, Heip CHR (2006) Bioturbation: a fresh look at Darwin's last idea. Trends in Ecology & Evolution 21: 688-695

Miller RJ, Smith CR, DeMaster DJ, Fornes WL (2000) Feeding selectivity and rapid particle processing by deep-sea megafaunal deposit feeders: A ^{234}Th tracer approach. Journal of Marine Research 58: 653-673

Mironov AN (1973) New deep-sea echinoid species of the genus *Echinocrepis* and distribution patterns of the family Pourtalesiidae (Echinoidea, Meridosternina). Transactions of the P.P. Shirshov Institute of Oceanology 91: 239-247

Mironov AN (1975) Mode of life of the pourtalesiid sea-urchins (Echinoidea: Pourtalesiidae). Transactions of the P.P. Shirshov Institute of Oceanology 103: 281-288

Mironov AN (2008) Pourtalesiid sea urchins (Echinodermata: Echinoidea) of the northern Mid-Atlantic Ridge. Marine Biology Research 4: 3-24

Mooi R, David B (1996) Phylogenetic analysis of extreme morphologies: deep-sea holoasteroid echinoids. Journal of Natural History 30: 913-953

Mortensen T (1950) A monograph of the Echinoidea, Spatangoida, Vol. 5, Part 1. Reitzel, Copenhagen

Paul AZ, Thorndike EM, Sullivan LG, Heezen BC, Gerard RD (1978) Observations of the deep-sea floor from 202 days of time-lapse photography. Nature 272: 812-814

Ramsay K, Kaiser MJ, Moore PG, Hughes RN (1997) Consumption of fisheries discards by benthic scavengers: utilization of energy subsidies in different marine habitats. Journal of Animal Ecology 66: 884-896

Reimers CE, Jahnke RA, McCorkle DC (1992) Carbon fluxes and burial rates over the continental slope and rise off central California with implications for the global carbon cycle. Global Biogeochemical Cycles 6: 199-224

Ruhl HA (2007) Abundance and size distribution dynamics of abyssal epibenthic megafauna in the northeast Pacific. Ecology 88: 1250-1262

Ruhl HA (2008) Community change in the variable resource habitat of the abyssal northeast Pacific. Ecology 89: 991-1000

Ruhl HA, Smith KL, Jr. (2004) Shifts in deep-sea community structure linked to climate and food supply. Science 305: 513-515

Sarmiento JL, Siegenthaler U (1992) New production and the global carbon cycle. In: Falkowski PG, Woodhead AD (eds) Primary Production and Biogeochemical Cycles in the Sea. Plenum Press, New York, pp 317-332

Saucede T, Mooi R, David B (2004) Evolution to the extreme: origins of the highly modified apical system in pourtalesiid echinoids. Zoological Journal of the Linnean Society 140: 137-155

Smallwood BJ, Wolff GA, Bett BJ, Smith CR, Hoover D, Gage JD, Patience A (1999) Megafauna can control the quality of organic matter in marine sediments. Naturwissenschaften 86: 320-324

Smith AB (2004) Phylogeny and systematics of holasteroid echinoids and their migration into the deep-sea. Paleontology 47: 123-150

Smith CR, Berelson W, DeMaster DJ, Dobbs FC, Hammond D, Hoover DJ, Pope RH, Stephens M (1997) Latitudinal variations in benthic processes in the abyssal equatorial Pacific: control by biogenic particle flux. Deep-Sea Research II 44: 2295-2317

Smith KL, Jr., Baldwin RJ, Ruhl HA, Kahru M, Mitchell BG, Kaufmann RS (2006) Climate effect on food supply to depths greater than 4,000 meters in the northeast Pacific. Limnology and Oceanography 51: 166-176

Smith KL, Jr., Kaufmann RS (1999) Long-term discrepancy between food supply and demand in the deep eastern North Pacific. Science 284: 1174-1177

Smith KL, Jr., Kaufmann RS, Baldwin RJ, Carlucci AF (2001) Pelagic-benthic coupling in the abyssal eastern North Pacific: An 8-year time-series study of food supply and demand. Limnology and Oceanography 46: 543-556

Smith KL, Jr., Kaufmann RS, Wakefield WW (1993) Mobile megafaunal activity monitored with a time-lapse camera in the abyssal North Pacific. Deep-Sea Research I 40: 2307-2324

Smith KL, Kaufmann RS, Baldwin RJ (1994) Coupling of near-bottom pelagic and benthic processes at abyssal depths in the Eastern North Pacific-Ocean. Limnology and Oceanography 39: 1101-1118

Solan M, Cardinale BJ, Downing AL, Engelhardt KAM, Ruesink JL, Srivastava DS (2004) Extinction and ecosystem function in the marine benthos. Science 306: 1177-1180

Solan M, Kennedy R (2002) Observation and quantification of *in situ* animal-sediment relations using time-lapse sediment profile imagery (t-SPI). Marine Ecology Progress Series 228: 179-191

Stemmann L, Jackson GA, Ianson D (2004) A vertical model of particle size distributions and fluxes in the midwater column that includes biological and physical processes—Part I: model formulation. Deep-Sea Research I 51: 865-884

Thorndike EM, Gerard RD, Sullivan LG, Paul AZ (1982) Long-term, time-lapse photography of the deep ocean floor. In: Scrutton RA, Talwani M (eds) The Ocean Floor. John Wiley & Sons, Ltd., New York, pp 255-275

Thunell RC, Moore WS, Dymond J, Pilskaln CH (1994) Elemental and isotopic fluxes in the Southern California Bight: a time-series sediment trap study in the San Pedro Basin. Journal of Geophysical Research 99: 875-889

Thunell RC, Varela R, Llano M, Collister J, Muller-Karger F, Bohrer R (2000) Organic carbon fluxes, degradation, and accumulation in an anoxic basin: sediment trap results from the Cariaco Basin. Limnology and Oceanography 45: 300-308

Tunnicliffe V, Garrett JF, Johnson HP (1990) Physical and biological factors affecting the behavior and mortality of hydrothermal vent tubeworms (Vestimentiferans). Deep-Sea Research Part a-Oceanographic Research Papers 37: 103-125

Vardaro MF, Parmley D, Smith KL, Jr. (2007) A study of possible "reef effects" caused by a long-term time-lapse camera in the deep North Pacific. Deep-Sea Research I 54: 1231-1240

II

**A Study of Possible ''Reef Effects'' Caused by a Long-Term
Time-Lapse Camera in the Deep North Pacific**

ELSEVIER

A study of possible "reef effects" caused by a long-term time-lapse camera in the deep North Pacific

M.F. Vardaro[a,c,*], D. Parmley[b], K.L. Smith Jr.[c]

[a] Scripps Institution of Oceanography, University of California at San Diego, 9500 Gilman Drive, La Jolla, CA 92093-0208, USA
[b] Torrey Pines Institute for Molecular Studies, 3550 General Atomics Court 2-129, San Diego, CA 92121-1122, USA
[c] Monterey Bay Aquarium Research Institute, 7700 Sandholdt Road, Moss Landing, CA 95039-9644, USA

Abstract

The aggregation response of fish populations following the addition of artificial structures to seafloor habitats has been well documented in shallow-water reefs and at deeper structures such as oil extraction platforms. A long-term time-lapse camera was deployed for 27 four-month deployment periods at 4100 m in the eastern North Pacific to study abyssal megafauna activity and surface–benthos connections. The unique time-series data set provided by this research presented an opportunity to examine how deep-sea benthopelagic fish and epibenthic megafauna populations were affected by an isolated artificial structure and whether animal surveys at this site were biased by aggregation behavior. Counts were taken of benthopelagic grenadiers, *Coryphaenoides* spp., observed per week as well as numbers of the epibenthic echinoid *Echinocrepis rostrata*. No significant correlation ($r_s = -0.39$; $p = 0.11$) was found between the duration of deployment (in weeks) and the average number of *Coryphaenoides* observed at the site. There was also no evidence of associative behavior around the time-lapse camera by *E. rostrata* ($r_s = -0.32$; $p = 0.19$). The results of our study suggest that abyssal fish and epibenthic megafauna do not aggregate around artificial structures and that long-term time-lapse camera studies should not be impacted by aggregation response behaviors.
© 2007 Elsevier Ltd. All rights reserved.

Keywords: Underwater photography; Ocean floor; Long-term time-lapse; Aggregation; Grenadier fish; Megafauna; USA; California; NE Pacific

1. Introduction

Associative behavior is the aggregation of different species at a single structure or topographic area not driven solely by the incentive of prey species or

*Corresponding author. Monterey Bay Aquarium Research Institute, 7700 Sandholdt Road, Moss Landing, CA 95039-9644, USA. Tel.: +1 831 775 1839; fax: +1 831 775 1736.
E-mail addresses: mvardaro@mbari.org (M.F. Vardaro), ksmith@mbari.org (D. Parmley), dparms@gmail.com (K.L. Smith Jr.).

small-scale habitat requirements (Fréon and Dagorn, 2000). Such behavior has been observed in many pelagic fish species, most notably tuna (Fréon and Dagorn, 2000; Parin and Fedoryako, 1999; Uda, 1933). The attraction of assemblages to natural or artificial structures has not been completely explained, although many competing hypotheses have been proposed. For example, structures and topographic highs could serve as shelter from predators (Soemarto, 1960), a means for predators to concentrate smaller prey species

(Kojima, 1956), a spatial reference point to aid navigation in the open ocean (Klima and Wickham, 1971), or a meeting point for members of the same species to associate and form larger schools (Dagorn and Fréon, 1999). The practical implication of the "reef effect" is a localized increase in the density and activity of fish and invertebrate species, potentially leading to inflated counts of local population size during censuses.

Shallow-water platforms and artificial reefs can be colonized by invertebrates and fish within days (Golani and Diamant, 1999). Longer-term observations show that colonization rates gradually increase over periods of months, finally leveling off at a stable population at around 6–8 months, although densities and species compositions can vary over yearly time scales (Relini et al., 2002). Artificial reefs also appear to be sites of increased reproductive success, rather than simply concentrating the surrounding populations around a single structure (Stephens and Pondella, 2002). Deep-sea colonization rates by invertebrates are much lower (Beaulieu, 2001; Grassle, 1977; Smith and Hessler, 1987) and populations are more diffuse (Rex, 1981), making long time-series measurements vital to the study of deep ocean habitats. The unique properties of deep-water environments (lack of downwelling light, low population densities, reduced food supply, etc.) allow testing of the various rationales for aggregation behavior by removing many of the variables that have been used to explain associative behavior in shallow-water environments.

Fifteen years of hourly photographs taken with a time-lapse camera system were analyzed to evaluate the impact of aggregation effects on counts of fish and epibenthic invertebrates at an abyssal site in the eastern North Pacific (Station M; 34°50'N, 123°00'W; 4100 m depth). The camera system was deployed at 4100 m for 4-month periods almost continually since 1989, providing a long time-series record of biological activity on and near the seafloor. We hypothesized that the numbers of mobile animals observed by the time-lapse camera would increase significantly over the deployment period. Here we examine the observations and the possible effects of the camera system on the animal populations at the site over intervals of weeks to months.

2. Materials and methods

The time-lapse camera system (Fig. 1) was first deployed at Station M in 1989 (Smith et al., 1993),

and has since collected 27 time-lapse image data sets of approximately 4 months each. Station M lies in the eastern North Pacific and is subject to strong seasonal pulses of surface productivity (Smith et al., 1992). The seafloor at 4100 m has very little topographic relief (<100 m over $1600 km^2$) and is composed of silty-clay sediment with seasonal deposits of flocculent phytodetritus. Currents near the seafloor average $3.8 cm s^{-1}$, can reach a maximum of $18.2 cm s^{-1}$ and flow to the south during periods of highest current speeds and towards the north and west during the periods of low current speeds (Beaulieu and Baldwin, 1998). Time-lapse photography has revealed abundant evidence of bioturbation and other epifaunal activity at the site in the form of numerous trails, furrows and mounds that can be centimeters to meters across (Smith et al., 1993). No organisms or features taller than glass sponge stalks, $\sim 10–20 cm$ in height (Beaulieu, 2001), were observed during any time-lapse deployment.

The camera took one still photograph of the seafloor every hour and the film was recovered and the equipment redeployed during maintenance cruises three times a year. The time-lapse camera consists of a Benthos 377 camera mounted on a titanium frame at an angle of 31° from horizontal with the lens ~ 2 m above the seafloor. The camera is equipped with a 28-mm Nikonos lens, providing angular coverage of 50° in the horizontal and 35° in the vertical plane, and holds 400 ft of 35-mm color-negative film (Fuji, Type 8514, 500 ASA). Up to 3500 images can be collected in 4.6 months. Two 400-W-s strobes, one mounted on either side of the camera housing, illuminate approximately $20 m^2$ of the seafloor beginning at a distance of 1.8 m from the camera frame and extending approximately 6.5 m from the base of the camera frame (see Smith et al. 1993 for a more complete description of the time-lapse camera). The entire camera frame was examined after each recovery to identify any encrusting animals and remove any other biofouling. However, the time-lapse camera system returned to the surface after a 4-month deployment with no visible encrusting growths or attached organisms.

The oblique photographs taken by the time-lapse camera (Fig. 2) were analyzed using a perspective-grid method (Wakefield and Genin, 1987; Wolf, 1983). Each image was projected onto a flat surface and digitized with a Science Accessories Corp.[®] electronic digitizer interfaced with a computer. Fish and the echinoid *Echinocrepis* that appeared in the

\
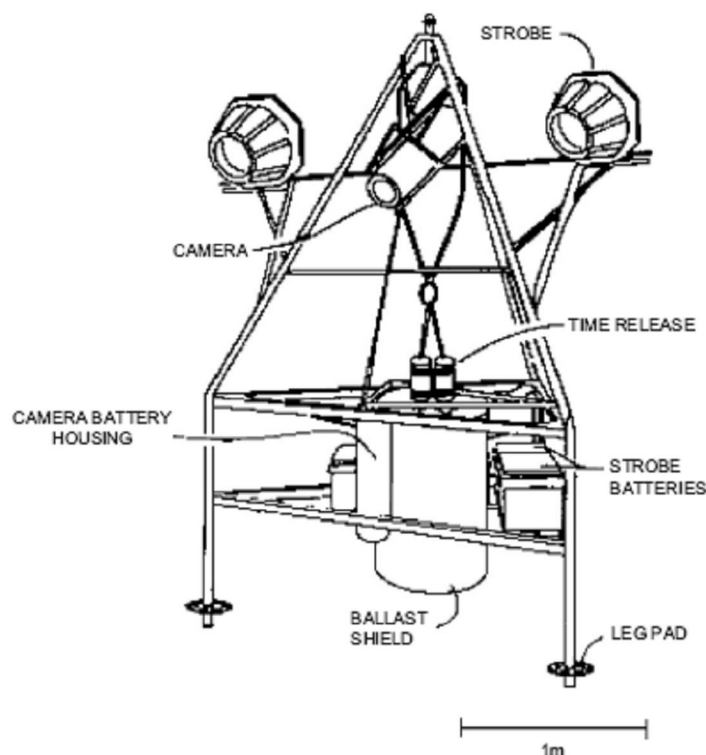
Fig. 1. The time-lapse camera deployed at Station M (adapted from Smith et al., 1993).

time-lapse record were tentatively identified based on appearance, apparent behavior and species geographic range. The presence and relative orientation (swimming or on the seafloor) of individual fish and echinoids observed in the photographic record were digitally recorded and entered into a spreadsheet. Each appearance of an animal in the time-lapse record was counted separately, as there was no practical way to distinguish individuals that may have appeared in multiple frames.

Statistical analyses of the data were performed to determine if there was a positive correlation between the numbers of fish seen at the deployment site and the number of weeks the time-lapse camera was on the seafloor. A weekly time interval was chosen to maximize the number of animals included while retaining sufficient resolution to see changes over time. The numbers of fish seen during each week (168 frames) of the camera deployment were summed, and these weekly sums were then averaged for the entire time series to provide a mean number of animals observed during each week of deployment time. A non-parametric Spearman correlation was run on the summed weekly data from each 4-month deployment. A separate Spearman correlation was run on the combined average weekly data from all of the camera deployments. The same tests were then run on the numbers of echinoids seen over the time-lapse camera deployment period.

3. Results

A total of 1406 fishes and 178 *Echinocrepis* echinoids were observed during the entire time-lapse record, which was composed of 27, 4-month deployments over 15 years (Table 1). The most abundant fish species on and near the seafloor were grenadier fish ($n = 1337$), either *Coryphaenoides*

Fig. 2. A single frame from the long time-series photographic record collected at Station M using a time-lapse camera. A fish (*Coryphaenoides* spp.) can be seen in the right foreground; also visible are epibenthic fauna including several hexactinellid sponge "stalks" which extend from the sediment surface. The viewing area is approximately $20 \, \text{m}^2$.

armatus or *Coryphaenoides yaquinae*. These species are indistinguishable in photographic images (D. Bailey, personal communication), and both are common scavenging predators in the deep North Pacific (Priede et al., 1990). Other fishes observed included *Bathysaurus* sp. ($n = 61$; probably *B. mollis*, based on the depth and North Pacific location of the deployment site) and an unidentified species, most likely an Alepocephalid, *Conocara salmoneum* or *Alepocephalus tenobrosus* (J. Drazen, personal communication). Because 95.1% of the individuals observed in the time-lapse record were *Coryphaenoides* species, only *Coryphaenoides* were included in the statistical analysis. Roughly seven times as many *Coryphaenoides* individuals were photographed while swimming ($n = 1176$) than while foraging on the seafloor ($n = 161$), which was inferred from the distinctive head-down tilted posture (Sakurai and Kido, 1992) and possible contact with the sediment surface (Fig. 3). No direct feeding activity was observed.

Only one of the individual deployments, Station 2411 (Table 1), showed a significant correlation between deployment time and the number of *Coryphaenoides* observed ($r_s = -0.57$; $p < 0.05$). None of the data from the other individual deployment periods exhibited significant correlations, either positive or negative. No significant correlation was found between the duration of the time-lapse camera deployment (in weeks) and the number of *Coryphaenoides* per week during all 27 deployments ($r_s = -0.06$; $p = 0.25$) or the combined average number per week ($r_s = -0.39$; $p = 0.11$) observed at the site (Fig. 4a).

A conspicuous mobile epibenthic megafaunal species at Station M, the echinoid *Echinocrepis rostrata*, also did not show evidence of associative behavior around structures. Weekly totals of the number of individual *E. rostrata* observed were obtained in a manner similar to the fish data. Only two of the individual deployments, Stations 612 ($r_s = -0.54$; $p = 0.05$) and 2022 ($r_s = 0.62$;

Table 1
Time-lapse camera deployments and correlations between weekly fish numbers (*Coryphaenoides* spp.) and Echinoid numbers (*Echinocrepis rostrata*) over the deployment period

Station	No. of frames	Deploy date (MM/DD/YY)	Recovery date (MM/DD/YY)	Days deployed	Fish observed	Fish Spearman correlation	E. rostrata observed	E. rostrata Spearman correlation
223	2773	10/29/1989	02/22/1990	116	63	$r_s = 0.15; p = 0.59$	3	$r_s = -0.05; p = 0.84$
323	2999	02/23/1990	06/28/1990	125	35	$r_s = -0.10; p = 0.70$	4	$r_s = 0.17; p = 0.51$
448	2801	06/29/1990	10/24/1990	117	72	$r_s = -0.43; p = 0.10$	4	$r_s = -0.19; p = 0.49$
612	2927	02/22/1991	06/22/1991	122	43	$r_s = 0.20; p = 0.50$	3	$r_s = -0.54; p = 0.05^a$
715	718	06/23/1991	07/23/1991	30	16	$r_s = 0.32; p = 0.68$	0	N/A
1616	3422	02/22/1993	07/15/1993	143	43	$r_s = 0.30; p = 0.22$	5	$r_s = 0.18; p = 0.48$
1707	2664	07/17/1993	11/05/1993	111	42	$r_s = -0.02; p = 0.96$	7	$r_s = -0.38; p = 0.16$
2022	3085	06/18/1994	10/25/1994	129	52	$r_s = -0.06; p = 0.81$	5	$r_s = 0.62; p = 0.01^a$
2311	2760	10/26/1994	02/18/1995	115	61	$r_s = -0.42; p = 0.09$	10	$r_s = -0.01; p = 0.98$
2411	2533	02/18/1995	06/04/1995	106	51	$r_s = -0.57; p = 0.02^a$	6	$r_s = 0.02; p = 0.95$
2612	2533	06/04/1995	11/18/1995	106	65	$r_s = 0.29; p = 0.24$	6	$r_s = 0.28; p = 0.24$
2718	1789	11/18/1995	02/01/1996	75	23	$r_s = 0.21; p = 0.53$	6	$r_s = 0.36; p = 0.28$
2918	2922	02/01/1996	06/03/1996	122	56	$r_s = 0.21; p = 0.41$	2	$r_s = -0.19; p = 0.47$
3027	3086	06/03/1996	10/10/1996	129	66	$r_s = -0.28; p = 0.27$	4	$r_s = -0.41; p = 0.12$
3301	3934	11/11/1996	04/24/1997	164	51	$r_s = -0.24; p = 0.34$	4	$r_s = 0.33; p = 0.17$
3408	2972	04/24/1998	08/31/1998	124	70	$r_s = 0.12; p = 0.65$	4	$r_s = -0.44; p = 0.07$
3510	2629	08/31/1998	12/19/1998	110	43	$r_s = -0.20; p = 0.46$	13	$r_s = 0.01; p = 0.97$
3708	3143	06/16/2001	10/25/2001	131	41	$r_s = 0.17; p = 0.49$	0	N/A
3822	2850	10/26/2001	02/23/2002	119	42	$r_s = 0.25; p = 0.34$	7	$r_s = 0.09; p = 0.74$
3909	2532	02/24/2002	06/10/2002	106	44	$r_s = 0.02; p = 0.95$	6	$r_s = -0.42; p = 0.12$
4010	2012	06/11/2002	09/09/2002	84	49	$r_s = -0.51; p = 0.08$	0	N/A
4211	3141	10/12/2003	02/26/2004	131	68	$r_s = 0.46; p = 0.06$	22	$r_s = 0.17; p = 0.48$
4302	2444	02/27/2004	07/30/2004	102	46	$r_s = -0.20; p = 0.47$	1	$r_s = -0.43; p = 0.11$
4407	2107	08/01/2004	10/27/2004	88	47	$r_s = -0.14; p = 0.65$	10	$r_s = 0.41; p = 0.16$
4512	2856	10/29/2004	02/23/2005	119	66	$r_s = -0.18; p = 0.48$	12	$r_s = 0.29; p = 0.26$
4609	2729	02/24/2005	06/14/2005	114	37	$r_s = 0.08; p = 0.76$	16	$r_s = -0.34; p = 0.20$
4806	3108	11/14/2005	8/15/2006	130	57	$r_s = 0.24; p = 0.34$	18	$r_s = -0.18; p = 0.47$

[a]Results in bold denote a significant correlation.

$p = 0.01$), exhibited significant correlations between deployment time and the weekly number of *Echinocrepis* echinoids observed. A separate Spearman test of the data from all 27 deployments showed no correlation between the duration of deployment and the total number of animals observed per week ($r_s = -0.02$; $p = 0.67$). The weekly numbers were then averaged together to find the mean number of animals seen per week post-deployment (Fig. 4b). No positive correlation between the duration of deployment of the time-lapse camera and the average weekly number of *E. rostrata* echinoids observed over that period was found ($r_s = -0.32$; $p = 0.19$).

4. Discussion

The results indicate no aggregations of *Coryphaenoides* spp. or *E. rostrata* within the 20 m² field-of-view of the time-lapse camera system at Station M. The absence of any sustained aggregation could be explained by the reduced numbers of megafauna at abyssal depths, the open structure of the camera frame, the length of deployment, or deep-sea animal behavior. The low density of prey and food falls on the abyssal plain (Rex, 1981; Smith and Baco, 2003) requires most active predators to move constantly, possibly negating sustained aggregation behavior around structures (Armstrong et al., 1992; Childress, 1995; Collins et al., 1998; Priede et al., 1994). Some studies have found evidence of schooling in deep-sea fish, but nearly all of these aggregations occurred on seamounts, deep-sea coral reefs or in association with spawning behavior, and all were in waters shallower than 4100 m (Drazen et al., 2003; Gunn et al., 1989; Husebø et al., 2002; Krieger and Wing, 2002; Pankhurst, 1988; Rogers, 1994). Seamounts, reefs and large rock outcroppings are theorized to attract fish aggregations for a number of reasons. Currents concentrate plankton, particulate organic matter and other food sources around these structures, the hard substrate provides a surface

M.F. Vardaro et al. / Deep-Sea Research I 54 (2007) 1231–1240

a

b
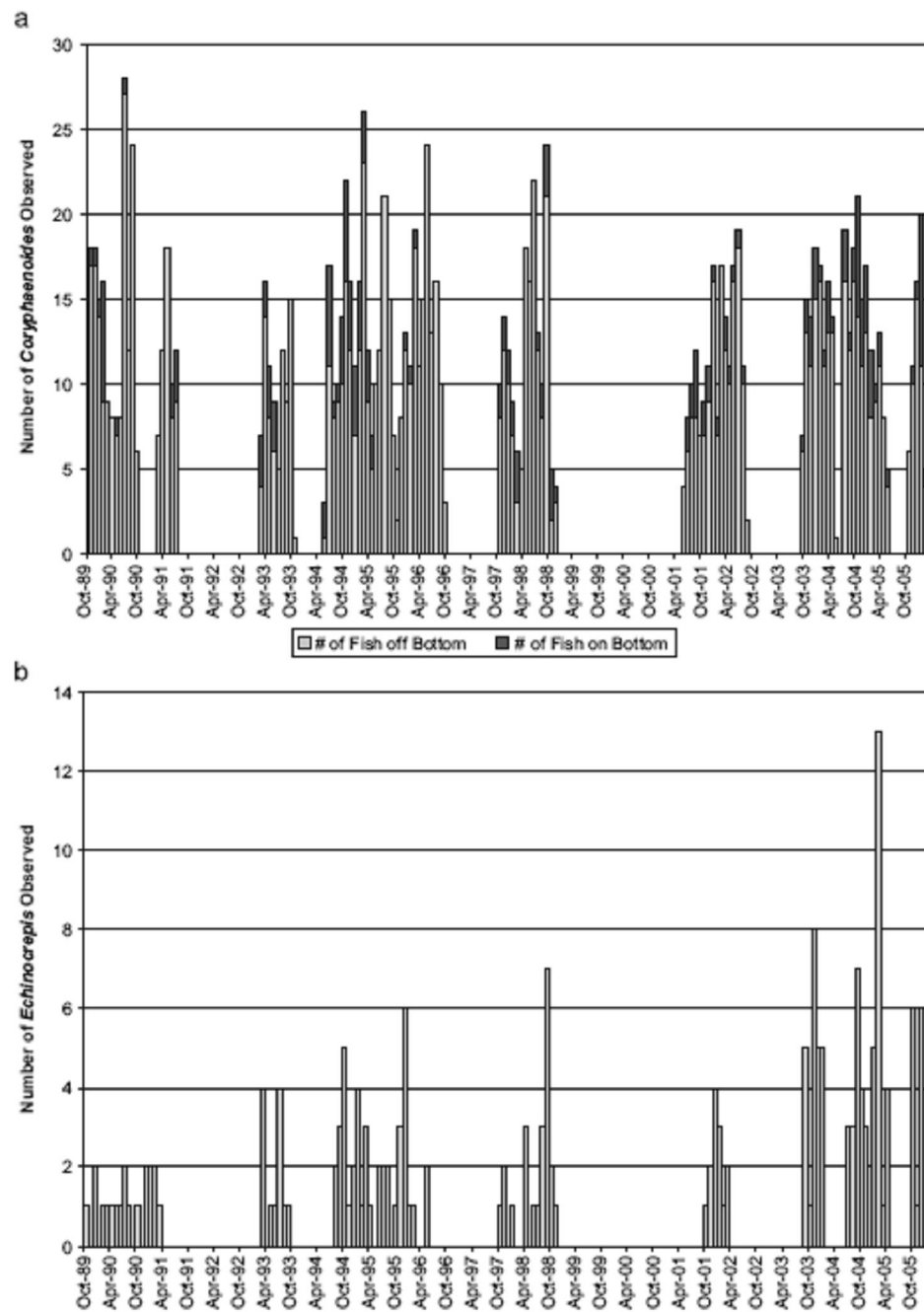
Fig. 3. Chart of monthly abundance of *Coryphænoides* fish (a) and *Echinocrepis* echinoids (b) at Station M over the 15-year seasonal deployment period, with periodic gaps due to equipment failure or ship unavailability.

\
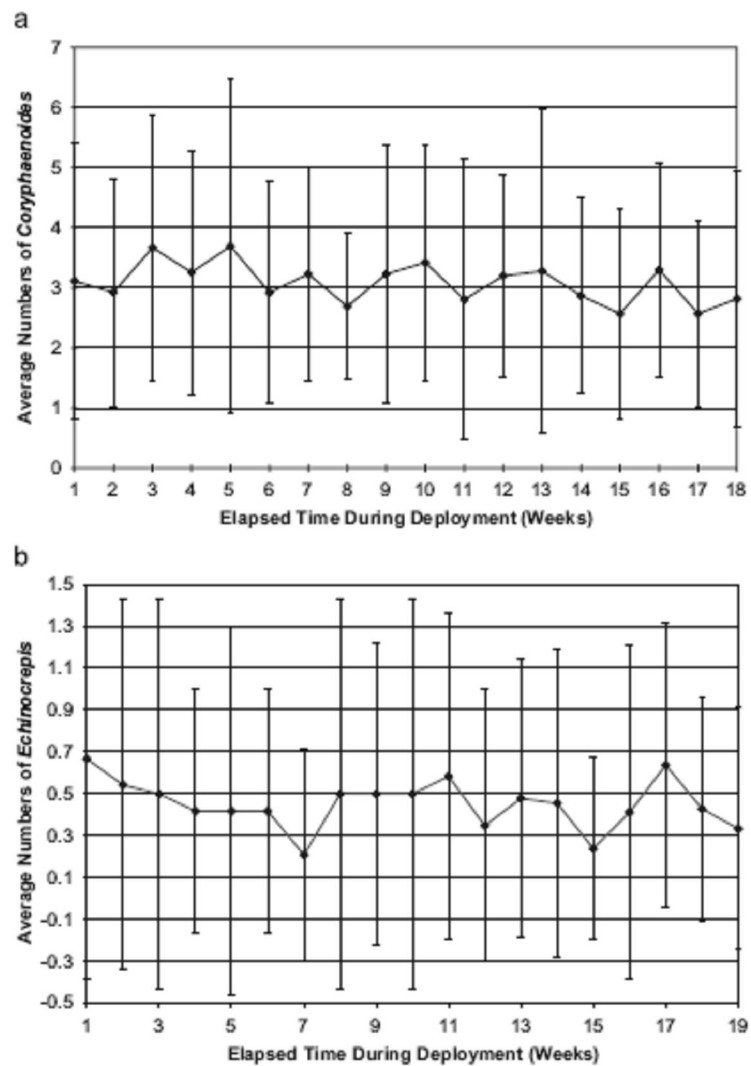
Fig. 4. Average *Coryphaenoides* fish (a) and *Echinocrepis* echinoid (b) abundance at Station M over the deployment period of the time-lapse camera system. The number of animals seen in the photo images was averaged over every week after the camera was deployed for all 27 deployments. No positive correlation was found between deployment time and numbers of near-seafloor *Coryphaenoides* ($r_s = -0.37$; $p = 0.14$) or *Echinocrepis* ($r_s = -0.32$; $p = 0.19$). Error bars indicate the standard deviation.

for egg attachment or for colonization by epifaunal invertebrates that could serve as potential prey and the complex surfaces of seamounts and coral reefs can serve as shelter from predators. Conversely, fish and echinoids inhabiting the abyssal plain may not possess any instinctual need for shelter, and the relatively open structure of the time-lapse camera reduces its potential attractiveness as an attachment point for eggs or epifaunal invertebrates. While currents at Station M are usually weak compared to currents in slope and seamount habitats, they have been recorded at speeds of nearly $20 \, \text{cm s}^{-1}$ (Beaulieu and Baldwin, 1998), which is strong enough to cause significant turbulence around a solid object on the seafloor and lift particulate matter into the water column. However, the open

structure of the camera frame provides little resistance to bottom currents, resulting in less trapping of particulate matter.

The lack of epifauna attached to the time-lapse camera frame following a deployment suggests that it does not provide habitat for potential prey animals such as bivalves, crustaceans and other organisms often observed attached to shallower water systems. Such faunal assemblages would supply substrate and a food source sufficient to support larger animals that could eventually result in the attraction of bathypelagic predatory fish. The enrichment of the seafloor by fecal pellets and other detritus secondary to colonization of the frame might then attract deposit-feeding epibenthic megafauna. However, the 4-month deployment time of the time-lapse camera could be insufficient to allow the settlement and growth of attached species. There may be a longer time lag between the deployment of a deep-sea structure, subsequent colonization by epifaunal invertebrates and ensuing aggregation than was observed during these experiments. Shallow-water artificial reefs and other structures can have a noticeable effect on the local community within a period of 1 week (Davis et al., 1982), but deep-sea structures do not appear to attract concentrations of encrusting fauna at speeds or in numbers comparable to hard surfaces located in shallower waters (Beaulieu, 2001; Grassle, 1977; Smith and Hessler, 1987). Surveys of shipwrecks in deep water (Husebø et al., 2002) and of drums of radioactive waste that were sunk in 914–1829 m of water off the Farallon Islands in the 1970s (Columbo and Kendig, 1990; Schell and Sugai, 1980) indicate that deep-sea structures do eventually support elevated local fish and invertebrate populations. Much longer deployments of deep-sea equipment platforms might provide adequate time for the attachment and development of abyssal sessile species.

Mobile epibenthic megafauna represent another potential food source that could attract predatory fish to seafloor structures. Abyssal megafaunal animals such as the echinoid *Echinocrepis* are known to occur in distributions ranging from near-random to patchy across the eastern North Pacific seafloor (Lauerman and Kaufmann, 1998; Lauerman et al., 1996). Large breeding aggregations of echinoids and holothurians have been observed in the deep-sea in several locations worldwide (Billett and Hansen, 1982; Young et al., 1992). However, these distribution patterns appear to be related to the arrival of sinking detrital aggregates and other food sources rather than the presence of natural or artificial structures on the seafloor. Although aggregations of mobile benthic megafauna are often seen in the vicinity of shallow-water artificial reefs (Fabi et al., 2002) and seamounts (Probert et al., 1997), the time-lapse camera data from Station M have provided no evidence of aggregation around structures at abyssal depths. If hard substrate suitable for attachment or shelter is a limiting resource in the deep sea (Drazen et al., 2003; Voight and Grehan, 2000), rapid colonization and aggregation around artificial structures such as the time-lapse camera would be expected. Again, the deployment period of the time-lapse camera system may be insufficient to allow for local increases in the numbers of mobile epibenthic megafauna.

Some studies suggest that deep-sea fish such as *Coryphaenoides* do exhibit schooling behavior near the seafloor on the edge of the continental shelf, at depths greater than 1000 m (Nero et al., 1997), which may act to confuse the sensory field of a potential predator or to utilize the combined search ability of the entire school to find prey (Auster et al., 1992). However, the utility of fixed structures as shelter from predators (Soemarto, 1960) appears to be reduced in the abyss because of the low population density and rare occurrence of large predators (Rex, 1981). Although bioluminescence triggered by contact with a structure could provide a point of reference for organisms able to detect light, the adaptive advantages of using structures as navigational tools or meeting points (Klima and Wickham, 1971) may be obviated by the lack of downwelling light and relatively featureless mud bottom at Station M. The absence of sunlight also removes the need for shade (Damant, 1921; Helfman, 1981), which is another possible cause of shallow-water aggregation around structures. The ability of an individual to locate a potential mate may be enhanced by aggregation behavior around objects in shallow-water or open-ocean environments (Dagorn and Fréon, 1999). However, the possible increased mating success conferred by a stationary aggregation is likely outweighed in the deep sea by the corresponding decrease in time that could be devoted to food finding behavior. The importance of constant motion is supported by the fact that seven times as many *Coryphaenoides* were photographed while swimming than while foraging in contact with the seafloor.

The time-lapse camera is fixed at an oblique angle that views an area approximately 1.8 m from the base of the camera frame, so no information is gathered on the faunal populations within the structure or outside of the camera's field of view. Nevertheless, any localized aggregations of animals around the camera frame should be reflected in an increase in activity within the field of view of the camera as well. Grenadiers, for example, tend to swim actively while remaining relatively close to the seafloor (Priede et al., 1990). Although the study took place at one site in a limited area of the North Pacific, the results may be representative of similar water depths with comparable fish and epifaunal populations. For example, a 6-month baited time-lapse camera deployment in the NE Atlantic at a depth of 2710 m drew large aggregations of *C. armatus* over the first 15 days, which rapidly diminished to less than three individuals per frame and then to single, infrequently seen, individuals by 45 days (Kemp et al., 2006). This experiment became an unbaited camera platform for several months in the deep Atlantic and the downward-looking camera recorded no fish aggregation in and around the frame, despite the residual presence of the bait carcass and a small population of scavenging crustaceans.

The apparent lack of aggregation behavior around the time-lapse camera in the deep North Pacific has significant implications for the study of abyssal populations. Many pelagic and shallow-water fish and invertebrate species congregate around natural and artificial structures, and deep-sea predatory species have been observed to briefly gather around baited camera platforms (Kemp et al., 2006; Priede et al., 1991, 2002). However, it appears that artificial structures alone do not cause significant associative behavior in abyssal fish or detritus-feeding echinoids around the time-lapse camera. Although more study is warranted on the effects of deployments longer than 4 months, long-term time-lapse photography remains a useful tool in studying the "undisturbed" ecology of the abyssal plain.

Acknowledgments

References

Armstrong, J.D., Bagley, P., Priede, I.G., 1992. Photographic and acoustic tracking observations of the behaviour of the grenadier *Coryphaenoides* (*Nematonurus*) *armatus*, the eel *Synaphobranchus bathybius*, and other abyssal demersal fish in the North Atlantic Ocean. Marine Biology 112, 535–544.

Auster, P.J., Griswold, C.A., Youngbluth, M.J., Bailey, G., 1992. Aggregations of myctophid fishes with other pelagic fauna. Environmental Biology of Fishes 39, 133–139.

Beaulieu, S.E., 2001. Colonization of habitat islands in the deep sea: recruitment to glass sponge stalks. Deep-Sea Research I 48, 1121–1137.

Beaulieu, S., Baldwin, R., 1998. Temporal variability in currents and the benthic boundary layer at an abyssal station off central California. Deep-Sea Research II 45, 587–615.

Billett, D.S.M., Hansen, B., 1982. Abyssal aggregations of *Kolga hyalina* Danielssen and Koren (Echinodermata: Holothurioidea) in the Northeast Atlantic Ocean: a preliminary report. Deep-Sea Research 29 (7a), 799–818.

Childress, J.J., 1995. Are there physiological and biochemical adaptations of metabolism in deep-sea animals? Trends in Ecology and Evolution 10 (1), 30–36.

Collins, M.A., Priede, I.G., Addison, S., Smith, A., Bagley, P.M., 1998. Acoustic tracking of the dispersal of organic matter by scavenging fishes in the deep-sea. Hydrobiologia 371/372, 181–186.

Columbo, P., Kendig, M.W., 1990. Analysis and evaluation of a radioactive waste package retrieved from the Farallon Islands 900-meter disposal site. Department of Nuclear Energy, Brookhaven National Laboratory, Upton, NY, p. 65.

Dagorn, L., Fréon, P., 1999. Tropical tuna associated with floating objects: a simulation study of the meeting point hypothesis. Canadian Journal of Fishing and Aquatic Science 56, 984–993.

Damant, G.C.C., 1921. Illumination of plankton. Nature 108, 42–43.

Davis, N., VanBlaricom, G.R., Dayton, P.K., 1982. Man-made structures on marine sediments: effects on adjacent benthic communities. Marine Biology 70, 295–303.

Drazen, J.C., Goffredi, S.K., Schlining, B., Stakes, D.S., 2003. Aggregations of egg-brooding deep-sea fish and cephalopods on the Gorda Escarpment: a reproductive hot spot. Biological Bulletin 205, 1–7.

Fabi, G., Luccarini, F., Panfili, M., Solustri, C., Spagnolo, A., 2002. Effects of an artificial reef on the surrounding soft-bottom community (central Adriatic Sea). ICES Journal of Marine Science 59, S343–S349.

Fréon, P., Dagorn, L., 2000. Review of fish associative behaviour: toward a generalisation of the meeting point hypothesis. Reviews in Fish Biology and Fisheries 10, 183–207.

Golani, D., Diamant, A., 1999. Fish colonization of an artificial reef in the Gulf of Elat, northern Red Sea. Environmental Biology of Fishes 54, 275–282.

Grassle, J.F., 1977. Slow recolonisation of deep-sea sediment. Nature 265, 618–619.

\

Gunn, J.S., Bruce, B.D., Furlani, D.M., Thresher, R.E., Blaber, S.J.M., 1989. Timing and location of spawning of blue grenadier, *Macruronus novaezelandiae* (Teleostei: Merlucciidae), in Australian coastal waters. Australian Journal of Marine and Freshwater Research 40, 97–112.

Helfman, G.S., 1981. The advantage to fishes of hovering in shade. Copeia 2, 392–400.

Husebø, Å., Nøttestad, L., Fosså, J.H., Furevik, D.M., Jørgensen, S.B., 2002. Distribution and abundance of fish in deep-sea coral habitats. Hydrobiologia 471, 91–99.

Kemp, K.M., Jamieson, A.J., Bagley, P.M., McGrath, H., Bailey, D.M., Collins, M.A., Priede, I.G., 2006. Consumption of large bathyal food fall, a six-month study in the NE Atlantic. Marine Ecology Progress Series 310, 65–76.

Klima, E.F., Wickham, D.A., 1971. Attraction of coastal pelagic fishes with artificial structures. Transactions of American Fishing Society 1, 86–99.

Kojima, S., 1956. Fishing for dolphins in the western part of the Japan Sea. II. Why do the fish take shelter under floating materials? Bulletin on Japanese Society of Scientific Fishing 21 (10), 1049–1052.

Krieger, K.J., Wing, B.L., 2002. Megafauna associations with deepwater corals (*Primnoa* spp.) in the Gulf of Alaska. Hydrobiologia 471, 83–90.

Lauerman, L.M.L., Kaufmann, R.S., 1998. Deep-sea epibenthic echinoderms and a temporally varying food supply: results from a one year time series in the NE Pacific. Deep-Sea Research II 45, 817–842.

Lauerman, L.M.L., Kaufmann, R.S., Smith Jr., K.L., 1996. Distribution and abundance of epibenthic megafauna at a long time-series station in the abyssal northeast Pacific. Deep-Sea Research I 43 (7), 107–1103.

Nero, R.W., Thompson, C.H., Love, R.H., 1997. Abyssopelagic grenadiers: the probable cause of low frequency sound scattering at great depths off the Oregon and California coasts. Deep-Sea Research I 44 (4), 627–645.

Pankhurst, N.W., 1988. Spawning dynamics of orange roughy, *Hoplostethus atlanticus*, in mid-slope waters of New Zealand. Environmental Biology of Fishes 21 (2), 101–116.

Parin, N.V., Fedoryako, B.I., 1999. Pelagic fish communities around floating objects in the open ocean. In: Scott, M.D., Bayliff, W.H., Lennert-Cody, C.E., Schaefer, K.M. (Eds.), Proceedings of the International Workshop on the Ecology and Fisheries for Tunas Associated with Floating Objects, 11–13 February 1992. Inter-American Tropical Tuna Commission Special Report 11. La Jolla, CA, pp. 447–458.

Priede, I.G., Smith Jr., K.L., Armstrong, J.D., 1990. Foraging behaviour of abyssal grenadier fish: inferences from acoustic tagging and tracking in the North Pacific Ocean. Deep-Sea Research 37, 81–101.

Priede, I.G., Bagley, P., Armstrong, J.D., Smith, K.L., Merrett, N.R., 1991. Direct measurement of active dispersal of food-falls by abyssal demersal fishes. Nature 351, 647–649.

Priede, I.G., Bagley, P.M., Smith Jr., K.L., 1994. Seasonal change in activity of abyssal demersal scavenging grenadiers *Coryphaenoides* (*Nematonurus*) *armatus* in the eastern North Pacific Ocean. Limnology and Oceanography 39 (2), 279–285.

Priede, I.G., Deary, A.R., Bailey, D.M., Smith Jr., K.L., 2002. Low activity and seasonal change in population size structure of grenadiers in the oligotrophic abyssal central North Pacific Ocean. Journal of Fish Biology 63, 187–196.

Probert, P.K., McKnight, D.G., Grove, S.L., 1997. Benthic invertebrate bycatch from a deep-water trawl fishery, Chatham Rise, New Zealand. Aquatic Conservation: Marine and Freshwater Ecosystems 7, 27–40.

Relini, G., Relini, M., Torchia, G., Palandri, G., 2002. Ten years of censuses of fish fauna on the Loano artificial reef. ICES Journal of Marine Science 59, S132–S137.

Rex, M.A., 1981. Community structure in the deep-sea benthos. Annual Reviews on Ecological System 12, 331–353.

Rogers, A.D., 1994. The biology of seamounts. Advances in Marine Biology 30, 305–350.

Sakurai, Y., Kido, K., 1992. Feeding behavior of *Careproctus rastrinus* (Liparididae) in captivity. Japanese Journal of Ichthyology 39, 110–113.

Schell, W.R., Sugai, S., 1980. Radionuclides at the US radioactive waste disposal Site near the Farallon Islands. Health Physics 39 (3), 475–496.

Smith, C.R., Baco, A.R., 2003. Ecology of whale falls at the deep-sea floor. Oceanography and Marine Biology: An Annual Review 41, 311–354.

Smith, C.R., Hessler, R.R., 1987. Colonization and succession in deep-sea ecosystems. Trends in Ecology and Evolution 2 (12), 359–363.

Smith Jr., K.L., Baldwin, R.J., Williams, P.M., 1992. Reconciling particulate organic carbon flux and sediment community oxygen consumption in the deep North Pacific. Nature 359, 313–316.

Smith Jr., K.L., Kaufmann, R.S., Wakefield, W.W., 1993. Mobile megafaunal activity monitored with a time-lapse camera in the abyssal North Pacific. Deep-Sea Research I 40 (11/12), 2307–2324.

Soemarto, 1960. Fish behaviour with special reference to pelagic schooling species: Lajang (*Decapterus* spp.). Eighth Proceedings of Indo-Pacific Fisheries Council 3, 89–93.

Stephens II, J., Pondella, D., 2002. Larval productivity of a mature artificial reef: the ichthyoplankton of King Harbor, California, 1974–1997. ICES Journal of Marine Science 59, S51–S58.

Uda, M., 1933. Types of skipjack schools and their fishing qualities. Bulletin on Japanese Society of Scientific Fishing 2 (3), 107–111.

Voight, J.R., Grehan, A.J., 2000. Egg brooding by deep-sea octopuses in the North Pacific Ocean. Biological Bulletin 198, 94–100.

Wakefield, W.W., Genin, A., 1987. The use of a Canadian (perspective) grid in deep-sea photography. Deep-Sea Research 34, 469–478.

Wolf, P.R., 1983. Elements of Photogrammetry: With Air Photo Interpretation and Remote Sensing. McGraw-Hill, New York.

Young, C.M., Tyler, P.M., Cameron, J.L., Rumrill, S.G., 1992. Seasonal breeding aggregations in low-density populations of the bathyal echinoid *Stylocidaris lineata*. Marine Biology 113, 603–612.

\

This chapter, in full, is a reprint from a May 2007 Deep-Sea Research, Part I (Vardaro MF, Parmley D, Smith KL, Jr. (2007) A study of possible "reef effects" caused by a long-term time-lapse camera in the deep North Pacific. Deep-Sea Research I 54: 1231-1240). The dissertation author was the primary investigator and the principal author of this manuscript, and permission to reprint this article here was given by both additional authors and the publisher, Elsevier.

\

III

Genetic and anatomic relationships between three morphotypes of the echinoid
Echinocrepis rostrata

Abstract

Three morphotypes of an irregular echinoid, genus *Echinocrepis,* are commonly observed in the deep North Pacific Ocean by remote time-lapse photographs and video from submersibles. Genetic tests were conducted to determine the phylogenetic relationships among the three morphotypes (designated tan, purple and white) to aid in bioturbation and population studies involving *Echinocrepis*. Ninety-eight specimens of *Echinocrepis* were collected by manned submersible and remotely operated vehicle (ROV) between 2005 and 2007. Gonad tissue samples for microscopy and genetic sequencing were removed from the specimens. The mitochondrial (mt) 16S rDNA sequence, a portion of the mitochondrial genome commonly used in determination of species, was amplified from 18 of the tissue samples (six specimens from each morphotype) and their similarity was compared using Bayesian analysis. Results show that all three morphotypes have statistically similar mt 16S rDNA sequences and are most likely the same species, *Echinocrepis rostrata*. The white morphotype has a significantly smaller body size ($p<0.0001$) than the other two morphotypes, has less gonad tissue, and a slightly different body shape, suggesting that it is a juvenile form of *E. rostrata*. Resolving the three morphotypes into one species simplifies identification of *E. rostrata* from photographs and leads to a greater understanding of the life history and reproductive cycle of a species vital to deep-sea bioturbation and carbon sequestration.

Introduction

Comparison of short, standardized gene sequences ("barcodes") that undergo relatively rapid molecular evolution can be employed to determine relatedness among

closely related organisms (Avise 1994; Floyd et al. 2002; Hebert et al. 2003; Moura et al. 2007), even within morphologically cryptic species (Moura et al. 2007; Johnson et al. 2008). DNA "barcoding" techniques have been used to examine variation on local to global scales for many different types of marine species (Miya and Nishida 1997; Burton 1998; de Vargas et al. 1999; Webb et al. 2006; Johnson et al. 2008, etc.). However, fewer gene sequence identification experiments have been conducted on deep-sea benthic megafauna (France et al. 1996; Chase et al. 1998; France and Hoover 2002; Johnson et al. 2008, etc.). Studies are hindered in part by the risk and costs of deep-sea exploration, and a general lack of specimens of the quantity and quality required for reliable sequencing and analysis. Advances in submersible technology have allowed intact samples of many previously indistinguishable and undescribed species to be recovered. Morphologically cryptic species can be problematic when describing geographic ranges, which can be overestimated if multiple cryptic species are conflated into a single group or underestimated if several morphotype variants are mistakenly described as distinct species (Johnson et al. 2008). In addition, taxa with morphologically distinct life stages have also been classified as separate species before molecular techniques linked larval and adult morphotypes (Shank et al. 1998).

One of the most common organisms observed during a long time-series study of pelagic-benthic coupling in the abyssal northeast Pacific (Station M; 4100 m, 34°50'N, 123°00'W) was *Echinocrepis rostrata*, an irregular echinoid (Smith et al. 1993; Kaufmann and Smith 1997; Ruhl 2007). The genus *Echinocrepis* contains two described species: *E. cuneata*, recovered only in the Southern Ocean, and *E. rostrata*, found only in the North Pacific. *Echinocrepis cuneata* was originally described by Agassiz (1881) and

E. rostrata was added to the genus by Mironov (1973). The *E. rostrata* specimens described by Mironov were "greenish-violet" in color, which probably corresponds to the purple morphotype described here. The fate of particulate organic carbon (POC) that reaches the seafloor is heavily influenced by the actions of benthic megafauna, such as *Echinocrepis*, that feed on and/or bury the surface-derived phytodetritus through bioturbation (Aller 1982; Kristensen and Blackburn 1987; Pfannkuche 1993; Pfannkuche et al. 1999; Smallwood et al. 1999; Miller et al. 2000; Smith et al. 2000). The large numbers of *Echinocrepis* found at Station M and their capacity for reworking wide areas of the seafloor made them ideal organisms for studies on deep-sea bioturbation and pelagic-benthic interactions. Complicating such research was the unknown phylogenetic relationship among the three morphotypes of *Echinocrepis* observed at Station M in time-lapse photographs and ROV and submersible video footage. If three different species were being observed, possible differences in food preference, foraging behavior or spawning pattern would need to be considered when conducting population-level research. Observations of size and density changes over time would also have to be separated out by species rather than considering all observations of *Echinocrepis* in the photographic record to be the same species.

The morphotypes were distinguishable by differences in pigmentation, size and shape (Fig. 1). Because *E. cuneata* has been found only in the Southern Ocean (Agassiz 1881), previous Station M studies (Smith et al. 1993; Kaufmann and Smith 1997; Ruhl 2007) concluded that the irregular echinoids at the site all belonged to the species *E. rostrata*. We examined the reproductive tissue and 16S mitochondrial DNA (mtDNA)

sequence variability of the three observed morphotypes of *Echinocrepis* echinoids at Station M to determine the phylogenetic relationship between the three morphotypes.

Materials and Methods

Specimen collection

All specimens of *Echinocrepis* were collected in the vicinity of a site known as Station M located ~220 km west of Point Conception, California, USA (35°16'N, 123°02'W) at a depth of ~4,000 m. Collections were conducted at a site that was in close proximity to Station M (34°50'N, 123°00'W; 4100 m depth) but slightly shallower in depth due to the safety limits of the submersibles. *Echinocrepis* specimens were collected for gene sequence analysis between 2005 and 2007 using the ROVs Jason II and Tiburon, and the Deep Submergence Vehicle (DSV) Alvin. Specimens were collected using a suction sampler attached to the robotic arm of the ROV, or by scoops and box-core grab sampling tools operated by the Alvin. Otter trawl samples, while extensive for the area, were excluded from this study because the fragility of *Echinocrepis* tests resulted in no collections of intact, uncontaminated specimens. All samples were sorted by size and appearance (color, body shape, and size), measured (length, oral width and height) and photographed. The specimens were then dissected; the gonadal tissue was removed, frozen in liquid nitrogen and ultimately stored in a -80ºC freezer. The remaining tissue and test fragments were preserved in 95% ethanol.

Molecular Methods

Genomic DNA was extracted from the frozen *Echinocrepis* gonad tissue samples using the Qiagen DNeasy purification protocol (Qiagen Inc., Valencia, CA). About 10 mg of gonad tissue from ten individuals of each morphotype were incubated overnight at 52ºC in a solution containing 20µL proteinase K to fully digest the tissue fragments. Once the DNA was isolated according to the DNeasy protocol, PCR was conducted in a solution that contained 30-100 ng of template DNA, 2.5 µL of 2.5 µM MgCl$_2$, 1 µL of each primer (10 µM final concentration), 2.5 units of *Taq* polymerase (AmpliTaq Gold, Applied Biosystems Inc., Foster, CA), 2.5 µL of 2 mM stock solution of dNTPs, and sterile water to final volume of 25 µL. An approximately 500-650-bp fragment of the mt 16S rDNA coding region was amplified using the primer pair 16sar (5'-CGCCTGTTTACCAAAAACAT-3') and 16sbr (5'-CCGGTCTGAACTCAGATCACGT-3') (Palumbi et al. 1991). A Cetus 9600 DNA Thermal Cycler (Perkin-Elmer Corp. CT) was used to carry out the PCR at an initial denaturation of 95ºC/10 min, followed by 35 cycles of 94ºC/1 min, 55ºC/1 min, and 72ºC/1 min, and a final extension at 72ºC/7 min. PCR products were then diluted in 40 µL of sterile water and purified with a Multiscreen HTS PCR 96 vacuum manifold system (Millipore Corp. Billerica, MA). An ABI 3,100 capillary sequencer and BigDye terminator v. 3.1 chemistry (Applied Biosystems Inc., Foster, CA) were used to sequence the amplified DNA in both directions with the same primers used for PCR. Forward and reverse sequences were proofread, aligned and edited by eye using Geneious® software (Drummond et al. 2007). Genetic differences between the morphotypes were then identified by using Geneious® software to compare the amplified sequences. Finally,

consensus sequences were extracted and basic local alignment search tool (BLAST) sequence similarity searched (Altschul et al. 1997) against all 47 of the echinoid mt 16S sequences in the GenBank DNA database.

Statistical Methods

Statistical analyses of DNA diversity were conducted using Arlequin (v. 3.1, Excoffier et al. 2005) and DnaSP (Rozas et al. 2003). Parsimony networks were constructed using the program TCS v. 1.21 (Clement et al. 2000) with a connection limit of 95% and redrawn in Adobe Illustrator CS v. 11.0.0.

Phylogenetic analyses were conducted using the Mr. Bayes v. 3.1.3 program (Huelsenbeck and Ronquist 2001). Appropriate substitution models for mt 16S were determined with standard procedures in PAUP (Swofford 1993) using Mr. Model Test (www.ebc.uu.se/systzoo/staff/nylander) and the Akaike information criterion (AIC, Akaike 1974). Bayesian analyses involving six chains were run for at least 10 million generations with a printing, sampling frequency and burn-in period of 1,000. Analyses were run five times each and data were visualized using Tracer v. 1.3 (Rambaut and Drummond 2003) to determine the appropriate burn-in period and ensure data had reached convergence. Trees were visualized using FigTree V.1.0 (http://tree.bio.ed.ac.uk/software/figtree). All nodes with less than 0.95 posterior probability support were collapsed to basal polytomys.

One-way analysis of variance (ANOVA) statistical tests followed by least significant difference (LSD) *post hoc* tests were used to compare the means of the test

size measurements and the ratios of test height to test length, and test width to test length
for the three morphotypes.

Results

Of the 98 specimens of *Echinocrepis* collected, 38 were of the purple
morphotype, 30 were tan and 30 were white. The specimens were distinguished visually
by pigmentation differences as well as morphological variability in size, position of the
test apex and test shape (Fig. 5, 6). No differences in sex distribution ratio or internal
anatomy were found between the morphotypes, aside from the white morphotype which
had very little gonad tissue (Fig. 7). ANOVA tests showed significant differences
between the mean test length (TL; $F_{2,94}$= 162.92, p<0.0001), test width (TW; $F_{2,95}$=
147.90, p<0.0001) and test height (TH; $F_{2,95}$= 146.59, p<0.0001) of all three morphotypes
(Table 2; Fig. 8A). The mean values for the ratios of TW:TL and TH:TL were not
significantly different between the two larger morphotypes (p>0.05; Fig. 8B), but
ANOVA tests showed a significant difference between the TH:TL ratio of the white
morphotype and the purple and tan morphotypes ($F_{2,94}$= 19.70, p<0.0001) and the TW:TL
ratios of the white and purple morphotypes ($F_{2,94}$= 3.27, p<0.05).

Partial mt 16S rDNA sequences were recovered from 30 specimens. From those
sequences, the present analysis was restricted to six of each type, chosen to represent the
maximum diversity within each morphotype. Pairwise distances within each morphotype
ranged from 0 to 0.01%, and between morphotypes 0 to 0.10%. The *Echinocrepis*
sequences were compared with other echinoid 16S sequences in the GenBank DNA
database and plotted on a difference tree (Fig. 9). The posterior probability value derived

from the Bayesian analysis for the *Echinocrepis* sequences was 1.00, therefore the node is fully supported.

Discussion

When compared to other echinoid species in the GenBank BLAST database, very little variation was seen between the three *Echinocrepis* morphotypes. Based on the statistical analyses of the genetic distances, it is most likely that all three morphotypes belong to the same species. The geographic location of Station M and the anatomical characteristics of the specimens (Mironov 1973) identify the species as *Echinocrepis rostrata*.

There is some evidence to suggest that the white morphotypes are juveniles or immature individuals. In addition to their significantly smaller size, white *E. rostrata* specimens display characteristics such as reduced gonadal tissue, less tapered, more rounded body shape and shorter spines that indicate that they may not be fully developed. The smallest specimen recovered by submersible was 36 mm wide, 39 mm long and 22 mm high. The resolution of time-lapse photographs and high-definition video from manned and unmanned submersible dives allowed identification of much smaller individuals, down to an observed minimum of 13 mm in length. Growth bands in the tests of other deep-sea echinoids have been used to estimate age (Gage 1987), but may not be a reliable method due to variation in the timing of band deposition in shallow-water species (Russell and Meredith 2000). No experimental age determination was done on the *E. rostrata* samples in this study, but all of the smaller size class of *E. rostrata*

observed in the time-series record and submersible video footage were white morphotypes.

The explanation for the difference in pigmentation between the tan and the purple *E. rostrata* morphotypes remains unknown. Many echinoids exhibit high levels of within-species variability in color, shape and spine length (Millott 1953; Nichols 1959; Chesher 1968; Chesher 1970; Serafy 1973; Higgins 1974; Higgins 1975; Marcus 1983; Lewis and Storey 1984). However, variability between morphotypes of the same echinoid species has often been linked to environmental factors such as light levels (Kristensen 1964), wave activity (Lewis and Storey 1984) and sediment type (Higgins 1974; Higgins 1975), none of which apply to *E. rostrata*. Although the test shapes of the tan and purple *E. rostrata* were more similar to each other than to the white morphotype, there were significant differences in test width, length and height between the purple and tan morphotypes. The size disparity may indicate that the smaller tan *E. rostrata* are younger than the larger purple ones. The pigmentation may change from tan to purple (or vice versa) with age, similar to color progressions seen in some shallow water species (Millott 1953), and some individuals that appeared to be intermediate in color have been observed at the site. The color difference may also be related to the density of spines on a particular animal which could alter its appearance. A number of other types of spatangoid echinoids exhibit unexplained within-species color variations (Chesher 1968; Chesher 1970). Although the colors of the tan and purple *E. rostrata* appear very different in time-lapse photographs and ROV video records, once removed from seawater or placed in water warmer than ~4ºC the pigments begin to leach out of the specimens into the water and the morphotypes become difficult to distinguish. HPLC analyses of

the pigments found in the test and spines of purple and tan *E. rostrata* may provide more information about the chemical composition and elucidate possible differences between the pigments.

Confirmation that the three morphotypes of *E. rostrata* seen at Station M are the same species allows for population-level measurements and bioturbation studies to proceed without having to divide population numbers by morphotype or species. The physical variability between the morphotypes highlights the difficulty of determining deep-sea species based only on photographs or video footage. Future research will attempt to sequence the mitochondrial cytochrome c oxidase (CO1) gene, another commonly used "barcoding" sequence, and test tissue samples from *Echinocrepis* specimens collected at other sites worldwide.
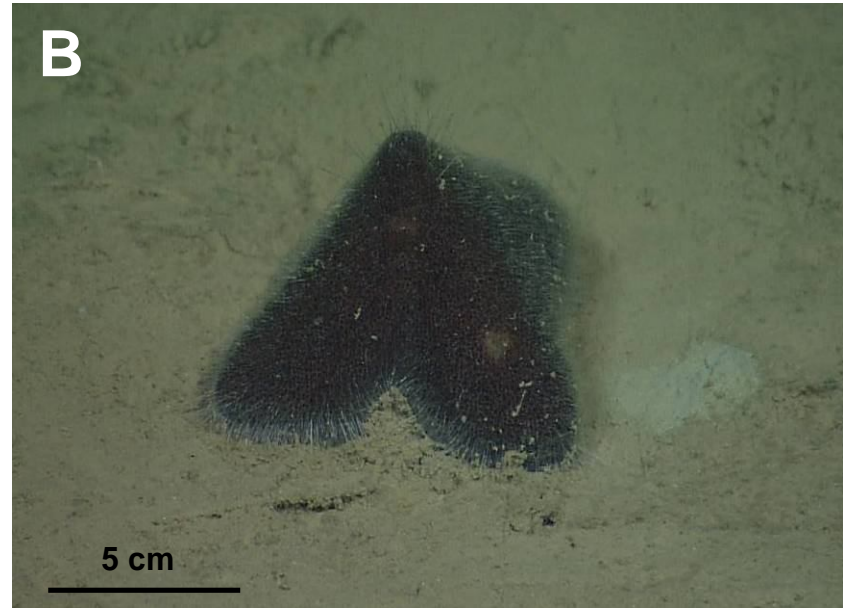
Figure 5. High-definition video captures from the ROV Tiburon illustrate the three morphotypes of *Echinocrepis rostrata* seen at Station M: tan (A), purple (B) and white (C). Another species of spatangoid echinoid, *Urechinus loveni* (syn. *Cystechinus loveni*) is visible in the bottom left of A. Scale is the same for all three images.
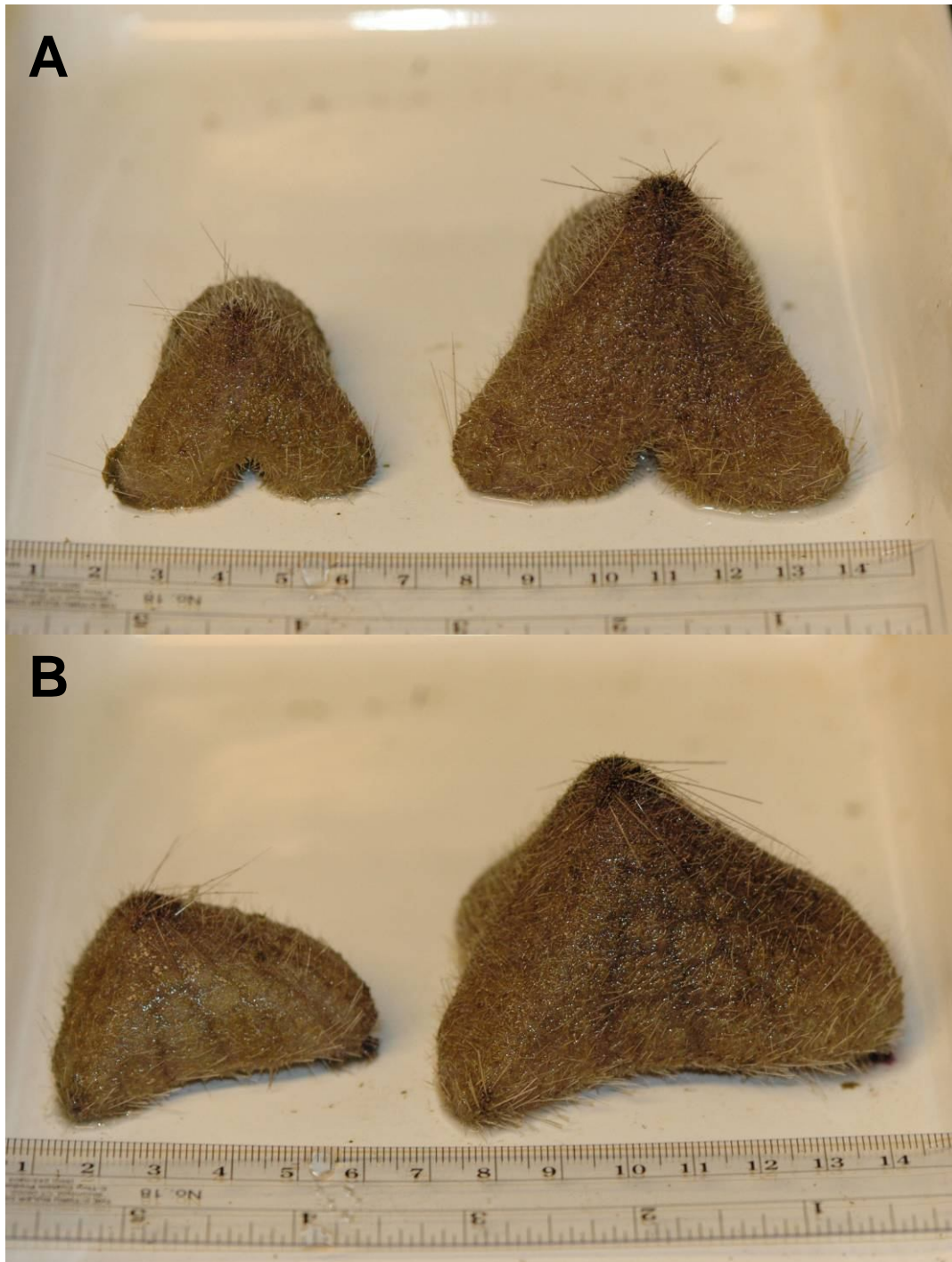
Figure 6. Front view (a) and lateral view (b) of a white (left) and a tan *E. rostrata* (right) recovered during the November, 2005 Jason II cruise. The white morphotype is significantly smaller and has a more rounded, less tapered shape. The pigmentation difference between the morphotypes is less pronounced at the surface.
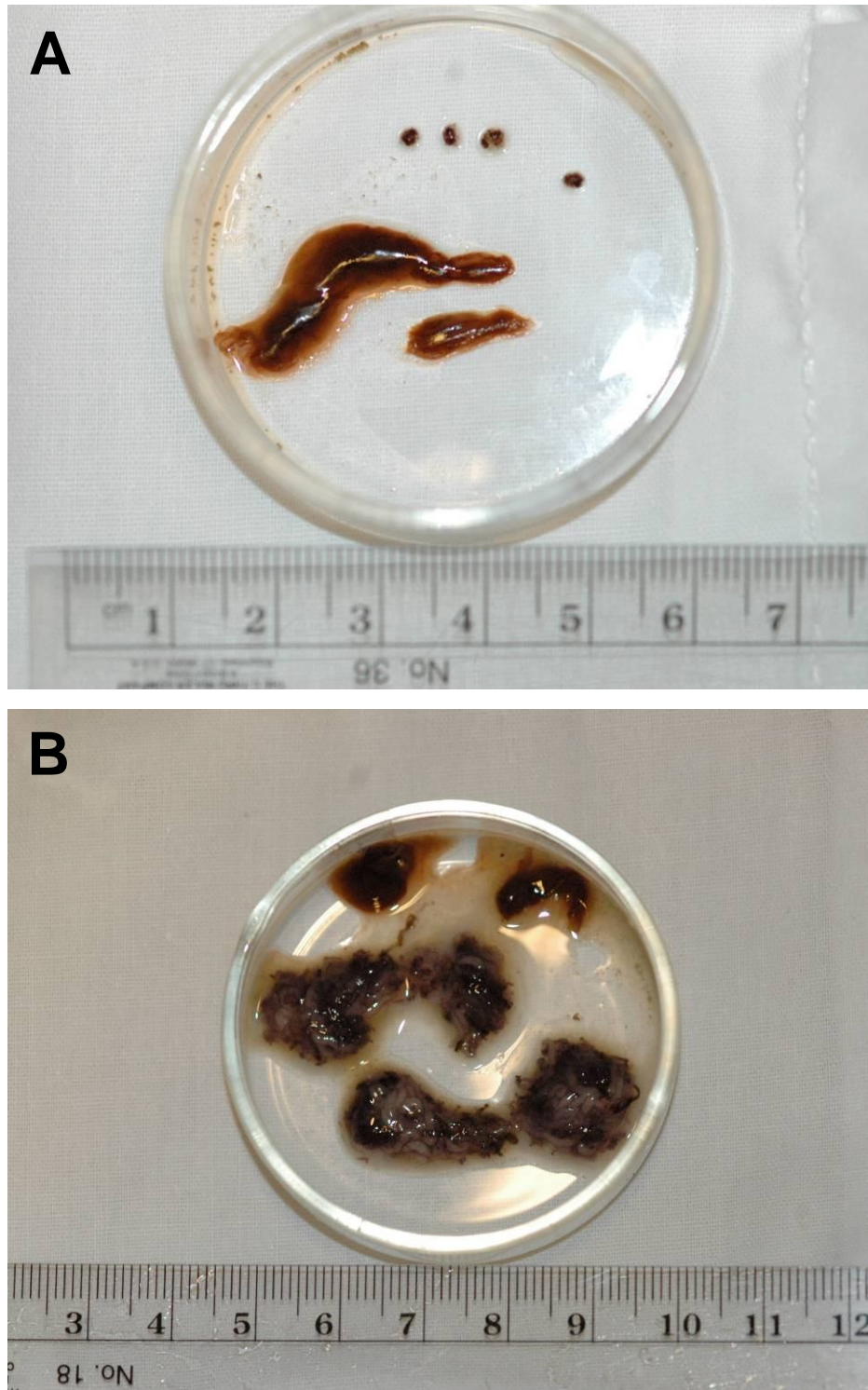
Figure 7. Amounts of gonadal tissue removed from a specimen of the white *E. rostrata* morphotype (A, top) and a purple *E. rostrata* morphotype (B, center). The reddish material in the center of the petri dish in A and the top of B is membranous support tissue, not gonad.

Table 2. ANOVA statistical test results on the size differentials between the *E. rostrata* morphotypes

Source	Sum squares	DF	Mean square	F statistic	p	LSD Contrast	Difference	95% CI	
Test Width (TW)	146.94	2	73.47	147.90	<0.0001	Purple v Tan	0.65	0.23 to 1.07	(significant)
Residual	47.19	95	0.50			Purple v White	2.88	2.46 to 3.30	(significant)
Total	194.13	97				Tan v White	2.23	1.78 to 2.67	(significant)
Test Length (TL)	204.27	2	102.13	162.92	<0.0001	Purple v Tan	0.93	0.46 to 1.40	(significant)
Residual	58.93	94	0.63			Purple v White	3.47	2.99 to 3.94	(significant)
Total	263.20	96				Tan v White	2.54	2.03 to 3.04	(significant)
Test Height (TH)	140.82	2	70.41	146.59	<0.0001	Purple v Tan	0.86	0.45 to 1.28	(significant)
Residual	45.63	95	0.48			Purple v White	2.86	2.45 to 3.28	(significant)
Total	186.45	97				Tan v White	2.00	1.56 to 2.44	(significant)
TH:TL ratio	0.109	2	0.055	19.70	<0.0001	Purple v Tan	0.025	-0.006 to 0.057	
Residual	0.261	94	0.003			Purple v White	0.081	0.049 to 0.113	(significant)
Total	0.371	96				Tan v White	0.055	0.022 to 0.089	(significant)
TL:TW ratio	0.025	2	0.013	3.27	0.0425	Purple v Tan	0.026	-0.012 to 0.063	
Residual	0.366	94	0.004			Purple v White	0.038	0.000 to 0.075	(significant)
Total	0.391	96				Tan v White	0.012	-0.027 to 0.052	
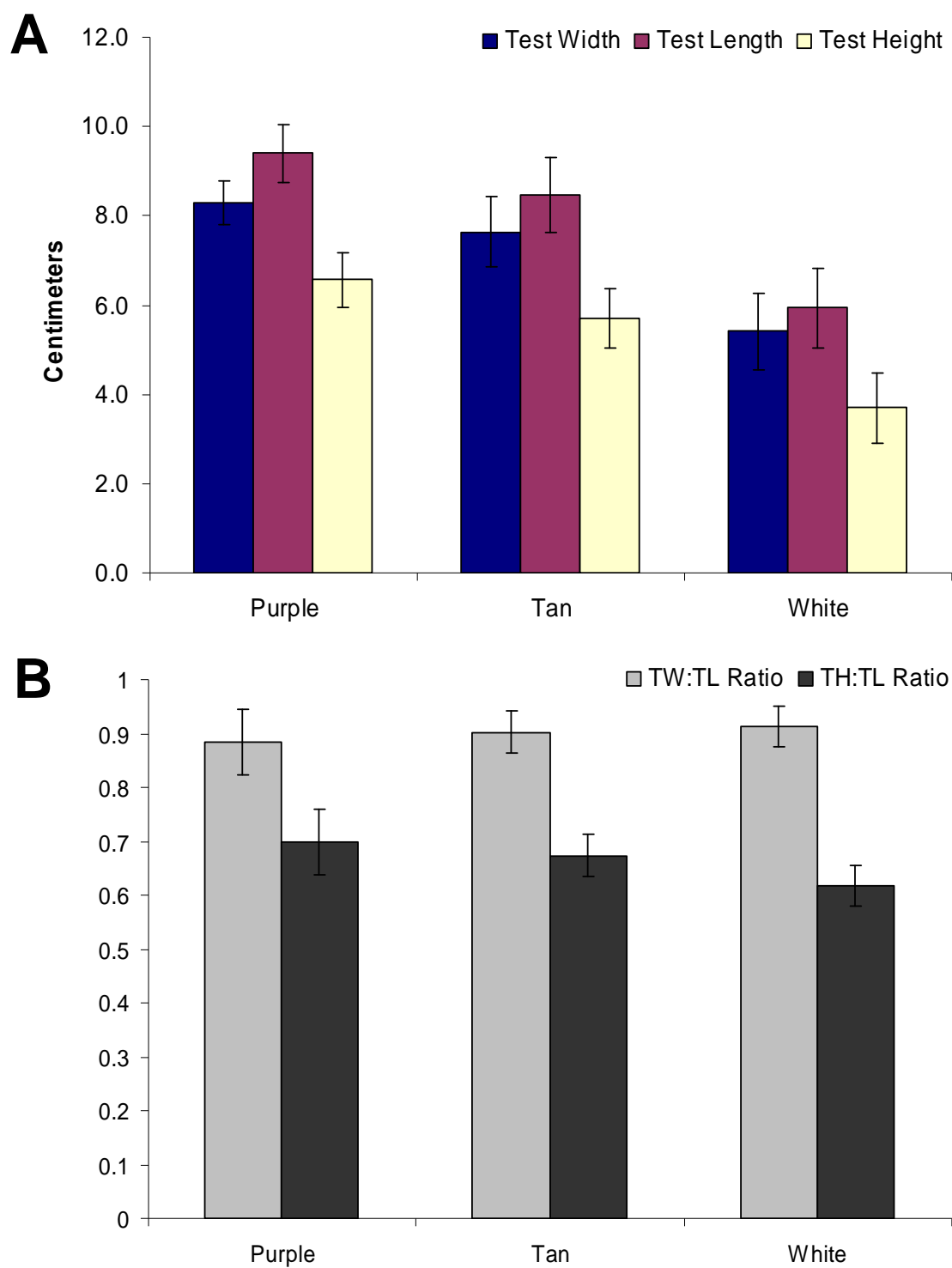
Figure 8. Charts of mean widths, lengths and heights of the three *E. rostrata* morphotypes drawn from the 98 specimens recovered (A). The white morphotype was significantly smaller than the other two. The ratios of test length (TL) to test width (TW) and test height (TH) were similar for all three morphotypes (B). Error bars indicate one standard deviation.
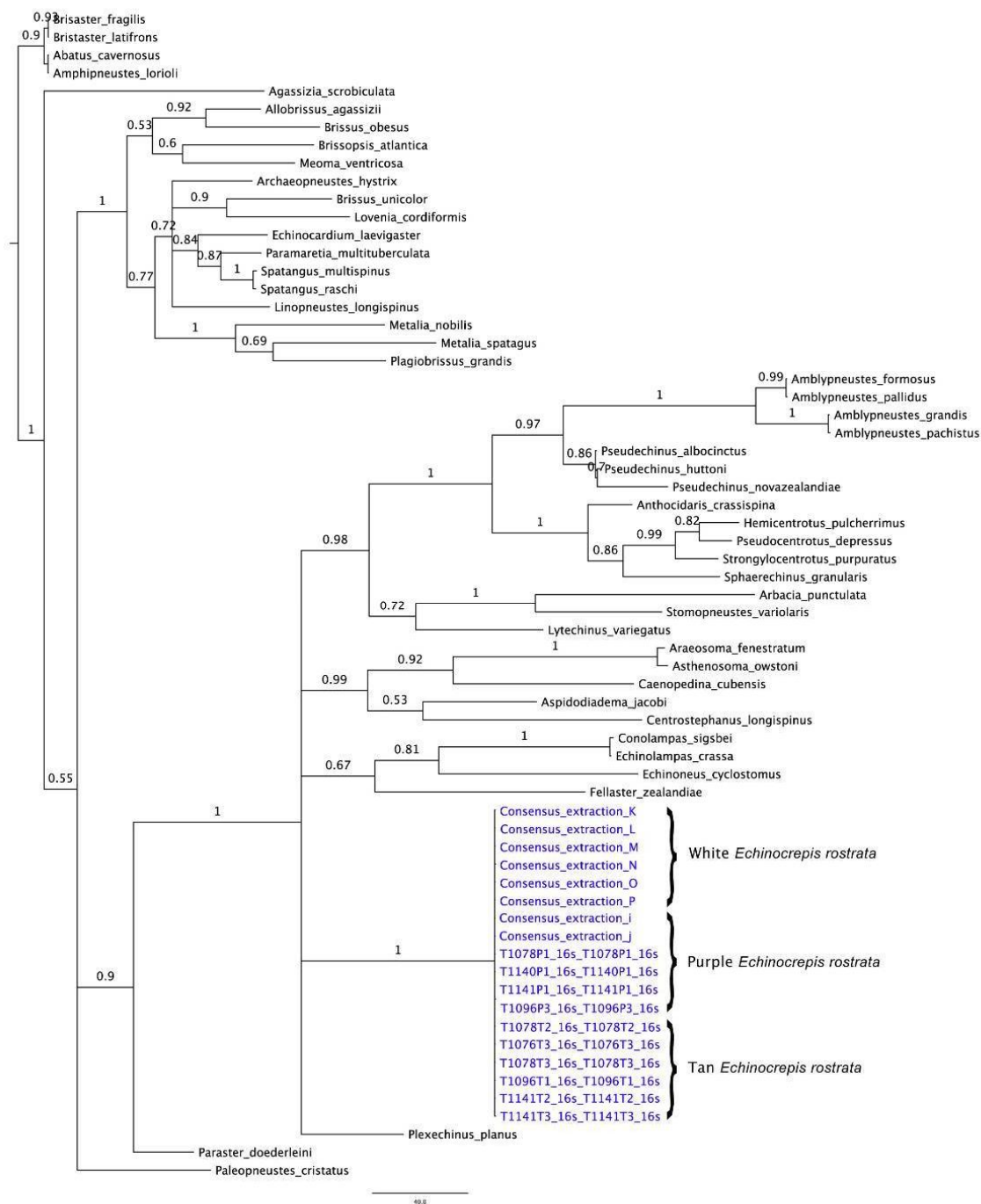
Figure 9. Bayesian tree constructed from the partial mt 16S rDNA sequences of 47 shallow and deep-water echinoid species drawn from the GenBank database and the 18 consensus sequences of the three *E. rostrata* morphotypes from Station M. The lack of variability among the mt 16S rDNA sequences from three morphotypes suggests that they are all the same species. Scale bar indicates % species divergence.

References

Agassiz A (1881) Report on the scientific results of the voyage of H.M.S. Challenger during the years 1873-76: Zoology; v. III, pt. 9, Report on the Echinoidea. Longmans & Co., London

Akaike H (1974) A new look at the statistical model identification. IEEE Transactions on Automatic Control 19: 437-499

Aller RC (1982) The effects of macrobenthos on chemical properties of marine sediment and overlying water. In: McCall PL, Tevesz MJS (eds) Animal-sediment relations---the biogenic alteration of sediments. Topics in geobiology, Vol 2. Plenum Press, New York, pp 53-102

Altschul SF, Madden TL, Schaffer AA, Zhang JH, Zhang Z, Miller W, Lipman DJ (1997) Gapped BLAST and PSI-BLAST: a new generation of protein database search programs. Nucleic Acids Research 25: 3389-3402

Avise JC (1994) Molecular markers, natural history and evolution. Chapman & Hall, New York

Burton RS (1998) Intraspecific phylogeography across the Point Conception biogeographic boundary. Evolution 52: 734-745

Chase MR, Etter RJ, Rex MA, Quattro JM (1998) Bathymetric patterns of genetic variation in a deep-sea protobranch bivalve, *Deminucula atacellana*. Marine Biology 131: 301-308

Chesher RH (1968) The systematics of sympatric species in West Indian spatangoids: a revision of the genera *Brissopsis*, *Plethotaenia*, *Paleopneustes*, and *Savianaster*. Studies in Tropical Oceanography 7: 1-168

Chesher RH (1970) Evolution in the genus *Meoma* (Echinoidea: Spatangoida) and a description of a new species from Panama. Bulletin of Marine Science 20: 731-761

Clement M, Posada D, Crandall KA (2000) TCS: a computer program to estimate gene genealogies. Molecular Ecology 4: 331-346

de Vargas C, Norris R, Zaninetti L, Gibb SW, Pawlowski J (1999) Molecular evidence of cryptic speciation in planktonic foraminifers and their relation to oceanic provinces. Proc. Natl. Acad. Sci. USA 96: 2864–2868

Drummond AJ, Ashton B, Cheung M, Heled J, Kearse M, Moir R, Stones-Havas S, Thierer T, Wilson A (2007) Geneious v3.5. Available from http://www.geneious.com/

Excoffier L, Laval G, Schneider S (2005) Arlequin ver. 3.1: an integrated software package for population genetics data analysis. Evolutionary Bioinformatics Online 1: 47-50

Floyd R, Abebe E, Papert A, Blaxter M (2002) Molecular barcodes for soil nematodes identification. Molecular Ecology 11: 839-850

France SC, Hoover LL (2002) DNA sequences of the mitochondrial COI gene have low levels of divergence among deep-sea octocorals (Cnidaria: Anthozoa). Hydrobiologia 471: 149–155

France SC, Rosel PE, Agenbroad JE, Mullineaux LS, Kocher TD (1996) DNA sequence variation of mitochondrial large-subunit rRNA provides support for a two-subclass organization of the Anthozoa (Cnidaria). Molecular Marine Biology and Biotechnology 5: 15-28

Gage JD (1987) Growth of the deep-sea irregular sea urchins *Echinosigra phiale* and *Hemiaster expergitus* in the Rockall Trough (N.E. Atlantic Ocean). Marine Biology 96: 19-30

Hebert PDN, Ratnasingham S, deWaard JR (2003) Barcoding animal life: cytochrome *c* oxidase subunit 1 divergences among closely related species. Proceedings of the Royal Society London B Biological Sciences 270 (Suppl. 1): S96–S99

Higgins RC (1974) Specific status of *Echinocardium cordatum*, *E. australe*, and *E. zealandicum* (Echinoidea: Spatangoida) around New Zealand, with comments on the relation of morphological variation to the environment. Journal of Zoology, London 173: 451-475

Higgins RC (1975) Observations on the morphology of *Echinocardium cordatum* (Echinoidea: Spatangoida) from diverse geographical areas. Journal of Zoology, London 177: 507-515

Huelsenbeck JP, Ronquist F (2001) MRBAYES: Bayesian inference of pylogenetic trees. Bioinformatics 17: 754-755

Johnson SB, Warén A, Vrijenhoek RC (2008) DNA barcoding of *Lepetodrilus* limpets reveals cryptic species. Journal of Shellfish Research 27: 43-51

Kaufmann RS, Smith KL, Jr. (1997) Activity patterns of mobile epibenthic megafauna at an abyssal site in the eastern North Pacific: results from a 17-month time-lapse photographic study. Deep-Sea Research I 44: 559-579

Kristensen E, Blackburn TH (1987) Fate of organic carbon and nitrogen in experimental marine sediment systems: Influence of bioturbation and anoxia. Journal of Marine Research 45: 231-257

Kristensen I (1964) The effect of raising *Diadema* at different levels of light intensity on pigmentation and preference for darkness. Caribbean Journal of Science 4: 441-443

Lewis JB, Storey GS (1984) Differences in morphology and life history traits of the echinoid *Echinometra lucunter* from different habitats. Marine Ecology Progress Series 15: 207-211

Marcus NH (1983) Phenotypic variability in echinoderms. In: Jangoux M, Lawrence JM (eds) Echinoderm Studies. A. A. Balkema, Rotterdam, pp 19-37

Miller RJ, Smith CR, DeMaster DJ, Fornes WL (2000) Feeding selectivity and rapid particle processing by deep-sea megafaunal deposit feeders: A ^{234}Th tracer approach. Journal of Marine Research 58: 653-673

Millott N (1953) Colour pattern and the definition of the species, *Diadema antillarum* philippi. Cellular and Molecular Life Sciences 9: 98-99

Mironov AN (1973) New deep-sea echinoid species of the genus *Echinocrepis* and distribution patterns of the family Pourtalesiidae (Echinoidea, Meridosternina). Transactions of the P.P. Shirshov Institute of Oceanology 91: 239-247

Miya M, Nishida M (1997) Speciation in the open ocean. Nature 389: 803-804

Moura CJ, Harris DJ, Cunha MR, Rogers AD (2007) DNA barcoding reveals cryptic diversity in marine hydroids (Cnidaria, Hydrozoa) from coastal and deep-sea environments. Zoologica Scripta 37: 93-108

Nichols D (1959) Mode of life and taxonomy in irregular sea urchins. Systematics Association Publication 3: 61-80

Palumbi SR, Martin A, Romano S, Mcmillan WO, Stice L, Grabowsky G (1991) A Simple Fool's Guide to PCR. University of Hawaii Press, Honolulu, HI

Pfannkuche O (1993) Benthic response to the sedimentation of particulate organic matter at the BIOTRANS station, 47 degree N, 20 degree W. Deep-Sea Research II 40: 135-150

Pfannkuche O, Boetius A, Lochte K, Lundgreen U, Thiel H (1999) Responses of deep-sea benthos to sedimentation patterns in the North-East Atlantic in 1992. Deep-Sea Research I 46: 573-596

Rambaut A, Drummond A (2003) Tracer, v. 1.3. available from http://beast.bio.ed.ac.uk/Tracer

Rozas J, Sánchez-DelBarrio JC, Messeguer X, Rozas R (2003) DnaSP, DNA polymorphism analyses by the coalescent and other methods. Bioinformatics 19: 2496-2497

Ruhl HA (2007) Abundance and size distribution dynamics of abyssal epibenthic megafauna in the northeast Pacific. Ecology 88: 1250-1262

Russell MP, Meredith RW (2000) Natural growth lines in echinoid ossicles are not reliable indicators of age: a test using *Strongylocentrotus droebachiensis*. Invertebrate Biology 119: 410-420

Serafy DK (1973) Variation in the polytypic sea urchin *Lytechinus variegatus* (Lamarck 1816) in the western Atlantic (Echinodermata, Echinoidea). Bulletin of Marine Science 23: 525-534

Shank TM, Lutz RA, Vrijenhoek RC (1998) Molecular systematics of shrimp from deep-sea hydrothermal vents: enigmatic "small orange" shrimp from the Mid-Atlantic Ridge are juvenile *Rimicaris exoculata*. Molecular Marine Biology and Biotechnology 7: 88-96

Smallwood BJ, Wolff GA, Bett BJ, Smith CR, Hoover D, Gage JD, Patience A (1999) Megafauna can control the quality of organic matter in marine sediments. Naturwissenschaften 86: 320-324

Smith CR, Levin LA, Hoover DJ, McMurtry G, Gage JD (2000) Variations in bioturbation across the oxygen minimum zone in the northwest Arabian Sea. Deep-Sea Research II 47: 227-257

Smith KL, Jr., Kaufmann RS, Wakefield WW (1993) Mobile megafaunal activity monitored with a time-lapse camera in the abyssal North Pacific. Deep-Sea Research I 40: 2307-2324

Swofford DL (1993) PAUP: phylogenetic analysis using parsimony. Smithsonian Institute, Washington, DC

Webb KE, Barnes DKA, Clark MS, Bowden DA (2006) DNA barcoding: A molecular tool to identify Antarctic marine larvae. Deep-Sea Research II 53: 1053-1060

IV

Gonadal anatomy and possible brooding by the deep-sea epibenthic echinoid
Echinocrepis rostrata **(Order Holasteroida: Family Pourtalesiidae)**

Abstract

Although fairly common in the deep northeast Pacific, the reproductive behavior of the deep-sea epibenthic echinoid *Echinocrepis rostrata* has never been described. The low overall densities of *E. rostrata* on the seafloor, very low fecundity (<1000 ova per female) and extremely large ova (600-700 μm) compared to shallow-water echinoids indicate that it is probably not a broadcast spawner. Only one incidence of contact between two animals was seen in hundreds of hours of *in situ* observations and there is no anatomical evidence of specialized brood pouches or internal fertilization. However, photographic evidence suggests that newly fertilized ova and possibly larvae adhere to the female's aboral epidermis, where at least the early stages of development take place. This brooding behavior would allow *E. rostrata* to make the most efficient use of its small number of gametes and minimize the energy investment involved in producing large amounts of germinal tissue in an abyssal environment characterized by highly variable food availability.

Introduction

Echinocrepis rostrata is unusual among deep-sea echinoids of the order Holasteroida in that it is permanently epibenthic. It is also fairly common for a member of the deep-sea megafauna, reaching densities approaching 1 individual m^{-2} (Ruhl 2007), and moves at an average rate of only 1.68 m day^{-1} (Chapter V). Thus this species is amenable to direct long-term observation by time-lapse photography and direct observation from submersibles (Smith et al. 1993; Lauerman et al. 1996; Kaufmann and

Smith 1997; Smith and Druffel 1998; Smith et al. 2002; Ruhl 2007; Vardaro et al. 2007). Although many aspects of the biology of *E. rostrata* are well-known, to date the reproduction of this species has not been described. Therefore, the purpose of this note is to illustrate the reproductive anatomy and to discuss likely incidence of brooding behavior.

Two species of *Echinocrepis* have been described: *E. cuneata* from the Southern Ocean and *E. rostrata* only in the North Pacific. *Echinocrepis cuneata* was originally described by Agassiz (1879; 1881) while *E. rostrata* was added to the genus almost a century later by Mironov (1973). Specimens collected by Mironov were described as "greenish-violet" which probably corresponds to the purple morphotype described in Ch. IV of the present dissertation. A tan morphotype was also described in the present study, and was shown to be the same species by mt 16S RNA sequencing. Since no obvious differences were found between the tan and purple specimens, the gonadal anatomy of the two morphotypes will be described together here.

Materials and Methods

Observations relevant to the present paper were made on several hundred specimens of *E. rostrata in situ* (Fig. 10A) and on 68 specimens brought to the surface by submersible and dissected. All specimens were collected in November 2005, August and December 2006 and February, June and September 2007 around a site known as Station M located ~220 km west of Point Conception, California, USA (35°16'N, 123°02'W) at a depth of ~4,000 m. Collections were conducted using the ROVs Jason II and Tiburon, and the Deep Submergence Vehicle (DSV) Alvin at a site that was in close proximity to

Station M (34º50'N, 123º00'W; 4100 m depth) but slightly shallower in depth due to the safety limits of the submersibles. Specimens were collected using a suction sampler attached to the robotic arm of the ROV, or by scoops and box-core grab sampling tools operated by the Alvin. Otter trawl samples, while extensive for the area, were excluded from this study because the fragility of *Echinocrepis* tests resulted in no collections of intact, uncontaminated specimens. All samples were sorted by size and appearance (color, body shape, and size), measured (length, oral width and height) and photographed. The specimens were then dissected and the gonads were removed. The gonad tissue was frozen in liquid nitrogen or fixed for histology either in 10% formalin or in 95% ethanol.

The fixed tissue was dehydrated in ethanol, embedded in Spurr's resin, sectioned with glass knives, stained in 0.1% toluidine blue, and mounted in immersion oil for optical microscopic investigation. Testes and ovaries were prepared, respectively, as 3 and 7 µm sections. Some of the ethanol and formalin-fixed gonads were prepared for scanning electron microscopy (SEM). After fixation, the specimens were washed in distilled water for 2 minutes and then dehydrated in an ethanol series and critical point dried from CO_2. The dried specimens were mounted on stubs with Scotch double-stick tape, rotary coated with a mixture of gold and palladium (60:40), and viewed with a Cambridge Instruments® 360 scanning electron microscope.

Results

All 68 of the specimens had four gonads at their aboral pole (Fig. 10B). As in irregular echinoids generally, the gonad at the AB interradius (the section that extends clockwise from the radius directly opposite the hydropore in regular five-sectioned

echinoids) had been lost (Hyman 1955). Of the 60 animals in which sex could be determined, the sex ratio was approximately equal (32 female: 28 male). Each gonad comprised numerous branching tubules and was ~0.5 – 2 cm in overall length. We did not determine gonad indices (percentage of gonad weight divided by total weight of the animal) because dissection was performed at sea with no access to a balance, but even the ripest specimens would have had a gonad index of under 1%. This is extremely small compared to shallow-water echinoids, where the gonad index can reach values around 30% (Boolootian et al. 1959; Holland and Giese 1965; Giese et al. 1966; Magniez 1983).

Specimens of *E. rostrata* testes were also collected and photographed. Testes from most of the males contained numerous spermatozoa in the lumen (Fig. 10C), although testes from some males were less ripe, containing few sperm (Fig. 10D). In unripe testes spermatocytes predominated in the germinal epithelium (Fig. 10D,E). The sperm identified from the male gonads (Fig. 10F,G) exhibited the conical, arrowhead shape typical of most echinoid sperm (Pearse and Cameron 1991). The sperm heads (at 3.5 µm) are only slightly longer than shallow-water echinoids, but considerably shorter than the approximately 10-µm long sperm of some deep-sea echinoids (Eckelbarger et al. 1989). The only unusual feature of *E. rostrata* sperm were the five small concavities near the posterior pole of the midpiece (Fig. 10G).

A cross-section of an ovarian lobe is shown in Figure 11A-C. The germinal epithelium included primary oocytes with diameters ranging between 7 µm and 700 µm. The primary oocytes were characterized by a large germinal vesicle containing a prominent nucleolus. Also present in the germinal epithelium were numerous nutritive phagocytes, some of which appear to be digesting a small proportion of the primary

oocytes that were undergoing degeneration. The ovarian lumen includes a relatively small number of female gametes of maximum size that proved to be haploid ova ("eggs"). These ova contained a small female pronucleus (Fig. 11A), instead of the large germinal vesicle characterizing the large primary oocytes. Figure 11D shows twelve uncompressed ova that were removed from an ovarian lumen. Although the ova were fixed in formalin, their diameters were probably comparable to those of living ova. Their average diameter was approximately 675 µm. This is considerably larger than the 85- to 150-µm diameter ova of shallow-living echinoids with planktotrophic larvae (Pearse and Cameron 1991).

Discussion

The large size of the eggs found in the gonad tissue strongly indicates that larval development of *E. rostrata* is lecithotrophic, omitting any planktotrophic phase, as is typical for many species of deep-sea echinoderms (Mortensen 1921; Tyler et al. 1982). Lecithotrophic development is consistent with the constant egg production found in *E. rostrata* specimens, which indicates that *E. rostrata* probably does not spawn seasonally (Tyler et al. 1982). Seasonal spawning of planktotrophic larvae by other deep-sea echinoderms has been linked to pulses of particulate organic carbon (POC) flux to the seafloor, because planktotrophic larvae require a ready source of food soon after hatching (Tyler et al. 1982; Tyler and Gage 1984; Ferrand et al. 1988). Lecithotrophic larvae, by contrast, can survive for long periods of time on stores of energy provided by large, yolky eggs (Shilling and Manahan 1994; Young et al. 1997) which allows them to disperse widely at any time of year regardless of the availability of an external food supply. The

seasonal and interannual variability of the food supply (POC flux) at Station M (Smith et al. 1992; Smith et al. 1994; Smith and Kaufmann 1999) may favor constant egg production and lecithotrophic larvae, which allows spawning and larval dispersal at any time of year. The *E. rostrata* larvae can then survive from their yolk and eventually recruit into the adult population whenever POC flux rates become favorable.

Some irregular echinoids that brood their young have conspicuous indentations in the test for retaining the developmental stages (Magniez 1983; Poulin and Féral 1996; Poulin and Féral 1998; Poulin et al. 2002). However, some echinoderms without such pouches brood their young directly on the surface of the female, for example the crinoid *Antedon mediterranea* (Holland 1991). There is limited evidence that *E. rostrata* may also exhibit surface brooding of the developmental stages without morphological specialization. Video recordings of a single tan individual of *E. rostrata* observed in December 2006 showed about 20 spherical objects clustered near the aboral pole of the animal (Fig. 12). The animal was collected using the ROV and dissection of the gonads showed it to be a female; unfortunately, the spheres on the surface were lost during collection. The diameter of the objects was uniform and very close to the 675 μm diameter of *E. rostrata* ova. It is probable that each sphere represented a recently fertilized ovum or an embryo in the early stages of development.

It is very unlikely that *E. rostrata* is a broadcast spawner. Only a very small quantity of eggs and sperm are present at any one time in females and males, respectively. In a ripe female, there are at most a few hundred ova ready to be spawned at any given time, compared with tens of millions of eggs in large, shallow-water echinoid species (Thompson 1979; McShane et al. 1996). Moreover, the density of adult

animals on the deep sea floor is relatively low (less than one individual m^{-2} according to Ruhl 2007). It is therefore likely that individuals of *E. rostrata* are required to come into close proximity to ensure effective fertilization, although we never saw any direct evidence for this. In observing several hundred hours of *E. rostrata* behavior in time-lapse photographs and real-time video, we saw two animals interact with each other only once and no obvious spawning ensued.

In sum, *E. rostrata* makes a relatively small investment in germinal tissue (which is presumably a good strategy in nutrient-limited environment like the deep sea). It seems likely that this species makes the most effective use of its small number of gametes by some kind of mating behavior that we have not yet observed. Presumably, this behavior involves close approximation of a male and female (and possibly multiple individuals) and involves the adhesion of the spawned ova to the female's aboral epidermis where at least the early stages of development take place.

Figure 10. *Echinocrepis rostrata* adults and male reproductive system as seen by light microscopy (LM) and scanning electron microscopy (SEM). (A) Purple morphotype from a frame of a videotape taken at about 4,000 m; the animal is crawling slowly on the sediment surface with its notched anterior end in advance (toward bottom left). (B) View of inner aboral surface of an animal (anterior end toward the right) after removal of all the viscera except the gonads (arrowed). (C) LM cross section of part of a testicular tubule with numerous spermatozoa in the lumen. (D) LM cross section of a testicular tubule with only a few spermatozoa in the lumen. (E) LM detail of 1D showing that the germinal epithelium comprises mostly spermatocytes with no detectable nutritive phagocytes. (F) SEM of a spermatozoan in side view showing the acrosome (arrow), conical nuclear region, midpiece (arrowhead) and flagellum. (G) SEM of a spermatozoan showing the flagellum arising from the posterior pole of the midpiece, which is indented by five shallow depressions.
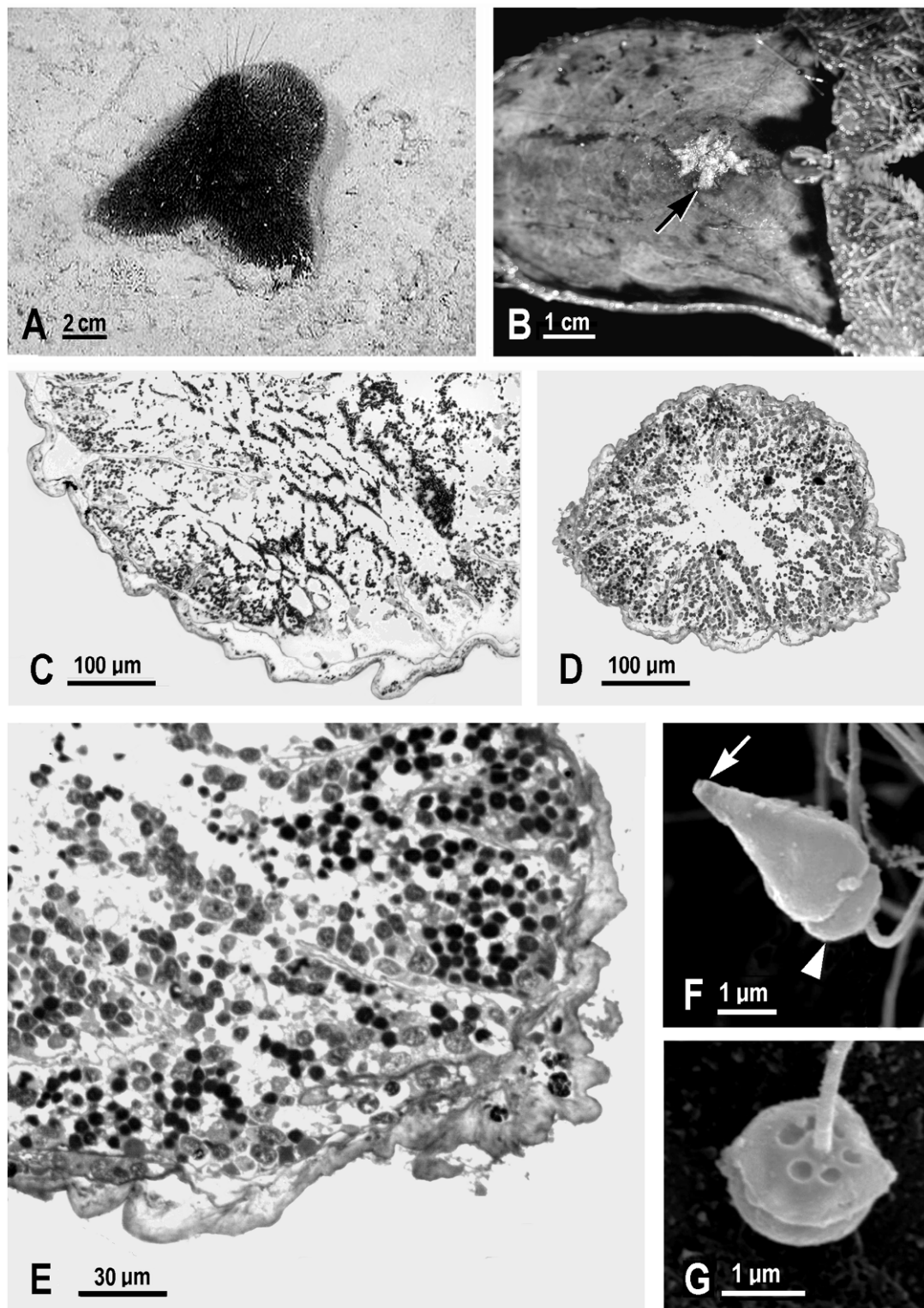
Figure 11. *Echinocrepis rostrata* female reproductive system seen by light microscopy. (A) Cross section of an ovarian tubule. The germinal epithelium includes many primary oocytes (po) ranging in diameter from about 10 μm (inset at top left) to hundreds of micrometers; also present are numerous nutritive phagocytes (np) some of which appear to be breaking down degenerating oocytes (arrowhead). The ovarian lumen contains ova (ov). (B) Detail of nutritive phagocytes in the germinal epithelium of an ovary. (C) The haploid female pronucleus near the periphery of an ovum. (D) Fixed, uncompressed ova with average diameters of approximately 675 μm.

A   200 µm

B   25 µm

C   25 µm

D   1000 µm
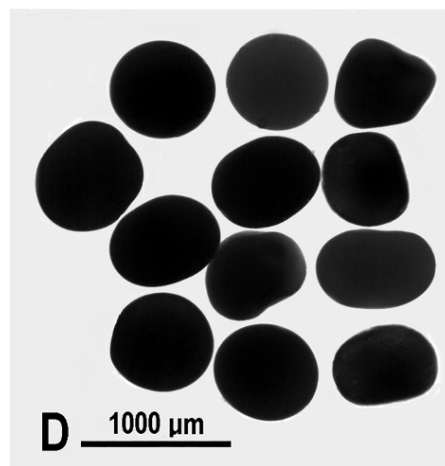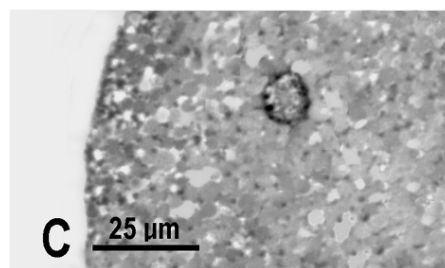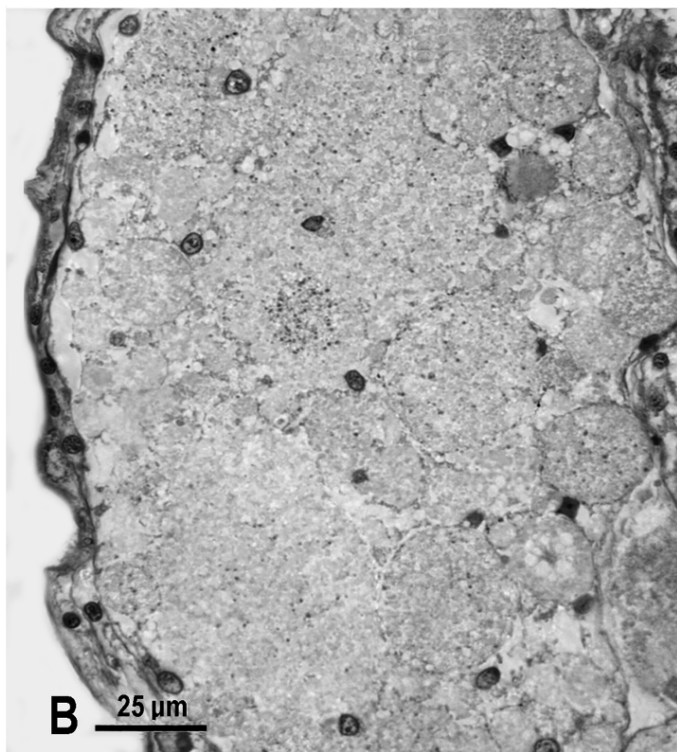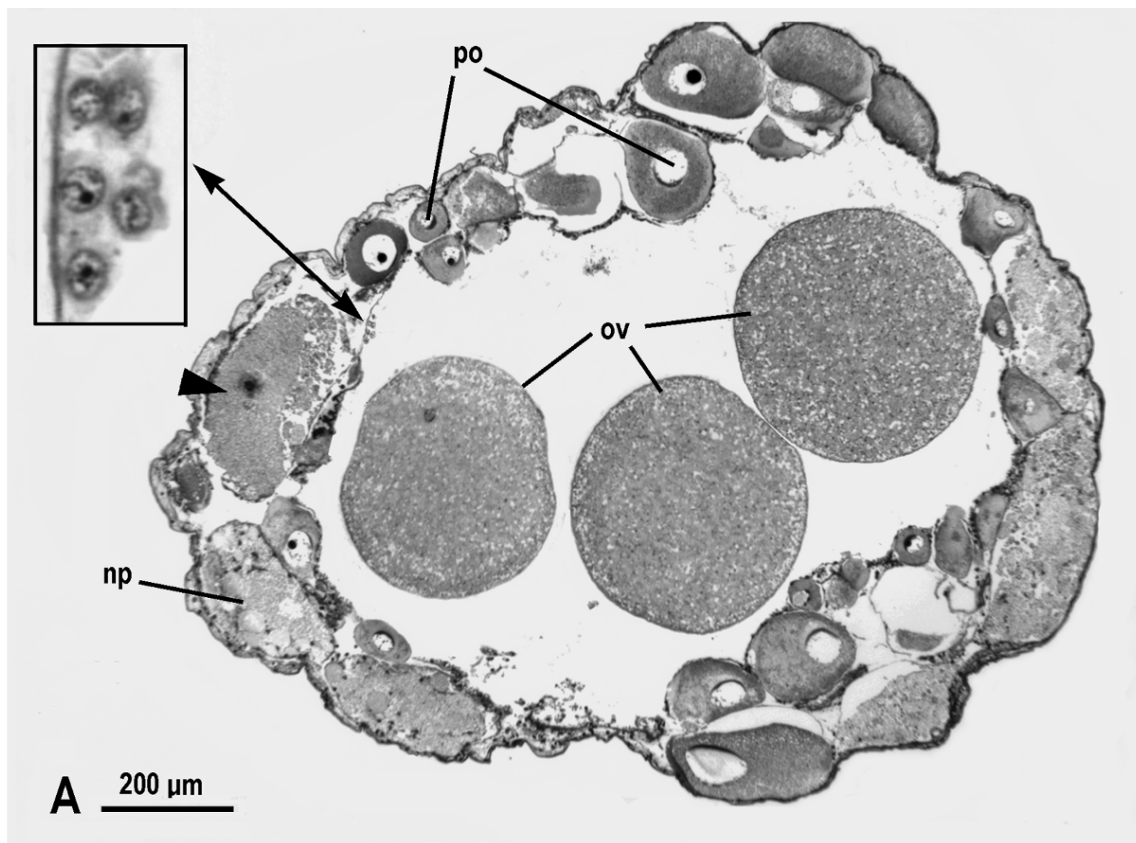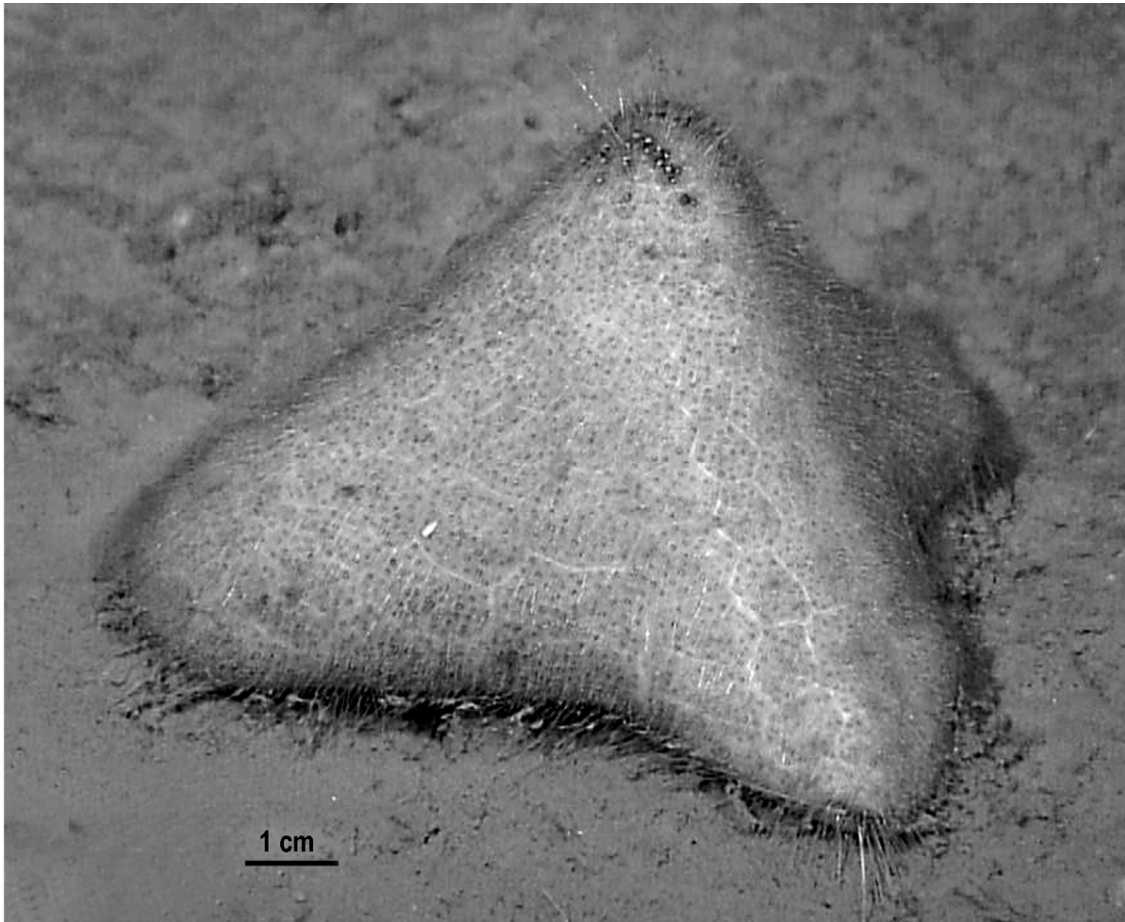
Figure 12. *Echinocrepis rostrata* female (tan color morph) from a frame of a videotape taken at about 4,000 m; anterior is toward the right. Approximately fifteen spheres (probably ova or early embryos) adhere to the epidermis of the animal near its aboral pole. The animal was captured, but the spheres were detached and lost by the time it reached the surface.

References

Agassiz A (1879) Preliminary report on the echini of the exploring expedition of H.M.S. "Challenger," Sir C. Wyville Thomson Chief of Civilian Staff. Proceedings of the American Academy of Arts and Sciences 14: 190-212

Agassiz A (1881) Report on the scientific results of the voyage of H.M.S. Challenger during the years 1873-76: Zoology; v. III, pt. 9, Report on the Echinoidea. Longmans & Co., London

Boolootian RA, Giese AC, Tucker JS, Farmanfarmaian A (1959) A contribution to the biology of a deep sea echinoid, *Allocentrotus fragilis* (Jackson). Biological Bulletin 116: 362-372

Eckelbarger KJ, Young CM, Cameron JL (1989) Modified sperm ultrastructure in four species of soft-bodied echinoids (Echinodermata: Echinothuriidae) from the bathyal zone of the deep sea. Biological Bulletin 177: 230-236

Ferrand JG, Vadon C, Doumenc D, Guille A (1988) The effect of depth on the reproductive cycle of *Brissopsis lyrifera* (Echinoidea, Echinodermata) in the Gulf of Lions, Mediterranean Sea. Marine Biology 99: 387-392

Giese AC, Farmanfarmaian A, Hilden S, Doezema P (1966) Respiration during the reproductive cycle in the sea urchin, *Strongylocentrotus purpuratus*. Biological Bulletin 130: 192-201

Holland ND (1991) Echinodermata: Crinoidea. In: Giese AC, Pearse JS, Pearse VB (eds) Reproduction of marine invertebrates, Volume 6. Boxwood Press, Pacific Grove, CA

Holland ND, Giese AC (1965) An autoradiographic investigation of the gonads of the purple sea urchin (*Strongylocentrotus purpuratus*). Biological Bulletin 128: 241-258

Hyman L (1955) The Invertebrates IV Echinodermata. McGraw-Hill, New York

Kaufmann RS, Smith KL, Jr. (1997) Activity patterns of mobile epibenthic megafauna at an abyssal site in the eastern North Pacific: results from a 17-month time-lapse photographic study. Deep-Sea Research I 44: 559-579

Lauerman LML, Kaufmann RS, Smith KL, Jr. (1996) Distribution and abundance of epibenthic megafauna at a long time-series station in the abyssal northeast Pacific. Deep-Sea Research I 43: 107-1103

Magniez P (1983) Reproductive cycle of the brooding echinoid *Abatus cordatus* (Echinodermata) in Kerguelen (Antarctic Ocean): changes in the organ indices,

biochemical composition and caloric content of the gonads. Marine Biology 74: 55-64

McShane PE, Gerring PK, Anderson OA, Stewart RA (1996) Population differences in the reproductive biology of *Evechinus chloroticus* (Echinoidea: Echinometridae). New Zealand Journal of Marine & Freshwater Research 30: 333-339

Mironov AN (1973) New deep-sea echinoid species of the genus *Echinocrepis* and distribution patterns of the family Pourtalesiidae (Echinoidea, Meridosternina). Transactions of the P.P. Shirshov Institute of Oceanology 91: 239-247

Mortensen TA (1921) Studies of the Development and Larval Forms of Echinoderms. G.E.C. Gad, Copenhagen

Pearse JS, Cameron RA (1991) Echinodermata: Echinoidea. In: Giese AC, Pearse JS, Pearse VB (eds) Reproduction of marine invertebrates, Volume 6. Boxwood Press, Pacific Grove, CA, pp 513–662

Poulin É, Féral J-P (1996) Why are there so many species of brooding Antarctic echinoids? Evolution 50: 820-830

Poulin É, Féral J-P (1998) Consequences of brood protection in the diversity of Antarctic echinoids. Océanis 24: 159-188

Poulin E, Palma AT, Féral J-P (2002) Evolutionary versus ecological success in Antarctic benthic invertebrates. Trends in Ecology & Evolution 17: 218-222

Ruhl HA (2007) Abundance and size distribution dynamics of abyssal epibenthic megafauna in the northeast Pacific. Ecology 88: 1250-1262

Shilling FM, Manahan DT (1994) Energy metabolism and amino acid transport during early development of Antarctic and temperate echinoderms. Biological Bulletin 187: 398-407

Smith KL, Jr., Baldwin RJ, Karl DM, Boetius A (2002) Benthic community responses to pulses in pelagic food supply: North Pacific Subtropical Gyre. Deep-Sea Research I 49: 971-990

Smith KL, Jr., Baldwin RJ, Williams PM (1992) Reconciling particulate organic carbon flux and sediment community oxygen consumption in the deep North Pacific. Nature 359: 313-316

Smith KL, Jr., Druffel ERM (1998) Long time-series monitoring of an abyssal site in the NE Pacific: an introduction. Deep-Sea Research II 45: 573-586

Smith KL, Jr., Kaufmann RS (1999) Long-term discrepancy between food supply and demand in the deep eastern North Pacific. Science 284: 1174-1177

Smith KL, Jr., Kaufmann RS, Wakefield WW (1993) Mobile megafaunal activity monitored with a time-lapse camera in the abyssal North Pacific. Deep-Sea Research I 40: 2307-2324

Smith KL, Kaufmann RS, Baldwin RJ (1994) Coupling of near-bottom pelagic and benthic processes at abyssal depths in the Eastern North Pacific-Ocean. Limnology and Oceanography 39: 1101-1118

Thompson RJ (1979) Fecundity and reproductive effort in the blue mussel (*Mytilus edulis*), the sea urchin (*Strongylocentrotus droebachiensis*) and the snow crab (*Chionoecotes opilio*) from populations in Nova Scotia and Newfoundland. Journal of the Fisheries Research Board of Canada 36: 955-964

Tyler PA, Gage JD (1984) Seasonal reproduction of *Echinus affinis* (Echinodermata : Echinoidea) in the Rockall Trough, northeast Atlantic Ocean. Deep-Sea Research 31: 387-402

Tyler PA, Grant A, Pain SL, Gage JD (1982) Is annual reproduction in deep-sea echinoderms a response to variability in their environment? Nature 300: 747-750

Vardaro MF, Parmley D, Smith KL, Jr. (2007) A study of possible "reef effects" caused by a long-term time-lapse camera in the deep North Pacific. Deep-Sea Research I 54: 1231-1240

Young CM, Sewell MA, Tyler PA, Metaxas A (1997) Biogeographic and bathymetric ranges of Atlantic deep-sea echinoderms and ascidians: the role of larval dispersal. Biodiversity and Conservation 6: 1507-1522

V

Climate Variation and Bioturbation on the Sea Floor in the Abyssal North Pacific

Abstract

Seasonal and interannual climate variation is known to cause changes in the quality and quantity of particulate organic carbon (POC) flux to the deep-sea. Changes in POC flux could affect bioturbation and ultimately the sequestration of organic carbon in the deep-sea. The 18-year time-series photographic record from Station M showed increased abundance of *Echinocrepis rostrata* since the late 1990's. Abundance, size and speed data from the photographic record were used to create an equation for bioturbation potential that allowed us to track long-term changes in bioturbation by *E. rostrata*. Bioturbation did not increase significantly over 18 years despite increased population size, but bioturbation was significantly correlated with POC flux. Thus, by changing POC flux and bioturbation rates, climate variations can lead to changes in rates of carbon sequestration in deep sea sediments, impacting the global carbon cycle.

Introduction

Fluctuations in climate influence deep-sea benthic community structure and activity through the marine carbon cycle. Recent research has shown that climate variation affects levels of photosynthetic activity at the sea surface and subsequent particle export (Kahru and Mitchell 2002; Bopp et al. 2005; Behrenfeld et al. 2006; Buesseler et al. 2007). Ocean warming is likely to increase stratification and decrease nutrient availability at the surface, leading to a shift towards smaller size classes of phytoplankton, greater recycling of nutrients in surface layers and decreases in particulate organic carbon (POC) flux out of the euphotic zone (Bopp et al. 2005). Thus photosynthetic activity and primary production are related to the quantity and quality of

POC flux that reaches the seafloor and ultimately influences the benthic community (Smith et al. 1994; Ruhl and Smith 2004; Ruhl 2007).

Although flux attenuation rates are variable, the majority of the organic carbon produced in the surface layers of the ocean is recycled in the upper ocean, either solubilised and remineralized by bacterial activity or consumed by zooplankton as it falls through the water column (Martin et al. 1987; Lampitt 1992; Lee et al. 1998; Kiørboe 2001; Kiørboe and Thygesen 2001; Stemmann et al. 2004; Buesseler et al. 2007). Organic carbon that reaches the seafloor provides food for benthic fauna, while some portion becomes sequestered through burial without being ingested (Reimers et al. 1992; Smallwood et al. 1999; Miller et al. 2000). This sequestration removes carbon from cycling back through the water column. The fate of POC that reaches the seafloor is heavily influenced by the actions of benthic megafauna that feed on and/or bury the surface-derived phytodetritus (Aller 1982; Kristensen and Blackburn 1987; Pfannkuche 1993; Pfannkuche et al. 1999; Smallwood et al. 1999; Miller et al. 2000; Smith et al. 2000). Here we show that climate variation and deep-sea bioturbation are positively correlated, and that increased POC flux leads to altered rates of bioturbation and changes in levels of carbon sequestration.

Materials & Methods

Time-Lapse Camera (TLC)

The study was conducted using a long time-series photographic record of the seafloor at 4,100 meters in the Northeast Pacific Ocean. An autonomous film camera system was first deployed at the site known as Station M in 1989 (Smith et al. 1993), and

continued through September 2007. The time-lapse camera (TLC) took one oblique

photograph of the seafloor every hour and was serviced 3 times a year. The TLC

consisted of a Benthos 377 camera mounted on a titanium frame at an angle of 31º from

horizontal with the lens ~2 m above the sea floor. The camera was equipped with a 28-

mm Nikonos lens, providing angular coverage of 50º in the horizontal and 35º in the

vertical plane, and holds 400 feet of 35-mm color-negative film (Fuji, Type 8514, 500

ASA). Up to 3500 images could be collected in 4.6 months. Two 400-W-s strobes, one

mounted on either side of the camera housing, illuminated approximately 20 m^2 of the

sea floor beginning at a distance of 1.8 m from the camera frame and extending

approximately 6.5 m from the base of the camera frame (see Smith *et al*. 1993 for a more

complete description of the time-lapse camera).

Camera Sled (CS)

Fifty-two seasonal photographic line-transects were also taken using a towed

camera sled (CS) between October 1989 and January 2005. Due to logistical restraints,

the frequency of these transects was variable, but they were typically conducted

seasonally. Line transect photography was conducted using a Benthos 372 35mm film

camera and Benthos 382 strobe mounted on a towed benthic camera sled, at a height of

82 cm and 22.5° below horizontal (Wakefield and Smithey 1989). The camera took one

photograph every five s as the sled moved along the bottom at ~2.8 km h^{-1}. The

overlapping images created a continuous image mosaic of the seafloor. A semi-balloon

otter trawl net towed behind the camera sled collected specimens from the line transect

area. Specimens recovered from the trawl net were then identified and used to facilitate

identification of the species observed in the line-transect photographs. The trawl net had a

6.1 m opening and 3.8 cm stretch mesh net with a 1.3 cm mesh cod-end liner (Wakefield

and Smithey 1989). The resulting photographic record monitored deep benthic sediment

community processes over 18 years. The CS tows provided instantaneous line-transect

measurements of epibenthic megafauna abundance and size, while the TLC system

monitored a single area of the seafloor for 4-month intervals with a detailed view of

temporal changes in activity and bioturbation (Fig. 13a,b). Animal specimens were

collected by remotely operated vehicle (ROV) and submersible during research cruises in

2006 and 2007.

Photographic Analysis

The oblique photographs taken by the TLC were analyzed using a perspective-

grid method (Wolf 1983; Wakefield and Genin 1987). Each image was projected onto a

flat surface and digitized with a Science Accessories Corp.® electronic digitizer

interfaced with a computer. The camera sled photographs were evaluated using a

Canadian grid system (Wakefield and Genin 1987) as well as the computer program

DISTANCE (Laake et al. 1994), based on line-transect theory (Buckland et al. 1993).

Using the digitized location of each individual along each transect, DISTANCE estimated

the visibility of an object at a distance perpendicular to the centerline of the transect. The

DISTANCE program then provided a probability density function and effective strip

width (ESW) for each species. The transect length was calculated using the sum of non-

overlapping distances between frames along the axis of the transect. Overlap was

estimated by measuring the relative positions of objects visible in sequential frames. The ESW was multiplied by the transect length to provide an estimation of abundance.

Climate Indices

Four climatic indices were also examined as part of the study, the Northern Oscillation Index (NOI, Schwing et al. 2002), Southern Oscillation Index (SOI, Trenberth and Shea 1987), the Multivariate ENSO Index (MEI, Wolter and Timlin 1998), the Bakun Upwelling Index (BUI, Bakun 1973), and the North Pacific Gyre Oscillation Index (NPGO, Di Lorenzo et al. 2008). The NOI is based on the difference in sea level air pressure anomalies (SLPA) between the N Pacific high, located in the NE Pacific and a climatologically low-pressure region near Darwin, Australia. The SOI is similar to the NOI, but is based on two S Pacific locations, one near Darwin, and the other near Tahiti. Although the SOI and the NOI are highly correlated, the NOI is correlated more closely with ecological variables in the NE Pacific (Schwing et al. 2002). The MEI is a more integrated anomaly index incorporating parameters such as sea surface temperature, clouds, and wind. Correlations with NOI and SOI have the same sign and correlations with the MEI have the opposite sign of the NOI and SOI. The BUI is measure of the volume of water that upwells along coastal California and Oregon. It uses geostrophic wind fields to identify the amount of offshore transport of coastal surface waters. The NPGO is derived from analyses of Northeast Pacific sea-surface temperature anomalies (SSTa) and sea-surface height anomalies (SSHa). The variability of the NPGO is driven by regional and basin-scale fluctuations in upwelling and horizontal advection, and has been significantly correlated with previously unexplained changes in salinity, nutrients

and chlorophyll. All time-lagged correlations used the non-parametric Spearman-Rank correlation with monthly data and 1-month lag intervals. Pearson (parametric) correlations have several assumptions that are violated by the biological data in this study including normality and homoscedasticity. Nonparametric tests were used here since they do not make assumptions about the distribution of the data. Numerical analyses were done using Excel (Microsoft®) and Statistica (StatSoft®).

Adjustments for multiple comparisons were not used. Multiple test adjustments to the p value, such as the Bonferroni or Box-Jenkins corrections, are often used to reduce Type I errors, but can also increase Type II errors and result in a loss of test power, especially for smaller sample sizes (Feise 2002). Subjective decisions about what constitutes a test, or group of tests, are also avoided by not using such corrections. Instead, conclusions regarding links with climate or food supply were based, in part, on whether the correlations met the basic criteria of sign and temporal relationship specified in Ruhl and Smith 2004.

Particulate Organic Carbon (POC) Flux

Particulate organic carbon (POC) flux to the seafloor was measured using a Teflon© coated parflux sediment trap with a 0.25 m^2 opening moored at 50 m above bottom (4050m water depth) (Baldwin et al. 1998; Baldwin and Smith 2003). Ten-day samples were taken at 50 and 600 meters above bottom (mab). Details of sediment trap data collection and analysis can be found in Baldwin et al. (1998). Temporal gaps in measured POC flux measurements over the time series necessitated the creation of a composite estimate of POC flux. This POC flux composite incorporates POC flux data

from 50 mab, then uses available data from the 600 mab sediment trap to fill in gaps

where possible, and finally an estimation of POC flux to 50 mab based on multiple

regression analysis of empirical data. The empirical estimate of POC flux at 50 mab was

generated using the Northern Oscillation Index, Bakun upwelling index, and satellite

estimated export flux from surface waters overlying the study site (Smith et al. 2006).

The export flux estimate used satellite-based net primary production (NPP) derived from

the Vertically Generalized Production Model (VGPM, Behrenfeld and Falkowski 1997)

and sea surface temperature using formulas from Laws (2004) for a 50 km radius around

the Station M site. The modeled POC flux data can explain about 50% of the sediment

trap measured POC flux and can therefore establish if the flux is high or low. The

VGPM based POC flux estimates were included from March 1997 until October 1997

because measured POC became available in November 1997. In January 1998 POC flux

estimates to 50 mab using the newly available Carbon-based Production Model (CBPM,

Behrenfeld et al. 2005) were used to fill in POC flux time-series gaps beginning in

January 1999. The CbPM model also can explain about 50% of the variation in measured

POC flux. The composite of both measured values and model-estimated values presented

a nearly continuous POC flux time-series to cross-correlate with climatic indices,

bioturbation rate and the parameters used to calculate the bioturbation rate (abundance,

size and speed).

Bioturbation Equation

   Echinocrepis rostrata, a deep-sea epibenthic, irregular echinoid, is common at

Station M and leaves distinctive trails in the sediment that allow quantification of the area

disturbed by their movements (Fig. 14a,b). Abundance, body size and activity of *E. rostrata* from the photographic record were used to create an equation for bioturbation potential similar to that generated for shallow-water environments (Solan et al. 2004a; Lohrer et al. 2005). Unlike prior research which used indices of bioturbation to compare the relative contributions of multiple epibenthic and infaunal populations to total sediment mixing rates in shallow water (Solan et al. 2004a), our study focused on the primary species, *E. rostrata*, as a proxy for bioturbation in a less complex deep-sea environment. The significant traits used in our calculation of area covered by bioturbation (B_i) were abundance (A_i, individuals m^{-2}), size (S_i, mm), movement speed (V_i, mm day^{-1}), and depth of sediment disturbance (D_i, mm):

$$B_i = A_i \times S_i \times V_i \times D_i \qquad (1)$$

Full descriptions of each trait and the details of their derivation from CS and TLC datasets are provided below.

We derived the abundance of *E. rostrata* from the CS line transects. The CS data were used because of the greater spatial coverage of the line transects ($\sim$125,797 m^2) compared to the TLC area ($\sim$560 m^2). In addition, the greater statistical power of the CS analyses performed using DISTANCE software (Laake et al. 1994) based on line transect theory (Buckland et al. 1993) provided a more robust measurement of abundance changes over time. Although abundance can be calculated from stationary measurements or "point transects," the mobility of *E. rostrata*, the number of individuals seen in the TLC records ($n_{TLC} = 202$), and the low number of individuals visible in the camera field of view at a particular point in time made it less appropriate to rely on TLC-based abundance. A rapid order of magnitude increase in *E. rostrata* abundance (Fig. 15a)

occurred between 2000 (0.2 individuals m^{-2}) and 2005 (0.8 individuals m^{-2}) and was

recorded from the CS transects (Ruhl 2007). A similar trend was seen in the number of

E. rostrata observed with the TLC (Fig. 13a,b). The average yearly number of *E.*

rostrata seen in the field of view of the TLC before 2000 was 0.4 individuals m^{-2}, which

doubled to 0.8 individuals m^{-2} year^{-1} after 2000.

The increase in abundance coincided with a decrease in the mean size of the

individuals observed per month in both the CS (Ruhl 2007) and TLC photographic

records. Sizes of *E. rostrata* for the bioturbation calculations were taken from the CS

data rather than the TLC data again because of the much larger sample size. Size drawn

from the CS photographs was of body length rather than the anterior width. Since

anterior width corresponds to the width of the trails of disturbed sediment left by *E.*

rostrata movement, we converted the length to width measurements using a ratio

(length:anterior width) derived from measurements taken of 98 *E. rostrata* specimens

collected by remotely operated vehicle (ROV) and submersible. Monthly mean widths of

E. rostrata observed by the CS decreased from 62 mm (+/- 9 mm) before 2000 to 43 mm

(+/- 13 mm) after 2000 (Fig 15a), while the mean width of *E. rostrata* observed by the

TLC decreased from 90 mm to 80 mm ($\pm$20 mm). Although the decrease in size seen in

the TLC data fell within the error range, the general trend of decreasing size over the

period of the time-series measurements agreed with the CS data. The disparity in

maximum and minimum sizes of *E. rostrata* observed between the CS and TLC data is

most likely due to the differences in spatial coverage and sample size. The CS camera, at

~1m above the seafloor, facilitated measurements of the smallest size class of *E. rostrata*

and the greater spatial coverage enabled the CS to photograph a larger number of

individuals (n_{CS} = 2782) than the TLC (n_{TLC} = 202).

Mean speed of *E. rostrata* individuals observed by the TLC (1.68 ± 0.85 m day^{-1})

did not exhibit a significant positive or negative trend (p > 0.05) over the entire time

series, from 1989 to 2007 (Fig 15a). However, a seasonal pattern in *E. rostrata*

movement speed did emerge. Speed correlated significantly (p<0.05) with sea surface

temperature, which has a primarily seasonal variation, in a non-parametric Spearman

correlation. There was also a significant positive correlation (r_s = 0.36; p<0.0001)

between the size of *E. rostrata* individuals and their speed (Fig. 17a) indicating that

larger organisms moved faster.

The mode of *E. rostrata* bioturbation, "plowing" through the top layer of the

sediment, remained consistent in both TLC and CS photographic records. No *E. rostrata*

were observed in the process of burrowing into the sediment, however on a few occasions

some individuals were covered with sufficient sediment to be nearly obscured. The depth

of the trails created by most *E. rostrata* observed during submersible and ROV dives at

Station M ranged from 0 to 2cm depth. Although not able to be reliably measured from

either TLC or CS photographs, this depth was determined by comparing the measured

heights of *E. rostrata* collected using the submersibles to the depths of the observed

furrows. Here we use an estimated mixing depth of one cm in the bioturbation equation.

Results

The quantity of bioturbation values (n=16) was a product of the occasional lack of

temporal overlap between CS and TLC deployments (Fig. 16). There were a total of 37

months with *E. rostrata* abundance and size data from the CS tows, but only 16 of those

months also included TLC deployments with visible *E. rostrata* that allowed

measurement of movement speed and estimation of the bioturbation rate. Bioturbation

rate calculated using the above values was positively correlated ($r_s = 0.65$; $p < 0.01$) to

POC flux to the seafloor, with changes in bioturbation activity lagging variations in food

supply by ~1 month (Table 3). However, the bioturbation rate did not change

significantly ($p > 0.05$) over the length of the time-series record (Fig. 15a). The lack of

secular change in bioturbation rates was not unexpected due to the relationship with POC

flux, which has also not undergone any secular change over the time period of the time-

series, and the long-term trends seen in the variables used to calculate bioturbation show

either no change (speed, trail depth) or opposing trends (size vs. abundance).

POC flux has previously been correlated to upwelling indicators such as the

Bakun Upwelling Index (BUI), the BUI anomaly and to sea surface temperature (SST)

(Fig. 15b,c) with time lags between upwelling events and changes in the food supply to

the deep sea of ~40 to 60 days at Station M (Baldwin et al. 1998). Climate indices

expressive of El Niño/La Niña such as the Northern Oscillation Index (NOI), the

Multivariate ENSO Index (MEI, Fig. 15d), and the Southern Oscillation Index (SOI)

have also been correlated with POC flux variations and shifts in benthic megafauna

abundance (Ruhl and Smith 2004). The North Pacific Gyre Oscillation Index (NPGO, Di

Lorenzo et al. 2008) is a relatively new indicator of climate variation, and has not

previously been correlated with Station M data. Sea surface temperature (SST) was

calculated for a 50 km radius around Station M using the ocean color and temperature

scanner (OCTS). SST was found to correlate significantly ($r_s = 0.58$; $p < 0.05$) with

bioturbation on a 3-month time lag (Fig. 15c; Table 3). Ruhl and Smith (2004) found that cross correlations between climate indices and several holothuroid species abundances peaked with abundance lagging climate by 11 to 22 months. We found that bioturbation was also correlated with these indices at time lags varying from 3-4 months for the BUI, SST and NPGO, and 16-20 months for the NOI, SOI and MEI (Table 1). The varying time-lags between changes in climate, temperature, upwelling and bioturbation can be attributed to the time necessary for climate variations to impact upwelling, SST and POC flux and for the ensuing flux changes to reach and affect the seafloor community. The parameters used to calculate the bioturbation rate (abundance, size and speed) correlated with POC flux variations on differing time scales. Abundance peaks lagged ~3 months behind POC flux changes, but there was no significant relationship between size and POC flux, for unknown reasons. Conversely, rates of speed shifted nearly instantaneously, with peaks lagging POC flux by ~0-1 months (Table 1). Speed also appeared to have seasonal peaks, coinciding with similar peaks in POC flux and SST (Fig. 15a,c). Some of the temporal lags between climate and bioturbation are the net outcome of changes in size, density and speed values.

Discussion

Epibenthic megafauna feeding and movement have proven to be major factors in incorporating detritus into the benthic food web (Solan et al. 2004b). Detrital material that reaches the seafloor attracts epibenthic fauna which respond to these patches of resources (Levinton and Kelaher 2004; Ruhl and Smith 2004). These epibenthic megafauna then facilitate incorporation of the POC into the sediment where it is rapidly

consumed by infauna and bacteria (Witte et al. 2003). If the activity levels of epibenthic megafauna such as *E. rostrata* are affected by climate-mediated changes in POC flux, the fate of carbon that reaches the seafloor will also be affected.

The calculated bioturbation rate, a product of the intermittent overlap between the CS and TLC deployments as previously stated, may obscure larger trends in bioturbation rate over time as well as seasonal signals. For example, a paired t-test showed that significantly lower numbers ($p < 0.01$) of *E. rostrata* were seen in TLC photographs during summer months than during winter months (Fig. 17b). However, no seasonal pattern was found in the CS abundance data, which may indicate that the difference in the frequency of occurrence variation between TLC and CS abundances was primarily due to changes in movement speed or migration behavior rather than a localized change in population size. These behavioral changes would affect local bioturbation rates, but the impact on sediment mixing over regional to basin scales remains unknown.

Shifting rates of bioturbation linked to climate could greatly impact sediment biology, chemistry and geology. If global warming leads to increased stratification of ocean layers and decreased particle flux (Bopp et al. 2005), rates of bioturbation would also be expected to decline. Decreasing rates of bioturbation would weaken sediment mixing, leading to reduced availability of surface derived POC to deep-sea infauna and bacteria (Reimers et al. 1992; Smallwood et al. 1999), resulting in less incorporation of surface-derived carbon into the infaunal food web (Aller 1982; Kristensen and Blackburn 1987). Less sediment mixing by epibenthic megafauna could potentially strain infauna and microbial populations that depend on the transport of POC deposits from the sediment-water interface deeper into the sediment (Danovaro et al. 2008; Thistle et al.

2008). Restructuring of the benthic community and the rise of new dominant species might also follow such changes in sediment mixing.

Variation in sediment stratification and species composition due to changes in bioturbation rates (McIntyre et al. 1967; Berger and Heath 1968; Guinasso and Schink 1975; Goreau 1980; Hutson 1980) can provide a means of tracking climatic shifts in the geologic record (Behl and Kennett 1996). Diversity oscillations and significant abundance changes in deep-sea benthic species have been linked to variation in climate both in the geologic record (Cronin and Raymo 1997; Cannariato et al. 1999; Cronin et al. 1999; Yasuhara et al. 2008) and in more recent benthic surveys (Ruhl and Smith 2004; Ruhl 2008). Declines in sediment mixing and phytodetritus breakdown by benthic infauna and microbes combined with the decomposition of the nutrient-starved infaunal population could lead to reductions in dissolved oxygen in the sediment and a positive feedback loop that could even further reduce levels of bioturbation. Although even total anoxia does not preclude the breakdown of phytodetritus on the seafloor (Hulthe et al. 1998), the combined impact of reduced bioturbation and impaired sediment oxygenation on the benthic community might render the benthos unable to efficiently respond to and break down large pulses of phytodetritus during more productive periods. This might result in the excess carbon being cycled back into the water column. Alternatively, decreasing bioturbation could lead to increased burial and sequestration of carbon. POC deposits that reach the abyss may simply accumulate on the seafloor if they are not mixed into the sediment and broken down by biological activity.

Deep sediment cores, pore water analyses and isotopic organic carbon tests are necessary to determine the actual fate of the POC being mixed by bioturbation, but it is

clear that climate-mediated changes in POC flux are correlated to deep epibenthic animal behavior and biologically mediated sediment mixing. Climate variation has far-reaching effects on the global carbon cycle, from surface productivity to deep sea bioturbation. Long-term time-series measurements are critical to resolving the links between the surface and deep-sea carbon cycling in the context of changing climate.
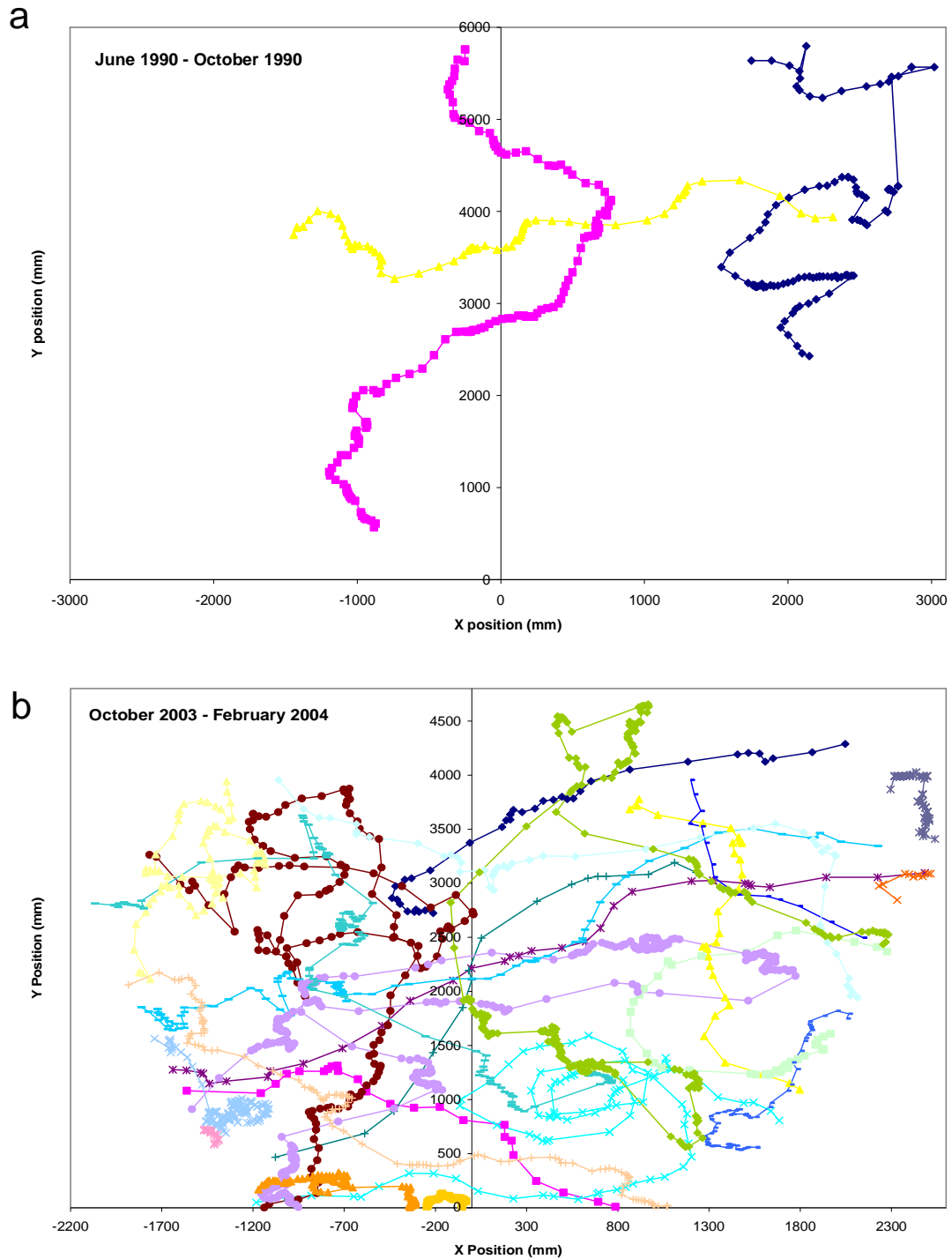
Figure 13. *Echinocrepis rostrata* movement patterns digitized from 4-month autonomous time-lapse camera deployment periods at Station M prior to (a) and subsequent to (b) the 1998 El Niño/La Niña cycle. Lines indicate individual *E. rostrata* trails through the field of view of the camera; units are in mm from the base field of view and the intervals between plotted points are hours.
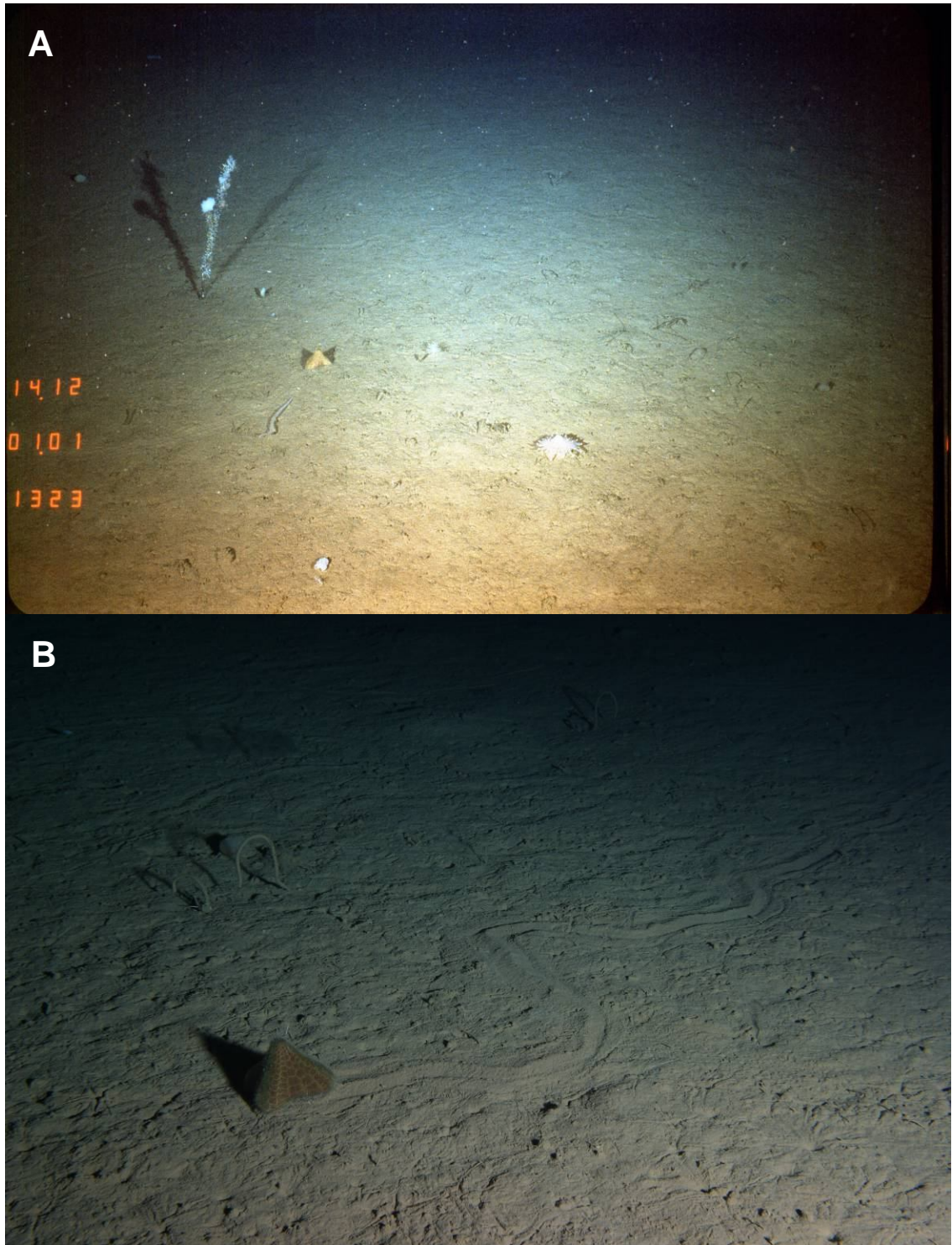
Figure 14. Examples of images from the autonomous time-lapse camera record (A) and the towed camera sled footage (B) taken at Station M, with an *Echinocrepis rostrata* visible in the center of the field of view in each shot. The characteristic trail left in the sediment by *E. rostrata* movement is markedly evident in the camera sled image.
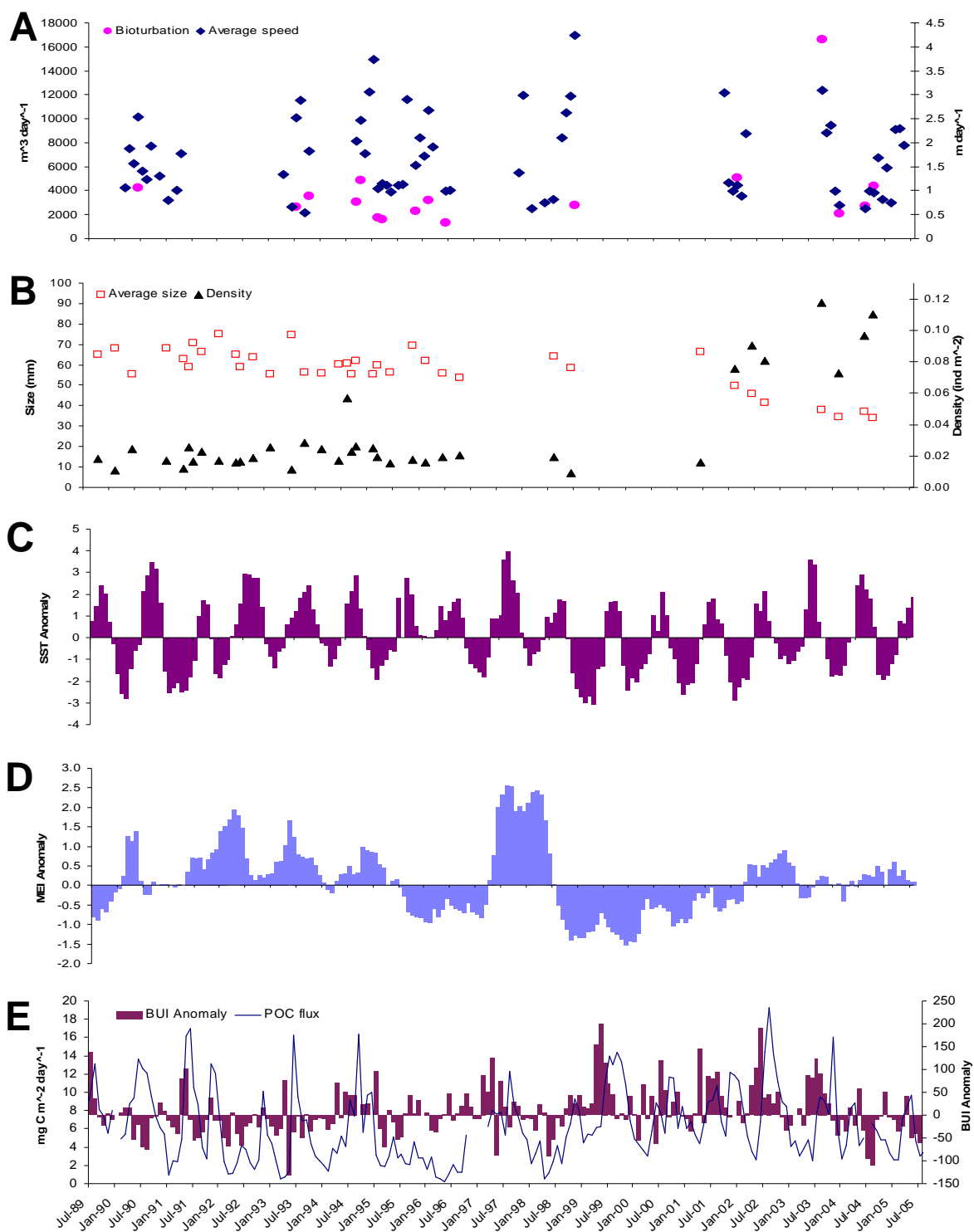
Figure 15. Bioturbation (circles) and *E. rostrata* speed (diamonds) (A), the inverse relationship between *E. rostrata* size (open squares) and density (closed triangles) previously published in Ruhl (2007) (B) the sea surface temperature (SST) anomaly (C), the MEI climate index anomaly (D) and the POC flux composite (blue line) and the BUI anomaly (red bars) (E), from 1989 to 2005.
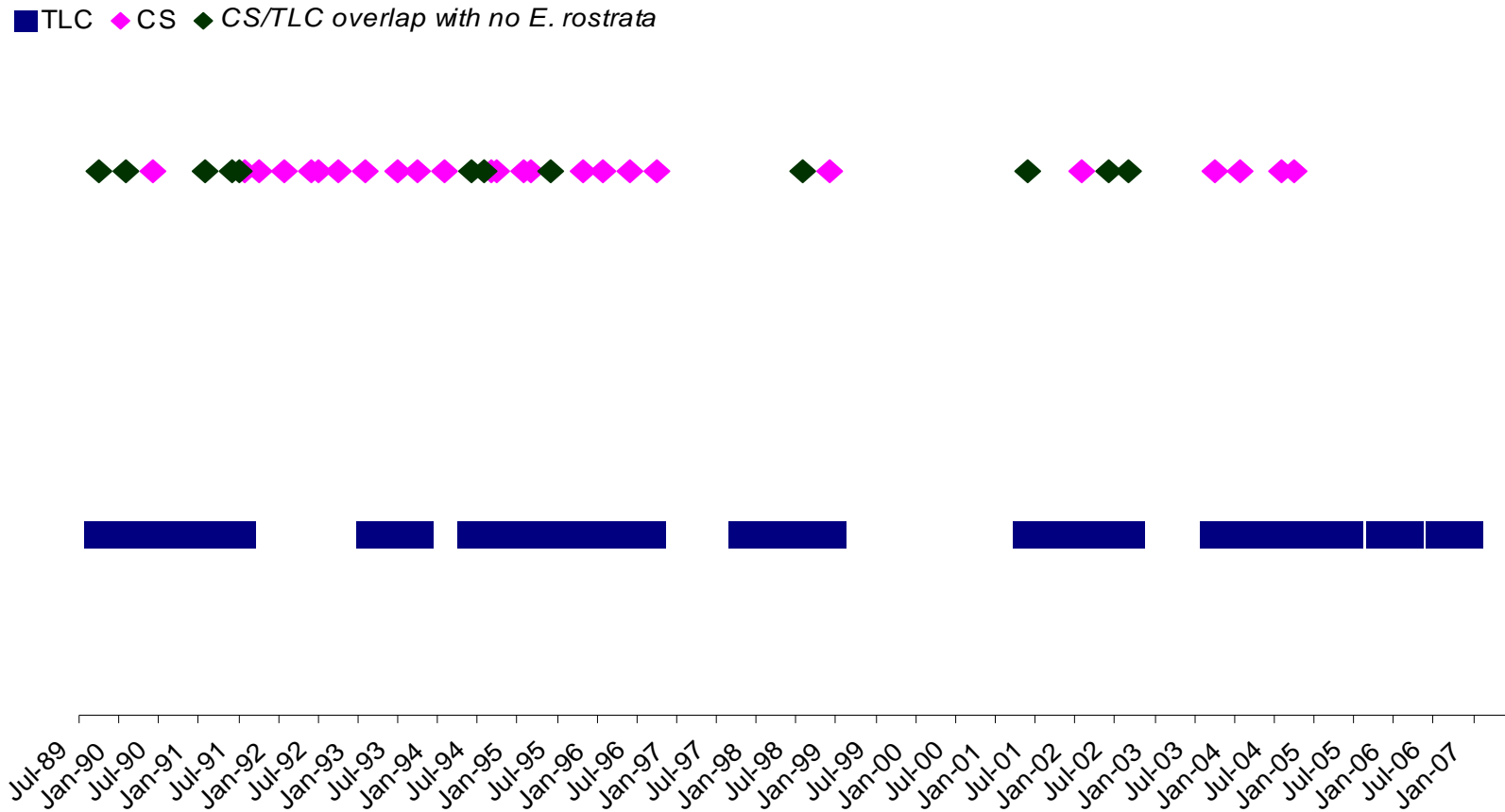
Figure 16. The temporal overlap between months with camera sled (CS) transects and time-lapse camera (TLC) deployments at Station M. The TLC was deployed during 28 of the 37 months with CS transects, but unfortunately 12 of the overlapping deployments were during months when no *E. rostrata* were observed by the TLC (green diamonds).

Table 3. Peaks in time-lagged Spearman rank cross-correlations (r) between climate indices and the factors used to calculate bioturbation. The "activity" term represents size and speed multiplied to derive the area covered by *E. rostrata* movement before adding density numbers to derive population-level bioturbation. The correlations and associated time lags (in months) shown are the peaks in cross correlations (those with the highest r) and are not intended to represent fixed temporal lags. Significant correlations are in bold. n = number of monthly estimates for each correlation

Category	n	NOI r	NOI p	NOI Time lag	SOI r	SOI p	SOI Time lag	MEI r	MEI p	MEI Time lag	NPGO r	NPGO p	NPGO Time lag
Density	37	0.16	0.33	11	0.15	0.37	9	-0.18	0.28	13	0.32	0.06	2
Size	37	0.22	0.18	10	0.14	0.41	14	-0.23	0.16	20	-0.29	0.08	8
Speed	71	-0.21	0.08	15	**-0.25**	**<0.05**	**16**	**0.29**	**<0.05**	**14**	-0.21	0.08	22
Activity	16	**-0.67**	**<0.01**	**12**	**-0.53**	**<0.05**	**15**	**0.61**	**<0.05**	**14**	**-0.55**	**<0.05**	**6**
Bioturbation	16	0.39	0.14	16	**0.53**	**<0.05**	**18**	**-0.51**	**<0.05**	**20**	**0.67**	**<0.01**	**3**
POC flux	206	**0.47**	**<0.001**	**6**	**-0.45**	**<0.001**	**9**	**0.36**	**<0.001**	**10**	**0.41**	**<0.001**	**17**

Category	n	BUI r	BUI p	BUI Time lag	BUI Anomaly r	BUI Anomaly p	BUI Anomaly Time lag	SST (50km radius) r	SST (50km radius) p	SST (50km radius) Time lag	POC flux composite r	POC flux composite p	POC flux composite Time lag
Density	37	**0.46**	**<0.01**	**4**	**0.38**	**<0.05**	**5**	-0.29	0.09	9	**0.39**	**<0.05**	**3**
Size	37	-0.3	0.07	5	**-0.53**	**<0.001**	**5**	0.20	0.23	21	0.21	0.25	18
Speed	71	**0.37**	**0.001**	**4**	**0.34**	**<0.01**	**1**	**0.29**	**<0.05**	**2**	**0.38**	**0.001**	**1**
Activity	16	-0.26	0.33	7	**-0.67**	**<0.01**	**7**	0.31	0.24	15	**-0.66**	**<0.01**	**4**
Bioturbation	16	**0.59**	**<0.05**	**4**	0.48	0.06	13	**0.58**	**<0.05**	**3**	**0.65**	**<0.01**	**1**
POC flux	206	**0.46**	**<0.001**	**2**	**0.31**	**<0.001**	**2**	**-0.53**	**<0.001**	**6**			

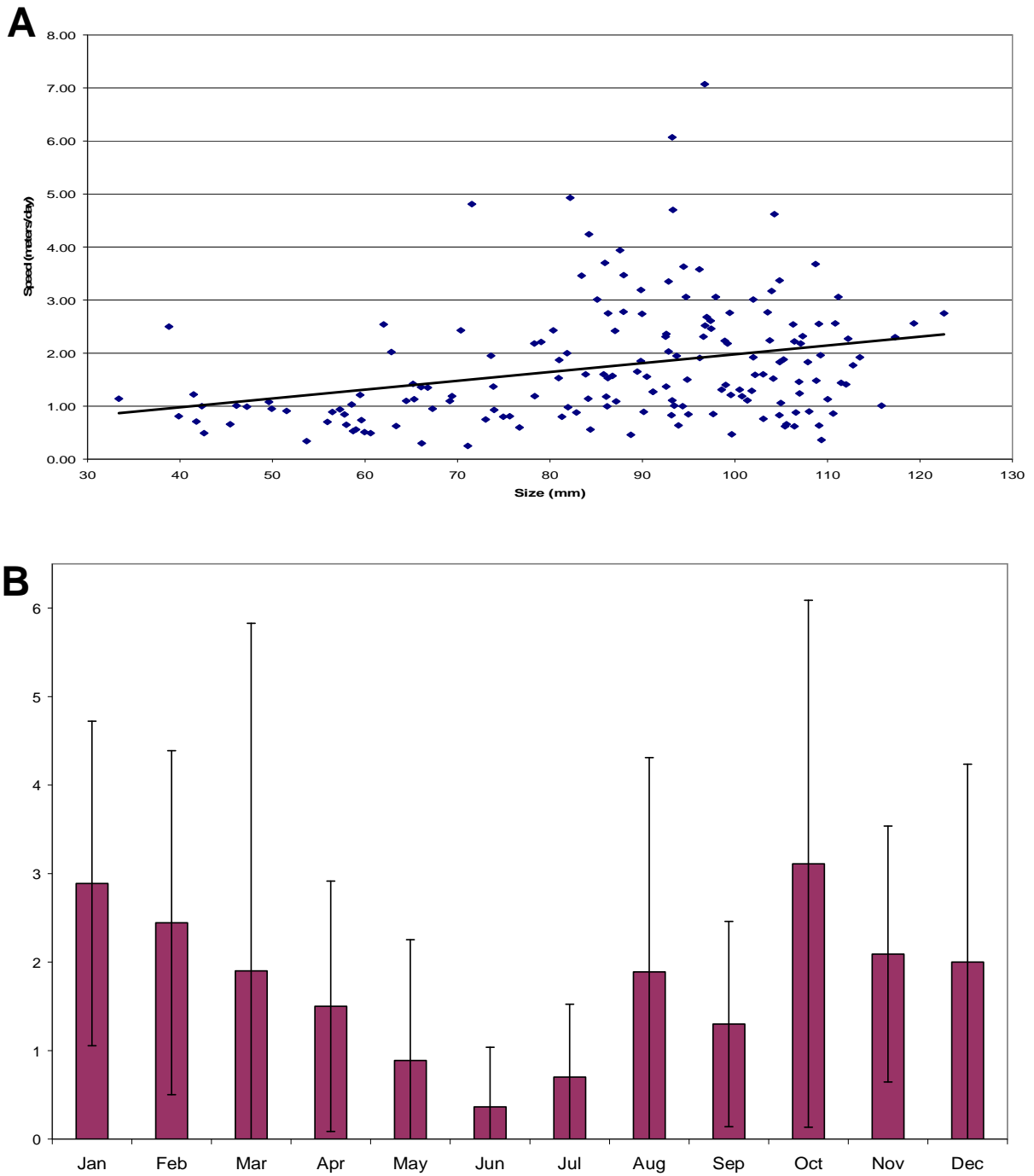**Figure 17**. The positive correlation ($r_s = 0.36$; $p < 0.0001$) between size and average speed of *Echinocrepis rostrata* (A) and the seasonal signal ($p < 0.01$) observed in the monthly average number of *E. rostrata* individuals observed over the 18 year time-lapse camera record (B). The error bars in (B) indicate one standard deviation.

References

Aller RC (1982) The effects of macrobenthos on chemical properties of marine sediment and overlying water. In: McCall PL, Tevesz MJS (eds) Animal-sediment relations---the biogenic alteration of sediments. Topics in geobiology, Vol 2. Plenum Press, New York, pp 53-102

Bakun A (1973) Coastal upwelling indices, west coast of North America, 1946-71. NOAA Tech. Rep. NMFS SSRF-671: 103p

Baldwin R, Smith KL, Jr. (2003) Temporal dynamics of particulate matter fluxes and sediment community response in Port Foster, Deception Island, Antarctica. Deep-Sea Research II 50: 1707-1725

Baldwin RJ, Glatts RC, Smith KL, Jr. (1998) Particulate matter fluxes into the benthic boundary layer at a long time-series station in the abyssal NE Pacific: composition and fluxes. Deep-Sea Research II 45: 643-665

Behl RJ, Kennett JP (1996) Brief interstadial events in the Santa Barbara basin, NE Pacific, during the past 60 kyr. Nature 379: 243-246

Behrenfeld MJ, Boss E, Siegel DA, Shea DM (2005) Carbon-based ocean productivity and phytoplankton physiology from space. Global Biogeochemical Cycles 19: doi:10.1029/2004GB002299

Behrenfeld MJ, Falkowski PG (1997) Photosynthetic rates derived from satellite-based chlorophyll concentration. Limnology and Oceanography 42: 1-20

Behrenfeld MJ, O'Malley RT, Siegel DA, McClain CR, Sarmiento JL, Feldman GC, Milligan AJ, Falkowski PG, Letelier RM, Boss ES (2006) Climate-driven trends in contemporary ocean productivity. Nature 444: 752-755

Berger WH, Heath GR (1968) Vertical mixing in pelagic sediments. Journal of Marine Research 26: 134-143

Bopp L, Aumont O, Cadule P, Alvain S, Gehlen M (2005) Response of diatoms distribution to global warming and potential implications: A global model study. Geophysical Research Letters 32: L19606 doi:19610.11029/12005GL023653

Buckland ST, Anderson DR, Burnham KP, Laake JL (1993) Distance sampling: estimating abundance of biological populations. Chapman and Hall, London, UK

Buesseler KO, Lamborg CH, Boyd PW, Lam PJ, Trull TW, Bidigare RR, Bishop JKB, Casciotti KL, Dehairs F, Elskens M, Honda M, Karl DM, Siegel DA, Silver MW, Steinberg DK, Valdes J, Van Mooy B, Wilson S (2007) Revisiting carbon flux through the ocean's twilight zone. Science 316: 567-570

Cannariato KG, Kennett JP, Behl RJ (1999) Biotic response to late Quaternary rapid climate switches in Santa Barbara Basin: Ecological and evolutionary implications. Geology 27: 63-66

Cronin TM, DeMartino DM, Dwyer GS, Rodriguez-Lazaro J (1999) Deep-sea ostracode species diversity: response to late Quaternary climate change. Marine Micropaleontology 37: 231-249

Cronin TM, Raymo ME (1997) Orbital forcing of deep-sea benthic species diversity. Nature 385: 624-627

Danovaro R, Gambi C, Dell'Anno A, Corinaldesi C, Fraschetti S, Vanreusel A, Vincx M, Gooday AJ (2008) Exponential decline of deep-sea ecosystem functioning linked to benthic biodiversity loss. Current Biology 18: 1-8

Di Lorenzo E, Schneider N, Cobb KM, Franks PJS, Chhak K, Miller AJ, McWilliams JC, Bograd SJ, Arango H, Curchitser E, Powell TM, Riviére P (2008) North Pacific Gyre Oscillation links ocean climate and ecosystem change. Geophysical Research Letters 35: L08607 doi:08610.01029/02007GL032838

Feise RJ (2002) Do multiple outcome measures require p-value adjustment? BMC Medical Research Methodology 2: 8

Goreau TJ (1980) Frequency sensitivity of the deep-sea climatic record. Nature 287: 620-622

Guinasso NL, Schink DR (1975) Quantitative estimates of biological mixing rates in abyssal sediments. Journal of Geophysical Research 80: 3032-3043

Hulthe G, Hulth S, Hall POJ (1998) Effect of oxygen on degradation rate of refractory and labile organic matter in continental margin sediments. Geochimica et Cosmochimica Acta 62: 1319-1328

Hutson WH (1980) Bioturbation of deep-sea sediments: Oxygen isotopes and stratigraphic uncertainty. Geology 8: 127-130

Kahru M, Mitchell BG (2002) Influence of the El Niño-La Niña cycle on satellite-derived primary
production in the California Current. Geophysical Research Letters 29: 1846 doi:1810.1029/2002GL014963

Kiørboe T (2001) Formation and fate of marine snow: small-scale processes with large-scale implications. Scientia Marina 65: 57-71

Kiørboe T, Thygesen UH (2001) Fluid motion and solute distribution around sinking aggregates. II. Implications for remote detection by colonizing zooplankters. Marine Ecology Progress Series 211: 15-25

Kristensen E, Blackburn TH (1987) Fate of organic carbon and nitrogen in experimental marine sediment systems: Influence of bioturbation and anoxia. Journal of Marine Research 45: 231-257

Laake JL, Buckland ST, Anderson DR, Burnham KP (1994) Distance users guide version 2.1. Colorado State University, Fort Collins, Colorado, USA

Lampitt RS (1992) The contribution of deep-sea macroplankton to organic remineralization: results from sediment trap and zooplankton studies over the Madeira Abyssal Plain. Deep-Sea Research 39: 221-233

Laws EA (2004) New production in the equatorial Pacific: a comparison of field data with estimates derived from empirical and theoretical models. Deep-Sea Research I 51: 205-211

Lee C, Murray DW, Barber RT, Buesseler KO, Dymond J, Hedges JI, Honjo S, Manganini SJ, Marra J, Moser C, Peterson ML, Prell WL, Wakeham SG (1998) Particulate organic carbon fluxes: compilation of results from the 1995 US JGOFS Arabian Sea Process Study. Deep-Sea Research II 45: 2489-2501

Levinton J, Kelaher B (2004) Opposing organizing forces of deposit-feeding marine communities. Journal of Experimental Marine Biology and Ecology 300: 65-82

Lohrer AM, Thrush SF, Hunt L, Hancock N, Lundquist C (2005) Rapid reworking of subtidal sediments by burrowing spatangoid urchins. Journal of Experimental Marine Biology and Ecology 321: 155-169

Martin JH, Knauer GA, Karl DM, Broenkow WW (1987) VERTEX: carbon cycling in the northeast Pacific. Deep-Sea Research 34: 267-285

McIntyre A, Bé AWH, Preikstas R (1967) Coccoliths and the Pliocene-Pleistocene boundary. Progress in Oceanography 4: 3-8

Miller RJ, Smith CR, DeMaster DJ, Fornes WL (2000) Feeding selectivity and rapid particle processing by deep-sea megafaunal deposit feeders: A [234]Th tracer approach. Journal of Marine Research 58: 653-673

Pfannkuche O (1993) Benthic response to the sedimentation of particulate organic matter at the BIOTRANS station, 47 degree N, 20 degree W. Deep-Sea Research II 40: 135-150

Pfannkuche O, Boetius A, Lochte K, Lundgreen U, Thiel H (1999) Responses of deep-sea benthos to sedimentation patterns in the North-East Atlantic in 1992. Deep-Sea Research I 46: 573-596

Reimers CE, Jahnke RA, McCorkle DC (1992) Carbon fluxes and burial rates over the continental slope and rise off central California with implications for the global carbon cycle. Global Biogeochemical Cycles 6: 199-224

Ruhl HA (2007) Abundance and size distribution dynamics of abyssal epibenthic megafauna in the northeast Pacific. Ecology 88: 1250-1262

Ruhl HA (2008) Community change in the variable resource habitat of the abyssal northeast Pacific. Ecology 89: 991-1000

Ruhl HA, Smith KL, Jr. (2004) Shifts in deep-sea community structure linked to climate and food supply. Science 305: 513-515

Schwing FB, Murphree T, Green PM (2002) The Northern Oscillation Index (NOI): a new climate index for the northeast Pacific. Progress in Oceanography 53: 115-139

Smallwood BJ, Wolff GA, Bett BJ, Smith CR, Hoover D, Gage JD, Patience A (1999) Megafauna can control the quality of organic matter in marine sediments. Naturwissenschaften 86: 320-324

Smith CR, Levin LA, Hoover DJ, McMurtry G, Gage JD (2000) Variations in bioturbation across the oxygen minimum zone in the northwest Arabian Sea. Deep-Sea Research II 47: 227-257

Smith KL, Jr., Baldwin RJ, Ruhl HA, Kahru M, Mitchell BG, Kaufmann RS (2006) Climate effect on food supply to depths greater than 4,000 meters in the northeast Pacific. Limnology and Oceanography 51: 166-176

Smith KL, Jr., Kaufmann RS, Wakefield WW (1993) Mobile megafaunal activity monitored with a time-lapse camera in the abyssal North Pacific. Deep-Sea Research I 40: 2307-2324

Smith KL, Kaufmann RS, Baldwin RJ (1994) Coupling of near-bottom pelagic and benthic processes at abyssal depths in the Eastern North Pacific-Ocean. Limnology and Oceanography 39: 1101-1118

Solan M, Cardinale BJ, Downing AL, Engelhardt KAM, Ruesink JL, Srivastava DS (2004a) Extinction and ecosystem function in the marine benthos. Science 306: 1177-1180

Solan M, Wigham BD, Hudson IR, Kennedy R, Coulon CH, Norling K, Nilsson HC, Rosenberg R (2004b) *In situ* quantification of bioturbation using time-lapse fluorescent sediment profile imaging (f-SPI), luminophore tracers and model simulation. Marine Ecology Progress Series 271: 1-12

Stemmann L, Jackson GA, Ianson D (2004) A vertical model of particle size distributions and fluxes in the midwater column that includes biological and physical processes—Part I: model formulation. Deep-Sea Research I 51: 865-884

Thistle D, Eckman JE, Paterson GLJ (2008) Large, motile epifauna interact strongly with harpacticoid copepods and polychaetes at a bathyal site. Deep-Sea Research I 55: 324-331

Trenberth KE, Shea DJ (1987) On the evolution of the Southern Oscillation. Monthly Weather Review 115: 3078-3096

Wakefield WW, Genin A (1987) The use of a Canadian (perspective) grid in deep-sea photography. Deep-Sea Research 34: 469-478

Wakefield WW, Smithey W (1989) Two camera sleds for quantitative study of deep-sea megafauna. Scripps Institution of Oceanography, La Jolla, California, USA

Witte U, Wenzhofer F, Sommer S, Boetius A, Heinz P, Aberle N, Sand M, Cremer A, Abraham W-R, Jørgenson BB, Pfannkuche O (2003) *In situ* experimental evidence of the fate of a phytodetritus pulse at the abyssal sea floor. Nature 424: 763-766

Wolf PR (1983) Elements of photogrammetry: with air photo interpretation and remote sensing. McGraw Hill, New York

Wolter K, Timlin MS (1998) Measuring the strength of ENSO - how does 1997/98 rank? Weather 53: 315-324

Yasuhara M, Cronin TM, deMenocal PB, Okahashi H, Linsley BK (2008) Abrupt climate change and collapse of deep-sea ecosystems. PNAS 105: 1556-1560

VI

The Effects of *Echinocrepis rostrata* Bioturbation on Abyssal Sediment Mixing

Abstract

Biological mixing of seafloor sediment, or bioturbation, plays an important role in determining the degree of recycling or burial of particles reaching the deep-sea floor. This study used deep-sea sediment cores recovered using manned and unmanned submersibles to determine the quantity of mixing that was attributable to bioturbation by *Echinocrepis rostrata*, a common deep-sea epibenthic echinoid. Thirty-two paired push core samples were collected between 2005 and 2007 from sediment trails recently created by *E. rostrata* and local undisturbed sediment at 4100 m depth in the eastern North Pacific. Radioactive isotope activity, carbon content and chlorophyll concentrations were measured in the top four cm of sediment from the push core samples. No significant differences were found in the ^{234}Th:^{210}Pb ratio, carbon content, or chlorophyll and phaeopigment concentrations between the control and bioturbated cores. The negative result may have been due to low particulate organic carbon (POC) flux rates at the study site during the sampling period, patchy distribution of newly deposited phytodetritus material in the areas cored, or negligible particulate matter ingestion and disturbance by *E. rostrata* in areas with small amounts of organic carbon. Future bioturbation studies will take background phytodetritus concentrations during sampling into account, and measure possible horizontal mixing by epibenthic megafauna.

Introduction

The fate of carbon that is buried in the deep sea sediments is largely determined by sediment disturbance caused by biological activity, or bioturbation (Gray 1974; Rhoads 1974; Aller 1982; Rhoads and Boyer 1982; Reimers et al. 1992; Smallwood et al.

1999; Miller et al. 2000). Bioturbation can also be a confounding influence on the temporal interpretation of sediment layers (McIntyre et al. 1967; Berger and Heath 1968; Guinasso and Schink 1975; Goreau 1980; Hutson 1980) and a means for transporting organic carbon deeper into the sediment, making it available to bacteria and infauna (Witte et al. 2003; Solan et al. 2004). However, relatively little is known about the role of deep-sea epibenthic megafauna in determining whether newly settled organic material will be buried or recycled into the water column. Epibenthic bioturbation can affect the geochemistry of sediments by disrupting fluid flow, homogenizing particle gradients created by macroinfauna and phytodetritus settlement, and by displacing, ingesting, and transporting sediment particles (Hoover 1995). Some infaunal and bacterial populations, which can be highly concentrated in surface sediments (Reimers and Smith 1986), are likely to be disturbed or buried by epibenthic bioturbation events, while newly settled organic carbon is simultaneously made available to the infaunal community that remains. The sampling experiments made possible by submersible technology allow for detailed studies of the controls on and consequences of deep-sea bioturbation and feeding behavior.

A long-term time-series study conducted at 4100m depth in the northeast Pacific Ocean demonstrated that one of the most common mediators of bioturbation at the study site was the irregular echinoid *Echinocrepis rostrata* (Smith et al. 1993). *Echinocrepis rostrata* is an epibenthic species that forages for phytodetritus and other food by "plowing" through the top layers of the sediment. In addition to ingesting organic carbon, the movement of *E. rostrata* through the top few cm of the sediment leaves distinctive trails, and may mix newly fallen particulate organic carbon (POC) and

phytodetritus aggregates deeper into the sediment. Recent findings from long-term photographic surveys at this study site (Ruhl 2007) show an order of magnitude increase in the abundance of *E. rostrata* between 2000 and 2005 following a strong El Niño/La Niña event in 1998-1999, as well as positive correlations between bioturbation activity and POC flux levels (Chapter V). If increases in ocean temperature amplify stratification and decrease nutrient availability at the surface, it could cause reductions in phytoplankton size, increase recycling of nutrients in surface layers and decrease particulate organic carbon (POC) flux (Bopp et al. 2005). The combination of factors make it important to discover how *E. rostrata* bioturbation affects deep-sea sediment and the carbon cycle. Decreasing rates of bioturbation due to a decline in POC flux would reduce sediment mixing, making surface derived POC inaccessible to deep-sea infauna and bacteria (Reimers et al. 1992; Smallwood et al. 1999), and resulting in reduced burial and remineralization of carbon.

Positive correlations between bioturbation by deep-sea epifauna and the diversity of infaunal sediment communities (e.g. Lohrer et al. 2004; Gallucci et al. 2008; Thistle et al. 2008) and rates of mixing of organic matter (e.g. DeMaster et al. 1994; Fornes et al. 1999; Smith et al. 2000) have been shown in previous studies. Submersible and remotely operated vehicle (ROV) technologies allow for more specific identification and sampling of sediment that has recently undergone bioturbation. We examined sediment push cores collected by manned and unmanned submersibles to determine how much mixing of deep-sea sediments is a result of *E. rostrata* bioturbation. Using stable isotopes to directly measure the mixing of the sediment before and after *E. rostrata*-mediated bioturbation provides previously unavailable data on the chemistry and homogenization

levels of recently disturbed sediment in the deep sea. Knowledge of the overall nutrient content of pre- and post-feeding surface sediments, estimated by measuring concentrations of chlorophyll and organic carbon, could also help to incorporate *E. rostrata* bioturbation into models of the deep-sea carbon cycle and carbon sequestration rates.

Materials and Methods

Push Core Collection

All of the sediment samples for this study were collected at a long-term time-series station in the northeastern Pacific Ocean known as Station M, located ~220 km west of Point Conception, California, USA (34°50'N, 123°00'W) at a depth of ~4,100 m. Station M is subject to strong seasonal pulses of surface productivity, a major factor in the selection of this study site (Smith et al. 1992). The sea floor at 4100 m has very little topographic relief (< 100 m over 1,600 km^2) and is composed of silty-clay sediment with seasonal deposits of flocculent phytodetritus. Sedimentation rates vary from 0-20 days for large phytodetritus aggregates to >100 days for small particulates (Lauerman et al. 1997). Currents near the seafloor average 3.8 cm s^{-1}, can reach a maximum of 18.2 cm s^{-1} and flow to the south during periods of highest current speeds and towards the north and west during the periods of low current speeds (Beaulieu and Baldwin 1998). Time-lapse photographs taken at this site have revealed abundant evidence of bioturbation and other epifaunal activity at the site in the form of numerous trails, furrows and mounds that range in width from centimeters to meters (Smith et al. 1993).

Sixteen pairs of 6.35 cm diameter push core sediment samples were taken at Station M using manned and unmanned submersibles during four cruises between

November 2005 and September 2007. Moving *E. rostrata* echinoids were identified on the seafloor by eye or video monitoring. The depth of the trails created by most *E. rostrata* at Station M ranged from 0 to 2cm depth. Only *E. rostrata* with distinct sediment trails ≥1 cm deep were chosen for sampling. Using the robotic arm of the submersible, a control core was inserted vertically into an undisturbed area of sediment next to the *E. rostrata* individual and an experimental core was inserted into the sediment directly behind the individual, centered in the trail (Fig. 18). After both cores were in place and the purge valves closed the cores were removed and placed in a quiver onboard the submersible for recovery.

Core sectioning

Once the submersible had been recovered by the surface vessel, the cores were immediately taken to a refrigerated van or cold room (~2°C) and sectioned. Of the 32 total cores recovered, eight cores were sectioned at 0.25 cm intervals down to a depth of 4 cm. The sections from four of these cores were placed in pre-weighed gamma vials and refrigerated until they could be transported back to the lab, where the sediment was then dried, ground, weighed and shipped to Claudia Benitez-Nelson at the University of South Carolina for ^{234}Th and ^{210}Pb isotope analysis. The other 24 cores were all sectioned at 0.25 cm intervals down to 1 cm and then every cm down to a depth of 4 cm. Each section was homogenized, and then split into two cryovials: one for phaeopigment analysis and one for carbon/hydrogen/nitrogen (CHN) analysis. The cryovials were then frozen in liquid nitrogen and then stored in a -80°C freezer until analysis.

Isotope analysis

The naturally occurring radionuclides ^{234}Th and ^{210}Pb, which are strongly adsorbed by particles in the water column, can be used to trace the ingestion of particulate matter by benthic organisms (Aller and DeMaster 1984; Moore and Dymond 1988). ^{234}Th is produced by ^{238}U decay and is scavenged by particles sinking through the water column. The short half-life (24.1 d) of ^{234}Th makes it very useful in identifying newly settled particles on ~100-d time scales. ^{210}Pb, produced in situ from ^{226}Ra and atmospheric input, has a long half-life (22.3 yr) relative to ^{234}Th. ^{210}Pb can be used to track particles on the order of 100 yr and is effectively stable over the time scales relevant to this study. Previous studies have found homogenization of ^{210}Pb activity levels down to depths of 2-3 cm in sediment recently disturbed by echinoid bioturbation activity (D.J. Hoover, personal communication).

Gamma ray spectrometry using an intrinsic well germanium detector with a resolution of 0.1% was performed to determine the activities, in counts per minute (cpm), of ^{234}Th and ^{210}Pb in the samples sent to South Carolina (Moore 1984; Thunell et al. 1994). Measured activities were converted to disintegrations per minute per gram (dpm g^{-1}) using liquid standards measured in the same geometry. To account for any possible fractionation due to compositional or grain size changes, excess (unsupported by decay of parent radionuclide) ^{210}Pb activity was used to normalize excess ^{234}Th activity. The ^{234}Th: ^{210}Pb activity ratio can be used to calculate apparent age differences between particulate matter from the sediment samples taken from disturbed and undisturbed areas of the seafloor. Such ages could indicate whether *E. rostrata* were mixing freshly settled (^{234}Th-rich) particles deeper into the older (^{234}Th-poor) sediment. Nonparametric Mann-

Whitney tests were performed on the mean values of ^{210}Pb activity, ^{234}Th activity, and the ^{234}Th: ^{210}Pb activity ratio from each core.

CHN analysis

Samples from 23 cores (one set of core sections was damaged during freezing and could not be used) were sent to the MSI Analytical Lab at UC Santa Barbara for CHN analysis. Each sample was freeze dried overnight and ground in a mortar and pestle. The elemental composition of organic material in the sediment samples was determined using an Automated Organic Elemental Analyzer (Dumas combustion method) which simultaneously analyzes the weight percentage of carbon (C), hydrogen (H), and nitrogen (N) in ~10 mg of sediment. Nonparametric Mann-Whitney tests were performed on the mean values of carbon and C:N ratio from each core, as well as the mean carbon and C:N ratio values from each individual 0.25 cm section. Inorganic carbon in each sample was measured using a UIC carbon coulometer and acidification module, but the proportion of inorganic to organic carbon in the sediment samples was negligible (0-100 ppm), even in the topmost layers of sediment.

Fluorometric analysis

Sections from 12 cores were kept in low-light conditions for chlorophyll and phaeopigment analysis on a fluorometer (Holm-Hansen et al. 1965). Sediment samples were freeze dried for 24 hours, then ground using a mortar and pestle, and weighed. One gram of sediment was placed in a 15 mL centrifuge tube, and then ~10 mL of 90% acetone was added to each tube. The sample tubes were incubated overnight in a -20ºC refrigerator to extract the pigments. The tubes were then centrifuged at 800g for 5

minutes, after which 10 mL of supernatant was decanted into a fluorometry tube.

Samples were run on a Turner Designs (Sunnyvale, CA) 10-AU Fluorometer to

determine the chlorophyll A concentration. After the chlorophyll number was recorded,

2 drops of 5% HCl were added to the sample to get a phaeopigment number. The results

from the fluorometer were then interpreted by an equation that incorporated sample

weight, solvent volume and instrument-specific response values to derive chlorophyll and

phaeopigment concentrations ($\mu g/g$). Nonparametric Mann-Whitney tests were

performed on the mean chlorophyll and phaeopigment concentrations ($\mu g/g$) from each

core, as well as the chlorophyll and phaeopigment concentrations ($\mu g/g$) of each

individual 0.25 cm section.

Results

Cores taken from areas that had recently been disturbed by *E. rostrata* showed

no evidence of any mixing of ^{234}Th-enriched material deeper into the sediment (Fig.

19A). ^{234}Th activity levels below a depth of 0.25 cm were not significantly elevated

above background concentrations (<0.20 cpm) to indicate bioturbation. The low ^{234}Th

values made it impossible to determine if bioturbation had mixed newer, ^{234}Th-rich,

material deeper into the sediment. In addition, there was no evidence of homogenization

of isotope values in the cores taken from bioturbated areas. No significant difference

($p>0.05$) in excess ^{210}Pb (Fig. 19B), excess ^{234}Th or the ^{234}Th: ^{210}Pb activity ratios was

found between the two control and two experimental cores.

The CHN analysis on 23 sediment cores found no significant differences

between the control and experimental cores that would conclusively indicate bioturbation

activity (Table 4). Data was recovered on the weight percentage of carbon, hydrogen and nitrogen, and the C:N ratio for each section of all the cores. Statistical tests showed no significant difference ($p>0.05$) between the carbon content in the control versus experimental sections. The carbon content and C:N ratio in the top cm of sediment was slightly higher in control cores ($\%C = 1.63 \pm 0.10$; C:N = 7.01 ± 0.48) than in the experimental cores ($\%C = 1.61 \pm 0.11$; C:N = 6.89 ± 0.51), although these differences were within the error range and not statistically significant.

The mean chlorophyll and phaeopigment content of the top cm of sediment was higher in the control ($conc_{chla} = 8.85 \pm 5.76$ µg/g; $conc_{phaeo} = 308.77 \pm 162.45$ µg/g) than in the experimental cores ($conc_{chla} = 7.82 \pm 4.92$ µg/g; $conc_{phaeo} = 259.90 \pm 131.41$ µg/g) as well as in the top four 0.25 cm core layers (Table 4). However, the mean chlorophyll and phaeopigment concentrations of each 0.25 cm sediment core layer and whole cores showed no significant difference ($p>0.05$) between control and experimental cores.

Discussion

Although previous studies have successfully examined sediment isotope values at Station M (Lauerman et al. 1997) and sites at similar depths (Aller and DeMaster 1984; Buesseler et al. 1992; Clough et al. 1997; Borole 2002; Demopoulos et al. 2003), the background ^{234}Th levels found at deep-sea sites were always very low (~10-20 dpm/g). Depletion of ^{234}Th in seafloor sediments is generally due to the time it takes for fresh phytodetritus material to reach the seafloor. The isotope values measured in the sediment samples from this study were much lower than expected, even given the extreme depth of Station M. The time delay between sample collection and measurement of isotope

concentrations (13 to 50 d), and possible factors such as unusually low influx of POC at the site may have resulted in depleted isotope values that provided little useful information on mixing depth due to bioturbation. The patchy nature of phytodetritus falls (Smith et al. 1994; Smith et al. 1996; Smith et al. 1998) and the lack of fresh samples of phytodetritus aggregates to compare to the background sediment made it difficult to detect mixing events. In addition, the short (24.1 d) half-life of ^{234}Th may have allowed the ^{234}Th content of the sediment samples to decay past the minimum detectable limit during the time that elapsed between sample collections and isotope measurements. This delay was an unavoidable result of weather difficulties, time required to return to shore, sample processing time, shipping time and a backlog of samples at the analytical lab that performed the spectroscopy. Conical sediment traps deployed at Station M nearly continuously since 1989 (Smith and Druffel 1998) have demonstrated that POC flux levels at Station M are highly variable seasonally and interannually, ranging from 0.18 to 25.21 mgC m^{-2} d^{-1}. The sample collections in November 2005 were conducted during a period of relatively low POC flux (<3 mgC m^{-2} d^{-1}), which would likely result in highly ^{234}Th-depleted sediment. Because the POC flux rates could not be determined until after the sediment trap samples recovered during the same cruise had been analyzed in the laboratory, there was no way to know whether POC flux rates were higher or lower than normal at the time. Sediment samples taken during a period of higher flux would be more likely to exhibit isotopic variation between bioturbated sediment and undisturbed sediment.

The absence of significant differences in the organic carbon or chlorophyll content of the control and experimental cores may also be related to the patchy nature of

phytodetritus aggregate falls, or to the feeding strategy of *E. rostrata*. Sampling of the gut contents of various deep-sea epibenthic megafauna has shown that most preferentially consume freshly deposited organic material, often in the form of phytodetritus aggregates (Pfannkuche and Lochte 1993; Lauerman et al. 1997; Miller et al. 2000; Demopoulos et al. 2003; Howell et al. 2004; Hudson et al. 2004). *Echinocrepis rostrata* have been observed changing the direction of movement towards newly fallen phytodetritus and consuming large aggregates on the seafloor (M. Vardaro, personal observation). Since POC flux is variable seasonally and interannually at the Station M study site, and the area of the seafloor that is covered by phytodetritus aggregates can be patchy on the scale of *E. rostrata*, even during extremely high flux events, it is possible that the sampling sites for this study were not enriched enough in carbon or chlorophyll to provide evidence of feeding behavior. The tracks that were sampled by the submersible may have been produced only by movement, not feeding, and any sediment mixing due to the movement of *E. rostrata* might not be detectable. Even if some of the organic material in the experimental cores was ingested, the absence of detectable amounts of phytodetrital material in the control cores could be responsible for the similarity between cores in front and behind the moving *E. rostrata* echinoids. The slightly higher carbon content and chlorophyll concentration in the top cm of the control cores compared to the slightly lower amounts of carbon and chlorophyll in the top cm of the experimental cores, while not statistically significant, suggests that some mixing or organic particle consumption was taking place. Sampling during a period of higher flux or coring only trails that pass through patches of phytodetritus would likely provide more evidence of mixing.

One potentially significant aspect of *E. rostrata* bioturbation that was not explicitly examined in this study was horizontal sediment transport. The mobility of *E. rostrata* could horizontally redistribute recently settled material across the sediment surface (Wheatcroft 1991; Smith et al. 1993) and change the chemistry of these particles in the process. By ingesting and concentrating phytodetritus aggregates, transporting them and then redistributing them as fecal material, horizontal heterogeneity of the seafloor would be increased. This horizontal component could be as important as the more commonly considered vertical component to the impacts of bioturbation on seafloor chemistry and geology. If *E. rostrata* bioturbation is more horizontally than vertically oriented, paired core samples from recently disturbed and control locations may not be sufficient to quantify the effect of *E. rostrata* movement and feeding on sediment chemistry. Horizontal bioturbation could be traced using artificial tracers such as dyes or luminophore beads, or additional core samples from multiple positions along the trail left behind a moving *E. rostrata* individual.

Although this study did not find conclusive evidence of the effect of *E. rostrata* bioturbation on sediment chemistry, previous work in the equatorial Pacific has shown that epifaunal echinoids can homogenize the top layers of sediment and redistribute phytodetrital material (Hoover 1995). The minimal differences between control and bioturbated cores in this study may have been due to low POC flux rates at Station M when compared to more eutrophic study areas, or to low feeding and/or mixing rates of *E. rostrata* in regions containing small amounts of newly arrived phytodetritus. The potential effects of bioturbation on carbon burial, infaunal and bacterial access to organic material, pore water flow and sediment particle sizes add significant complexity to

tracing the fate of organic carbon that reaches the deep sea. The collection of more sediment cores at different times of year and different time scales is necessary to parameterize bioturbation by *E. rostrata* and other epifauna if accurate models of carbon flux and sequestration are to be generated.
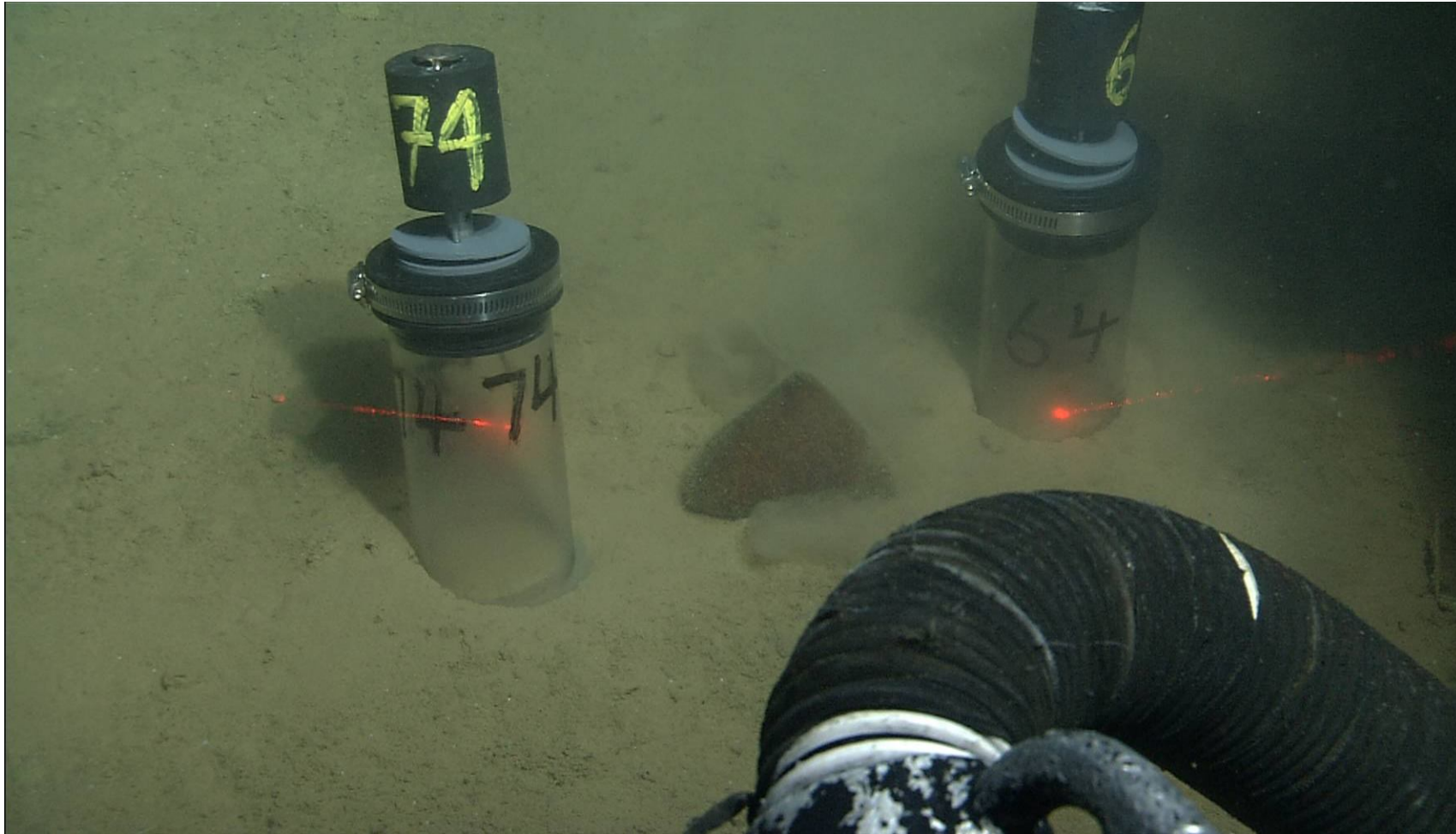
Figure 18. A high-definition still image from the ROV Tiburon, taken during sediment push core recovery. The *E. rostrata* echinoid in the center of the frame was moving from left to right. Thus, core 74 (left) was the experimental core placed in the trail behind the animal, and core 64 (right) was the control core, placed in undisturbed sediment in front of the animal. The ROV's suction sampler, used for collecting animals, is visible in the bottom right of the frame. The distance between the lasers is 29 cm.
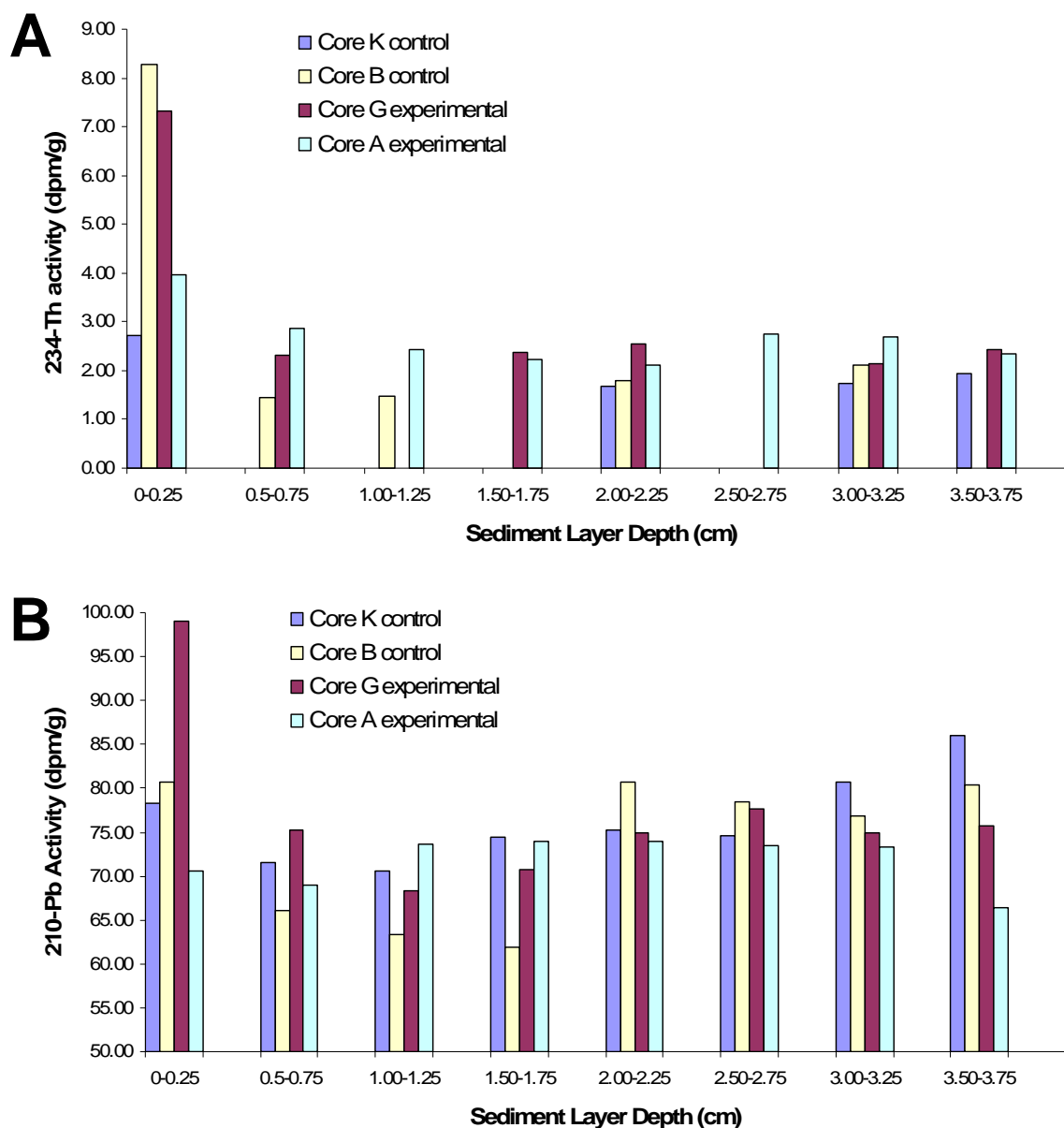
Figure 19. Measured activities of excess [234]Th (A) and [210]Pb (B) in disintegrations per minute per gram dry weight from the two pairs of cores taken in front (control) and behind (experimental) *E. rostrata* echinoids at Station M. Every other 0.25 cm section was skipped to minimize cost and sampling time. Zero values in the [234]Th data indicate levels of [234]Th activity too low to be detected by gamma ray spectroscopy.

Table 4. Mean carbon content (% by weight) and the carbon/nitrogen ratio from 23 sediment cores sent for CHN analysis. Mean chlorophyll a concentrations (µg/g) and phaeopigment concentrations (µg/g) are from the 12 cores analyzed fluorometrically.

Sediment Layer Depth (cm)	% Carbon			C/N Ratio			Chlorophyll (µg/g)			Phaeopigment (µg/g)		
	Control	Exp.	p-value	Control	Exp.	p-value	Control	Exp.	p-value	Control	Exp.	p-value
0-0.25	1.674 ±0.106	1.607 ±0.113	0.1179	7.25 ±0.34	6.97 ±0.48	0.0688	11.02 ±8.92	7.93 ±5.87	0.9372	427.77 ±208.51	334.55 ±154.58	0.3095
0.25-0.5	1.628 ±0.103	1.585 ±0.082	0.2875	6.96 ±0.55	6.87 ±0.60	0.7399	7.51 ±4.36	6.92 ±4.18	0.8182	320.46 ±159.71	251.60 ±135.80	0.2403
0.5-0.75	1.611 ±0.092	1.594 ±0.103	0.5619	6.91 ±0.36	6.86 ±0.53	0.6075	8.95 ±5.26	7.14 ±4.31	0.5887	257.48 ±122.32	229.76 ±113.60	0.4848
0.75-1.00	1.614 ±0.075	1.646 ±0.132	0.7045	6.90 ±0.62	6.85 ±0.49	0.8633	7.93 ±4.18	9.29 ±6.05	0.5887	229.39 ±97.81	223.68 ±121.52	0.9372
1.00-2.00	1.637 ±0.071	1.668 ±0.100	0.5027	7.01 ±0.48	6.67 ±0.36	0.1128	8.31 ±4.01	9.58 ±5.84	0.6991	205.02 ±97.94	205.95 ±103.31	0.9372
2.00-3.00	1.730 ±0.085	1.782 ±0.091	0.2469	7.10 ±0.52	7.22 ±0.41	0.4562	13.88 ±10.11	16.08 ±9.34	0.9372	219.59 ±98.04	259.53 ±123.85	0.4848
3.00-4.00	1.788 ±0.078	1.849 ±0.113	0.2276	7.25 ±0.42	7.41 ±0.46	0.4491	16.98 ±10.15	15.82 ±9.24	0.9372	264.84 ±125.82	286.44 ±140.23	1

References

Aller RC (1982) The effects of macrobenthos on chemical properties of marine sediment and overlying water. In: McCall PL, Tevesz MJS (eds) Animal-sediment relations---the biogenic alteration of sediments. Topics in geobiology, Vol 2. Plenum Press, New York, pp 53-102

Aller RC, DeMaster DJ (1984) Estimates of particle flux and reworking at the deep-sea floor using ^{234}Th/^{238}U disequilibrium. Earth and Planetary Science Letters 67: 308-318

Beaulieu S, Baldwin R (1998) Temporal variability in currents and the benthic boundary layer at an abyssal station off central California. Deep-Sea Research II 45: 587-615

Berger WH, Heath GR (1968) Vertical mixing in pelagic sediments. Journal of Marine Research 26: 134-143

Bopp L, Aumont O, Cadule P, Alvain S, Gehlen M (2005) Response of diatoms distribution to global warming and potential implications: A global model study. Geophysical Research Letters 32: L19606 doi:19610.11029/12005GL023653

Borole DV (2002) Analysis of ^{210}Pb in sediment trap samples and sediments from the northern Arabian Sea: evidence for boundary scavenging. Deep-Sea Research I 49: 1055-1069

Buesseler KO, Bacon MP, Cochran JK, Livingston HD (1992) Carbon and nitrogen export during the JGOFS North Atlantic Bloom Experiment estimated from ^{234}Th:^{238}U disequilibria. Deep-Sea Research 39: 1115-1137

Clough LM, Ambrose WG, Jr., Cochran JK, Barnes C, Renaud PE, Aller RC (1997) Infaunal density, biomass and bioturbation in the sediments of the Arctic Ocean. Deep-Sea Research II 44: 1683-1704

DeMaster DJ, Pope RH, Levin LA, Blair NE (1994) Biological mixing intensity and rates of organic carbon accumulation in North Carolina slope sediments. Deep-Sea Research II 41: 735-753

Demopoulos AWJ, Smith CR, DeMaster DJ, Fornes WL (2003) Evaluation of excess ^{234}Th activity in sediments as an indicator of food quality for deep-sea deposit feeders. Journal of Marine Research 61: 267-284

Fornes WL, DeMaster DJ, Levin LA, Blair NE (1999) Bioturbation and particle transport in Carolina slope sediments: a radiochemical approach. Journal of Marine Research 57: 335-355

Gallucci F, Sauter E, Sachs O, Klages M, Soltwedel T (2008) Caging experiment in the deep sea: efficiency and artefacts from a case study at the Arctic long-term observatory HAUSGARTEN. Journal of Experimental Marine Biology and Ecology 354: 39-55

Goreau TJ (1980) Frequency sensitivity of the deep-sea climatic record. Nature 287: 620-622

Gray JS (1974) Animal-sediment relationships. Oceanogr. Mar. Biol. Ann. Rev. 12: 223–261

Guinasso NL, Schink DR (1975) Quantitative estimates of biological mixing rates in abyssal sediments. Journal of Geophysical Research 80: 3032-3043

Holm-Hansen O, Lorenzen CJ, Holmes RW, Strickland JDH (1965) Fluorometric determination of chlorophyll. J. Cons. perm. int. Explor. Mer 30: 3-15

Hoover DJ (1995) Burrowing urchins in the abyssal equatorial Pacific: sediment reworking rates estimated using two independent tracer techniques. M.S. thesis

Howell KL, Billett DSM, Tyler PA, Davidson R (2004) Feeding ecology of deep-sea seastars (Echinodermata: Asteroidea): a pigment biomarker approach. Marine Ecology Progress Series 266: 103-110

Hudson IR, Wigham BD, Tyler PA (2004) The feeding behavior of a deep-sea holothurian, *Stichopus tremulus* (Gunnerus) based on *in situ* observations and experiments using a Remotely Operated Vehicle. Journal of Experimental Marine Biology and Ecology 301: 75-91

Hutson WH (1980) Bioturbation of deep-sea sediments: Oxygen isotopes and stratigraphic uncertainty. Geology 8: 127-130

Lauerman LML, Smoak JM, Shaw TJ, Moore WS, Smith KL, Jr. (1997) ^{234}Th and ^{210}Pb evidence for rapid ingestion of settling particles by mobile epibenthic megafauna in the abyssal NE Pacific. Limnology and Oceanography 42: 589-595

Lohrer AM, Thrush SF, Gibbs MM (2004) Bioturbators enhance ecosystem function through complex biogeochemical interactions. Nature 431: 1092-1095

McIntyre A, Bé AWH, Preikstas R (1967) Coccoliths and the Pliocene-Pleistocene boundary. Progress in Oceanography 4: 3-8

Miller RJ, Smith CR, DeMaster DJ, Fornes WL (2000) Feeding selectivity and rapid particle processing by deep-sea megafaunal deposit feeders: A ^{234}Th tracer approach. Journal of Marine Research 58: 653-673

Moore WS (1984) Radium isotope measurements using germanium detectors. Nuclear Instruments and Methods in Physics Research 223: 407-411

Moore WS, Dymond J (1988) Correlation of ^{210}Pb removal with organic carbon fluxes in the Pacific Ocean. Nature 331: 229-341

Pfannkuche O, Lochte K (1993) Open ocean pelago-benthic coupling: cyanobacteria as tracers of sedimenting salp faeces. Deep-Sea Research 40: 727-737

Reimers CE, Jahnke RA, McCorkle DC (1992) Carbon fluxes and burial rates over the continental slope and rise off central California with implications for the global carbon cycle. Global Biogeochemical Cycles 6: 199-224

Reimers CE, Smith KL, Jr. (1986) Reconciling measured and predicted fluxes of oxygen across the deep sea sediment-water interface. Limnology and Oceanography 31: 305-318

Rhoads DC (1974) Organism-sediment relations on the muddy sea floor. Oceanogr. Mar. Biol. Ann. Rev. 12

Rhoads DC, Boyer LF (1982) The effects of marine benthos on physical properties of sediments. A successional perspective. In: McCall PL, Tevesz MJS (eds) Animal-sediment relations—the biogenic alteration of sediments. Topics in geobiology, Vol 2. Plenum Press, New York, pp 3-52

Ruhl HA (2007) Abundance and size distribution dynamics of abyssal epibenthic megafauna in the northeast Pacific. Ecology 88: 1250-1262

Smallwood BJ, Wolff GA, Bett BJ, Smith CR, Hoover D, Gage JD, Patience A (1999) Megafauna can control the quality of organic matter in marine sediments. Naturwissenschaften 86: 320-324

Smith CR, Hoover DJ, Doan SE, Pope RH, DeMaster DJ, Dobbs FC, Altabet MA (1996) Phytodetritus at the abyssal seafloor across 10º of latitude in the central equatorial Pacific. Deep-Sea Research II 43: 1309-1338

Smith CR, Levin LA, Hoover DJ, McMurtry G, Gage JD (2000) Variations in bioturbation across the oxygen minimum zone in the northwest Arabian Sea. Deep-Sea Research II 47: 227-257

Smith KL, Jr., Baldwin RJ, Glatts RC, Kaufmann RS, Fisher EC (1998) Detrital aggregates on the sea floor: chemical composition and aerobic decomposition rates at a time-series station in the abyssal NE Pacific. Deep-Sea Research II 45: 843-880

Smith KL, Jr., Baldwin RJ, Williams PM (1992) Reconciling particulate organic carbon flux and sediment community oxygen consumption in the deep North Pacific. Nature 359: 313-316

Smith KL, Jr., Druffel ERM (1998) Long time-series monitoring of an abyssal site in the NE Pacific: an introduction. Deep-Sea Research II 45: 573-586

Smith KL, Jr., Kaufmann RS, Wakefield WW (1993) Mobile megafaunal activity monitored with a time-lapse camera in the abyssal North Pacific. Deep-Sea Research I 40: 2307-2324

Smith KL, Kaufmann RS, Baldwin RJ (1994) Coupling of near-bottom pelagic and benthic processes at abyssal depths in the Eastern North Pacific-Ocean. Limnology and Oceanography 39: 1101-1118

Solan M, Wigham BD, Hudson IR, Kennedy R, Coulon CH, Norling K, Nilsson HC, Rosenberg R (2004) *In situ* quantification of bioturbation using time-lapse fluorescent sediment profile imaging (f-SPI), luminophore tracers and model simulation. Marine Ecology Progress Series 271: 1-12

Thistle D, Eckman JE, Paterson GLJ (2008) Large, motile epifauna interact strongly with harpacticoid copepods and polychaetes at a bathyal site. Deep-Sea Research I 55: 324-331

Thunell RC, Moore WS, Dymond J, Pilskaln CH (1994) Elemental and isotopic fluxes in the Southern California Bight: a time-series sediment trap study in the San Pedro Basin. Journal of Geophysical Research 99: 875-889

Wheatcroft RA (1991) Conservative tracer study of horizontal sediment mixing rates in a bathyal basin, California borderland. Journal of Marine Research 49: 565-588

Witte U, Wenzhofer F, Sommer S, Boetius A, Heinz P, Aberle N, Sand M, Cremer A, Abraham W-R, Jørgenson BB, Pfannkuche O (2003) *In situ* experimental evidence of the fate of a phytodetritus pulse at the abyssal sea floor. Nature 424: 763-766

VII

Conclusions

Conclusions

This dissertation presented research that used time-lapse photography, animal collections and sediment core samples to prove that the rate of bioturbation of *Echinocrepis rostrata* echinoids at Station M was correlated to food supply and climate indices. Aggregation behavior and possible multiple species of *Echinocrepis* were ruled out as confounding factors which might have affected the data used to conduct the bioturbation study, while examination of the reproductive anatomy of *E. rostrata* showed that this species is unlikely to broadcast spawn or reproduce seasonally. More research is required to determine how bioturbation by epibenthic megafauna affects deep-sea sediment chemistry.

The apparent lack of aggregation behavior around the time-lapse camera in the deep North Pacific has significant implications for the study of abyssal populations. Aggregation behavior and the biases such behavior could cause have been cited as a key argument against the use of observations made with seafloor time-lapse camera systems (Carter et al. 1979). However, it appears that artificial structures alone do not cause significant associative behavior in abyssal fish or detritus-feeding echinoids around time-lapse cameras. The result of this study provided a sound basis to proceed with the main focus of my dissertation research, which used the 18 years of Station M time-lapse data to analyze the behavior and movement patterns of epibenthic megafauna. However, more study is warranted on time-lapse camera deployments lasting longer than four months, which may allow enough time for slow-growing deep-sea epifauna (Beaulieu 2001) to settle on the time-lapse camera frame, attracting other organisms and leading to aggregation behavior. Exploring the effects of longer exposure to the deep ocean

environment is especially important because of the growing number of long-term cabled array systems, such as the MARS and NEPTUNE arrays in the eastern Pacific Ocean, which will be deployed indefinitely at a range of depths with only limited service intervals.

By confirming through gene sequence analysis that the purple, white and tan *E. rostrata* individuals seen at Station M were likely the same species, the bioturbation study could go forward without having to separate the surveys of *E. rostrata* abundance and statistical analyses of abundance, size and movement speed by morphotype or species. While the size and color differences between the morphotypes were significant, the population numbers and effects of the three morphotypes *E. rostrata* on the sediment could be considered collectively. The physical variability between the morphotypes did demonstrate the difficulty of determining deep-sea species based only on photographs or video footage. Even the mt 16S rDNA results may not be sufficient to claim definitively that the three *E. rostrata* color morphs are one species. The mt 16S rDNA gene sequence is a more conserved gene than some of the other genes used in "barcoding" studies. Future research will attempt to sequence the mitochondrial cytochrome c oxidase (CO1) gene, which is even more prone to mutation than 16S, and test tissue samples from *Echinocrepis* specimens collected at other seafloor sites.

The discovery that *E. rostrata* produces a relatively small amount of germinal tissue is important to understanding the distribution and reproductive strategy of this deep-sea echinoid. The highly variable flux of POC at Station M and other deep-sea sites would provide an inhospitable climate for seasonal reproduction, since there would not always be sufficient food to support gonad growth, gamete production, larval

development and recruitment at a predictable time of year. Constant production of small numbers of large, yolky eggs allows *E. rostrata* to take advantage of pulses of phytodetritus that occur at irregular intervals by spawning and releasing their larvae into a more nutrient-rich environment. Although the mating behavior of *E. rostrata* has not been observed, the relatively low density of individuals and lack of seasonal spawning behavior makes large spawning aggregations and broadcast spawning unlikely. The investment in a small number of large ova also supports the larval brooding hypothesis, in which newly fertilized ova adhere to the external aboral surface of a female *E. rostrata* echinoid. Early larval development would occur in a protected environment as opposed to release into the water column, and, once developed, the larvae can recruit immediately into the benthic environment without relying on random dispersal by bottom currents. Although larval distribution is limited by brooding behavior, the increased survival rates of the larvae presumably compensates for that disadvantage (Poulin and Féral 1996; Poulin et al. 2002), and the wide distribution of *E. rostrata* supports that theory (Mironov 1973; Mironov 1976). The distribution of *E. rostrata* across the Pacific Ocean basin also highlights the suitability of conducting deep-sea bioturbation studies using this animal, as results can be extrapolated to apply to the entire abyssal plain.

The time-lagged correlations between climate indices, upwelling indices, POC flux rates and bioturbation rates show that climate-mediated changes in POC flux are connected to deep epibenthic animal behavior and biologically mediated sediment mixing. The increased abundance of *E. rostrata* following the 1998-1999 ENSO event (Ruhl 2007) did not increase overall levels of bioturbation, most likely because the population spike reflected increased larval recruitment and a shift towards smaller size

classes. However, when abundance, size and movement speed are all taken into consideration, the amount of sediment disturbed by *E. rostrata* is closely tied to POC flux, and therefore climate variation. Climate variation has far-reaching effects on the global carbon cycle and biological pump, from surface productivity to deep sea bioturbation. Long-term time-series measurements are critical to identifying the links between the surface and deep-sea carbon cycling.

Previous studies in the equatorial Pacific have shown that epifaunal echinoids can homogenize the top layers of sediment and redistribute newly fallen phytodetritus (Hoover 1995; Smith et al. 1996). However, my study did not find conclusive evidence of the effect of *E. rostrata* bioturbation on sediment chemistry. Low POC flux rates at Station M compared to study areas with higher levels of surface productivity and less interannual and seasonal variability may have resulted in the minimal differences found between control and disturbed sediment cores. Reduced movement and feeding of *E. rostrata* due to the small amounts of newly arrived phytodetritus may have also been a factor. More sediment coring at different times of year, as well as coring extensively in areas containing large amounts of phytodetritus and fresh disturbance by *E. rostrata* may provide more data on the effects of bioturbation on the sediment.

Broader Ecological Implications

This research strengthens our knowledge of the connections between surface conditions and the deep-sea, and extends the recognized impact of climate variation on animal behavior from population-level effects to large-scale sediment mixing. Bioturbation was first studied in terrestrial soil movement (Richter 1952), a process

recognized by Charles Darwin (1881) and one that is now acknowledged as an important factor in changing geochemical gradients, redistributing nutrients and restructuring bacterial and microfaunal communities (Meysman et al. 2006). However, bioturbation has an even greater global impact on the enormous sediment volume of the abyssal plain, which covers ~60% of the surface of the Earth (Glover and Smith 2003). The export of POC out of surface waters and into the deep sea delivers large amounts of carbon to the abyssal environment, supporting a highly diverse community of epifauna, infauna and bacteria (Martin et al. 1987; Lampitt 1992; Lee et al. 1998; Kiørboe 2001; Kiørboe and Thygesen 2001; Stemmann et al. 2004; Buesseler et al. 2007). The abyssal benthic community bioturbates the sediment, sequestering or remineralizing the POC, and upwelling then transports the carbon back to the surface waters, in the form of dissolved CO_2, at variable time scales ranging from hundreds to thousands of years (Broecker 1991; Bauer et al. 1992; Reimers et al. 1992; Smallwood et al. 1999; Miller et al. 2000).

Climate-related fluctuations in the levels of productivity at the surface result in corresponding changes in the quantity and quality of material that is deposited on the seafloor (Smith et al. 1994; Smith et al. 2001; Ruhl and Smith 2004) and the abundance of benthic organisms (Ruhl 2007). Long-term changes in ocean temperature, whether natural or anthropogenic, could reduce upwelling and nutrient delivery through increased stratification (Bopp et al. 2005). Increased temperatures may also reduce the percentage of surface production that is exported from surface waters into the deep ocean (Laws et al. 2000; Laws 2004). Although vertical mixing of the ocean occurs on the order of hundreds to thousands of years, the time scale of POC export flux can connect the surface to the abyss within weeks to months (Ruhl and Smith 2004; Smith et al. 2006).

Any shifts in the dominant species or distribution of the benthic community, secondary to climate-driven changes in POC flux rates, will change the nature and intensity of marine sediment bioturbation. The impacts of faunal-driven sediment mixing on the long-term carbon cycle remain essentially unknown. If long-term changes in ocean temperature and productivity disrupt the process of basin-scale abyssal bioturbation, the global carbon cycle could be affected in unforeseen ways.

Future Directions

Understanding and modeling deep-sea processes, such as the biological pump and oceanic carbon cycle, requires long-term datasets that can resolve the seasonal and interannual variability, population-level biological variability, and animal movements and behaviors that control those processes. Unfortunately, only two deep-sea sites worldwide have been the subject of long-term studies that exceed 5 years in length: Station M, the site of this dissertation project, located in the northeast Pacific Ocean at 4100m depth, studied since 1989, and the BENGAL project located on the Porcupine Abyssal Plain (PAP) at 4800m in the northeast Atlantic Ocean, studied since 1991 (Bett and Rice 1993; Bett et al. 2001; Billett et al. 2001; Lampitt et al. 2001). Both stations have observed considerable interannual variability in climate, productivity and animal behavior, and regime shifts in the dominant fauna over decadal time scales.

Funding for ship time, equipment deployments and servicing, information storage and data analysis are in short supply even for these two sites, despite the incalculable value of the unique datasets that have resulted from the observation of the deep-sea over long time scales. Establishing new long-term deep-sea study sites in other

parts of the ocean is essential to expanding the scope of the results from Station M and the PAP beyond those two sites to global ocean scales. Collaboration with deep-sea resource exploration and extraction projects can provide the support necessary to deploy new long-term observation platforms, and the ship and ROV time needed to service the platforms and recover collected data and samples. However, these sites are limited in global coverage to the locations of the offshore resource extraction projects, and stand-alone observation platforms have the same battery life limitations and data capacity restrictions as previous deep-sea projects.

The development of cabled seafloor arrays, which connect deep-sea observation platforms to high-bandwidth fiber-optic power and data cables, is revolutionizing the field of deep-sea biology. By providing power directly from shore to deep-sea observation platforms and sending real-time images and oceanographic data from the platforms back to monitoring facilities onshore, many of the logistical difficulties of deep-sea research can be eliminated. Once deployed, these arrays require minimal servicing, no recurring ship time costs and have minimal power and data storage restrictions. Several arrays are near functional status, such as the NEPTUNE and VENUS regional-scale monitoring projects in the northeast Pacific Ocean, and several more are either in the process of coming online or in the planning stages. There are significant technical hurdles to overcome, such as safely connecting new oceanographic modules to the underwater junction boxes and dealing with the storage and analysis of the immense amounts of real-time data that cabled arrays can produce. However, the ability to conduct long-term deep-sea observation and experimental projects at a fraction of the previous cost and in numerous new locations will provide a better understanding of

oceanic processes that vary on long time scales, such as pelagic-benthic coupling, deep-sea population dynamics, bioturbation and the carbon cycle.

References

Bauer JE, Williams PM, Druffel ERM (1992) Super ^{14}C activity of dissolved organic carbon fractions in the north-central Pacific and Sargasso Sea. Nature 357: 667-670

Beaulieu SE (2001) Colonization of habitat islands in the deep sea: recruitment to glass sponge stalks. Deep-Sea Research I 48: 1121-1137

Bett BJ, Malzone MG, Narayanaswamy BE, Wigham BD (2001) Temporal variability in phytodetritus and megabenthic activity at the seabed in the deep Northeast Atlantic. Progress in Oceanography 50: 349-368

Bett BJ, Rice AL (1993) The feeding-behavior of an abyssal Echiuran revealed by in-situ time-lapse photography. Deep-Sea Research I 40: 1767-1779

Billett DSM, Bett BJ, Rice AL, Thurston MH, Galeron J, Sibuet M, Wolff GA (2001) Long-term change in the megabenthos of the Porcupine Abyssal Plain (NE Atlantic). Progress in Oceanography 50: 325-348

Bopp L, Aumont O, Cadule P, Alvain S, Gehlen M (2005) Response of diatoms distribution to global warming and potential implications: A global model study. Geophysical Research Letters 32: L19606 doi:19610.11029/12005GL023653

Broecker WS (1991) The great ocean conveyor. Oceanography 4: 79-89

Buesseler KO, Lamborg CH, Boyd PW, Lam PJ, Trull TW, Bidigare RR, Bishop JKB, Casciotti KL, Dehairs F, Elskens M, Honda M, Karl DM, Siegel DA, Silver MW, Steinberg DK, Valdes J, Van Mooy B, Wilson S (2007) Revisiting carbon flux through the ocean's twilight zone. Science 316: 567-570

Carter L, Heffler D, Schafer CT (1979) Utilizing time-lapse photography and video systems in marine environments. Photogrammetric Engineering & Remote Sensing 45: 798

Darwin CR (1881) The Formation of Vegetable Mould Through the Action of Worms With Observations of Their Habits. John Murray, London

Glover AG, Smith CR (2003) The deep-sea floor ecosystem: current status and prospects of anthropogenic change by the year 2025. Environmental Conservation 30: 219-241

Hoover DJ (1995) Burrowing urchins in the abyssal equatorial Pacific: sediment reworking rates estimated using two independent tracer techniques. M.S. thesis

Kiørboe T (2001) Formation and fate of marine snow: small-scale processes with large-scale implications. Scientia Marina 65: 57-71

Kiørboe T, Thygesen UH (2001) Fluid motion and solute distribution around sinking aggregates. II. Implications for remote detection by colonizing zooplankters. Marine Ecology Progress Series 211: 15-25

Lampitt RS (1992) The contribution of deep-sea macroplankton to organic remineralization: results from sediment trap and zooplankton studies over the Madeira Abyssal Plain. Deep-Sea Research 39: 221-233

Lampitt RS, Bett BJ, Kiriakoulakis K, Popova EE, Ragueneau O, Vangriesheim A, Wolff GA (2001) Material supply to the abyssal seafloor in the Northeast Atlantic. Progress in Oceanography 50: 27-63

Laws EA (2004) New production in the equatorial Pacific: a comparison of field data with estimates derived from empirical and theoretical models. Deep-Sea Research I 51: 205-211

Laws EA, Falkowski PG, Smith WO, Jr., Ducklow H, McCarthy JJ (2000) Temperature effects on export production in the open ocean. Global Biogeochemical Cycles 14: 1231-1246

Lee C, Murray DW, Barber RT, Buesseler KO, Dymond J, Hedges JI, Honjo S, Manganini SJ, Marra J, Moser C, Peterson ML, Prell WL, Wakeham SG (1998) Particulate organic carbon fluxes: compilation of results from the 1995 US JGOFS Arabian Sea Process Study. Deep-Sea Research II 45: 2489-2501

Martin JH, Knauer GA, Karl DM, Broenkow WW (1987) VERTEX: carbon cycling in the northeast Pacific. Deep-Sea Research 34: 267-285

Meysman FJR, Middelburg JJ, Heip CHR (2006) Bioturbation: a fresh look at Darwin's last idea. Trends in Ecology & Evolution 21: 688-695

Miller RJ, Smith CR, DeMaster DJ, Fornes WL (2000) Feeding selectivity and rapid particle processing by deep-sea megafaunal deposit feeders: A ^{234}Th tracer approach. Journal of Marine Research 58: 653-673

Mironov AN (1973) New deep-sea echinoid species of the genus *Echinocrepis* and distribution patterns of the family Pourtalesiidae (Echinoidea, Meridosternina). Transactions of the P.P. Shirshov Institute of Oceanology 91: 239-247

Mironov AN (1976) Deep sea urchins of the northern Pacific. Transactions of the P.P. Shirshov Institute of Oceanology 99: 140-164

Poulin É, Féral J-P (1996) Why are there so many species of brooding Antarctic echinoids? Evolution 50: 820-830

Poulin E, Palma AT, Féral J-P (2002) Evolutionary versus ecological success in Antarctic benthic invertebrates. Trends in Ecology & Evolution 17: 218-222

Reimers CE, Jahnke RA, McCorkle DC (1992) Carbon fluxes and burial rates over the continental slope and rise off central California with implications for the global carbon cycle. Global Biogeochemical Cycles 6: 199-224

Richter R (1952) Fluidal-texture in Sediment-Gesteinen und ober Sedifluktion überhaupt. Notizbl. Hess. L.-Amt. Bodenforsch 3: 67-81

Ruhl HA (2007) Abundance and size distribution dynamics of abyssal epibenthic megafauna in the northeast Pacific. Ecology 88: 1250-1262

Ruhl HA, Smith KL, Jr. (2004) Shifts in deep-sea community structure linked to climate and food supply. Science 305: 513-515

Smallwood BJ, Wolff GA, Bett BJ, Smith CR, Hoover D, Gage JD, Patience A (1999) Megafauna can control the quality of organic matter in marine sediments. Naturwissenschaften 86: 320-324

Smith CR, Hoover DJ, Doan SE, Pope RH, DeMaster DJ, Dobbs FC, Altabet MA (1996) Phytodetritus at the abyssal seafloor across 10º of latitude in the central equatorial Pacific. Deep-Sea Research II 43: 1309-1338

Smith KL, Jr., Baldwin RJ, Ruhl HA, Kahru M, Mitchell BG, Kaufmann RS (2006) Climate effect on food supply to depths greater than 4,000 meters in the northeast Pacific. Limnology and Oceanography 51: 166-176

Smith KL, Jr., Kaufmann RS, Baldwin RJ, Carlucci AF (2001) Pelagic-benthic coupling in the abyssal eastern North Pacific: An 8-year time-series study of food supply and demand. Limnology and Oceanography 46: 543-556

Smith KL, Kaufmann RS, Baldwin RJ (1994) Coupling of near-bottom pelagic and benthic processes at abyssal depths in the Eastern North Pacific-Ocean. Limnology and Oceanography 39: 1101-1118

Stemmann L, Jackson GA, Ianson D (2004) A vertical model of particle size distributions and fluxes in the midwater column that includes biological and physical processes—Part I: model formulation. Deep-Sea Research I 51: 865-884